Addis Ababa University

Addis Ababa Institute of Technology

School of Mechanical & Industrial Engineering

MSc. Thesis on:

Numerical Analysis on the Impact Resistance and Energy Absorption Behavior of Motorcycle Helmet for Different Impact Conditions

A Thesis Submitted to the School of Graduate Studies of Addis Ababa Institute of Technology, Addis Ababa University in partial fulfillment for the Degree of Master of Science in Mechanical Engineering (Mechanical Design)

By:

Tsehayneh Negash

Advisor: - Dr. Araya Abera

Co-Advisor: - Mr. Tadesse Nega

Addis Ababa, Ethiopia

October, 2023

Addis Ababa University

Addis Ababa Institute of Technology

School of Graduate Studies

School of Mechanical and Industrial Engineering

MSc. Thesis on:

Numerical Analysis on Impact Resistance and Energy Absorption Behavior of Motorcycle Helmet for Different Impact Conditions

By:

Tsehayneh Negash

Approved by the Board of Examiners:

Dr. Araya Abera	_____	_____
Advisor	Signature	Date
Dr. Mulugeta Habtemariam	_____	_____
Internal Examiner	Signature	Date
Dr. Zenebe Mengestie	_____	_____
External Examiner	Signature	Date
Dr. Araya Abera	_____	_____
School Dean	Signature	Date
Dr. Sosina Mengistu	_____	_____
Associate Director for PG Program	Signature	Date

Declaration

I hereby declare that the work which is being presented in this thesis entitled "**Numerical Analysis on the Impact Resistance and Energy Absorption Behavior of Motorcycle Helmet for Different Impact Conditions**" is original work of my own, has not been presented for a degree of any other university and all the resource of materials used for this thesis have been duly acknowledged.

_____ _____

Tsehayneh Negash Date

This is to certify that the above declaration made by the candidate is correct to the best of my knowledge.

_____ _____

Dr. Araya Abera (Advisor) Date

Acknowledgment

First of all, I would like to thank the almighty God and his mother Virgin Mary; that is why all things are happened on the will of them.

Second, I would like to express my great-full thank for my Advisor Dr. Araya Abera for his continual guidance and supportive encouragement during the research; and my Co-advisor Mr. Tadesse Nega on behalf of his support in this research work. I also would like to thank the school for collaboration as well and a great gratitude to the staffs of AAiT railway excellence center.

Then, I would like to give a great thank for my senior staffs Belayneh Ytayew (PhD Cand.) and Mr. Aschalew Belete for their support at all levels of this thesis.

And finally, I would like to thank my parents for their support and encouragement during the stay of my postgraduate study.

Abstract

Head injuries are common during different activities of daily life – one is related to motorcycle vehicle traffic accident. The aim of this research was concerned on the analysis and evaluation of the effect of impact loads on the basis of impact velocities and angles in the case of accidents. The investigations were carried out using numerical analysis. The independent variables were impact velocities – ranged from 7.5 m/s to 17.5 m/s and impact angles – ranged from 0^0 to 90^0. Flat anvil and footpath scenarios were also conditions on which the effects of angles were determined. The peak linear acceleration (PLA) and head injury criteria (HIC) as well as energy absorption effect were the output parameters for the study. Solidworks 2022 SP1 30.1.0.82 and ANSYS – LS DYNA (HyperMesh 2019.1 – LsDyna (Keyword971_R10.1)) were employed for the modellings and numerical analysis. The Economics Commission for Europe (ECE 22.05) specification was selected to investigate the specified parameters related to the standards. Based on the obtained results when using stiff liner component, the PLA ranges from 199G to 622G (PLA per gravity) and HIC ranges from 1927 to 23900 when the impact velocity increases from 7.5 m/s to 17.5 m/s for frontal impact. Similar incremental trends were also recorded on the crown, rear and lateral impact positions. Using soft liner material, the effect of angles on the crown impact position at 16.5m/s were investigated and 153G of PLA and 1708 of HIC recorded at impact angle of 90^0. But when the value of the angle decreased, PLA and HIC values also continuously decreased. So, the severity of the accident increases with impact velocity and impact angels on flat anvil impacts. The extent of risk for the accidents which happened on footpath curve, minimized as the inclination of the resultant impact velocity was about 45^0 for the given specified impact velocity; this is because the impact load decomposed towards the two impact points. Using the model for the specified limit can provide the protection; but crossing the limit may result the risk too severe.

Key words: - Motorcycle Helmet; Helmet Shell; Impact Resistance; Liner Foam; Energy Absorption; Headform.

Table of Contents

List of Tables

List of Figures

Abbreviations

FE	Finite Element
FEM	Finite Element Model
FEA	Finite Element Analyzing
HIC	Head Injury Criterion
HIP	Head injury power
PVB	Polyvinyl Butyral
PLA	Peak Linear Acceleration
ABS	Acrylonitrile Butadiene Styrene
PC	Polycarbonate
EPS	Expanded Polystyrene
ICP	Intracranial Pressure
PA12	Polyamide 12
PLA	Peak Linear Acceleration
PRA	Peak Rotational Acceleration
HIII	Hybrid III
THUMS	Total Human Model for Safety
ECE	Economics Commission for Europe
RLA	Resultant Linear Acceleration

Nomenclatures

A_{max}	Peak Acceleration
σ_{vm}	Von-Misses Stress
g	Gravitational Constant; 9.81m/s^2
$a(t)$	Linear acceleration
$\alpha(t)$	Angular acceleration
ε_s	Shear strain
J	Joule
km/h	Kilometer per hour
mm	Millimeter
ms	Milliseconds

Chapter One

1 Introduction

1.1 Background

Head injuries are common during different activities of daily life; in accidents due to construction and industrial activities, accidents in case of football and racing games, traffic accidents on bicycle and motorcycle riders, etc. This case is most severe and needs consideration to reduce its effect using helmets. Industrial safety helmets are possessed to protect the falling object accidents during the industrial activities, but its testing energy is several times lower than that of the helmet for bicycle (testing energy ranges from 58J to 96J), equestrian (about 88J testing energy) and mountaineering (about 98J testing energy) [1].

Motorcycles have used for means of transportation with low prices and operation costs despite of the accidents due the speed unless protective helmet is used. The usage as well as the accidents related to those vehicle step up every year [2]. Motorcyclists used motorcycles due to their speed as relative to bicycle in transportation system and but resulting high accident rate as compared to bicycle accidents. The fatality rate of motorcycle accidents with in all traffic accidents accounts about 25% globally [3].

Road traffic accidents, despite of their severity, are major problems and common in worldwide on traffic aspects [4]. Motorcycle vehicle needs consideration regarding traffic accidents i.e., as whether using motorcycle helmet or not in riding. Motorcycle helmet provides the mechanical impact protection as possible in order to prevent the skull of the motorcyclist head from fracture due to complex kinematic impact during accidents [5]. This is because motorcycle accidents can cause severe injuries and fatalities, even when wearing helmets, due to the strength of motorcycle helmets lacks head protectability in actual impact accidents.

Using helmet safety in riding reduce the risk of head injuries up to 69% and the mortality rate will prevented up to 42% [6]. A helmet accomplishes this by slowing the stopping process. So that the head stops in around six milliseconds rather than one millisecond or less, and by trying to convert a small fraction of the collision energy to heat by the crushing or deformation of a

component. The helmet reduces the peak spike of energy to the head and brain by dispersing the crash energy over those incredibly brief six milliseconds. After the hit, it's crucial that the helmet doesn't spring backwards from the wearer's head. So, how minimize the severity of motorcyclists' head injuries is on be considering the design aspect of the components of the helmet. A well-designed component can distribute the impact energy to the whole component of the system and the energy will be easily absorbed [7]. And hence, many authors attempted to overcome the aforementioned problem. The research by [8] made their investigation on materials selection on the bases of energy absorption capacity and efficiency of recovery after impact to improve the performance of the system. On the other hand, the study by ***Fernandes & Alves de Sousa, 2013*** [9] made an improvement on the impact energy absorption performance of the component of the helmet by optimizing its physical size – the density and thickness of the liner foam.

The components, as stated by ***Bhudolia et al., 2021*** [10] & ***Dymek et al., 2022*** [11], consists of the outer shell which distributing the concentrated impact load through the whole helmet and the inner part which possess absorbing the distributed impact load to protect the head from injury in accidents. In order to improve the performance of the helmet re-examination of the model which made by the measurements of the shell during the impact was investigated. And also, the impact energy absorption performance during accidents depends on the foam component performance of the helmet as stated by ***Gilchrist & Mills, 1994*** [12]. As investigated by different researchers, the accidents related to motorcycle vehicles are serious causes of head injury and may results fatality. However, when using a motorcycle helmet, the severity of injuries could be minimized but cannot be totally prevented.

1.1.1 Types of Helmets

There are different types of helmets which used by motorcycle riders [13]. Figure 1.1 shows the three basic types of helmets available on the market, each of which has a number of variations as presented by ***Thai et al., 2021*** [14] as follow:

A. Half helmet

The lowest size and weight footprint is provided by the half helmet. A half helmet has a bowl-like form and just covers the summit of the head. Also, because of its tiny size and low weight, it

has less padding, liner, and shell material, all of which are vital in absorbing impact, making it the least protective form of helmet. A half helmet hardly complies with any basic covering requirements.

B. Open face

With the exception of the face, this type of helmet virtually completely encloses the head. Large visors that cover the rest of the face are occasionally provided by the manufacturer, although they are less durable against minor impacts than the chin bars from full-face helmets. According to studies, head injuries are substantially more likely while wearing an open face helmet.

C. Full-face

This is the bulkiest and heaviest of them all. A full-face helmet comprises strong shell and liner, additional material to protect the chin and the back head. It is the helmet that most frequently suggested since it offers the most amount of head coverage. The typical model includes a visor or windscreen to hide riders from unwanted objects like bugs, dust, or bad weather. Moreover, the thicker foam offers superior wind noise isolation to improve rider focus.

Half helmet Open-face helmet Full-face helmet

Source: *(Thai et al., 2021)*

Figure 1.1. Types of helmets.

The type of the helmet which considered in this research was full-face helmet due to the reasons – it covers most of the head parts of the rider, relatively low peak accelerations, which is a

measurable output parameter to determine whether the effect of the accident is within the safe mode or not, and also more recommended as stated by researchers ***Liu & Chen, 2017*** [15].

So, to maximize the prevention performance of the helmet, directions were given by researchers on the bases of material selection [16], physical size or topology optimization [17], environmental consideration [18], and concerning with the effect of impactors – impact velocity, impact angle, and anvils. Meanwhile the methods used – modeling the headform as much as mitigating the complexity of human head shape for experimental and numerical analysis – to investigate results nearly the actual accident phenomenon were implemented and were recommended.

In this research, the parameters which were considered during the study includes selecting of the material type for components, analyzing the effects of impact velocity and impact angle regarding to evaluating the severity of the accidents. But regarding those considerations, many attempts have been made to investigate experimentally as well as numerically on the determinant factors and behavior at different conditions. Performance of helmet at different material types (i.e., Acrylonitrile Butadiene Styrene (ABS), Polycarbonate (PC) as studied by ***Shankar et al., 2021*** [19]), impact velocities (i.e., v = 5.5 m/s - 13.9 m/ss, 11.5 m/s, 7.5 m/s in the studies by ***Gao, Wang, et al., 2022*** [3], ***Gao, He, et al., 2022*** [20], ***Aiello et al., 2007*** [21] respectively), crushing condition with respect to the impact angle (i.e., 30^0 intervals as stated by ***Zheng et al., 2022*** [22]) had been studied.

1.2 Statement of the problem

The impact load resistivity and energy absorption behavior of motorcycle helmet is still an issue in the transport sector since helmet is the best protective mechanism in riding accidents [23]. To do so, researches were done considering different aspects to improve the performance of motorcycle safety helmets. As some from the stated, the investigations were including the effects of material types on which the components were made, effect of impact velocities and impact angles during accidents, topology optimization of the helmet components, temperature conditions during conducting the experimental tests.

However, the effect of materials from different topology optimization aspects, impact velocity (i.e., below 5.5 m/s, between the intervals and above 13.9 m/s (which is 50 km/h) [3]), impact height, impact angle needs further considerations. Similarly the performance test was investigated only in ambient temperature and hygrometry conditions [24]. Regarding for the impact velocities, a maximum of 60 km/h urban speed is permitted by the speed limit regulation of Ethiopia for light weight vehicles including motorcycle. Therefore, that was significant to conduct a study for determining the helmet performance beyond those of the studied speed parameter limits and considering the maximum speed which permitted by the Ethiopian speed limit regulation.

For this research work, the gaps which considered in the investigation were effect of impact velocities, effect of impact angles relative to anvil types, and effect of liner foam material types on the output parameters (Peak Linear Acceleration – PLA, Head Injury Criteria – HIC and energy absorption behavior).

1.3 Objective

1.1.2 General Objective

The main objective of this research is numerical investigation on impact resistivity and energy absorption behavior of motorcycle helmet for different impact conditions.

1.1.3 Specific Objective

To achieve the main objective and find results for the specified research gaps, the following specific objectives are employed:

- To analyze the effect of impact velocity on impact load resistivity and energy absorption behavior of the helmet system;
- To evaluate the effect of impact angle on impact load resistivity and energy absorption behavior of the helmet system considering flat anvil accidents;
- To analyze the angle of inclination for the resultant impact velocities resulting minimum effect for the helmet system considering the footpath curve accidents.

1.4 Methodology

In this sub-section, the methodological sequences of the investigation were discussed as follow. The flow of this research started from the identification of research gaps from reviewing the stipulated literatures. The input parameters (independent parameters) in this study were impact velocities, which ranged from 7.5 m/s to 17.5 m/s within every 1 m/s difference and impact angles, which ranged from 0^0 to 90^0 with a 5^0 interval. Flat anvil and footpath scenarios were also conditions on which the effects of angles were determined. The peak linear acceleration (PLA) and head injury criteria (HIC) were the output (dependent) parameters for this study to measure the effect of impactors. The 3D model of the helmet system was developed on the basis of the Economic Commission of Europe (ECE 22.05) standards. Depending on the reviewed literatures, the material types for each component were assigned. For the modelling purpose, Solidworks 2022 SP1 30.1.0.82 software; and for the numerical analysis, ANSYS – LS DYNA (HyperMesh 2019.1 – LsDyna (Keyword971_R10.1)) software were used. Model validation was employed with the experimental investigations that were done previously. Then numerical investigations were done and discussions for the findings, conclusion and recommendation based on the findings were done. Finally, future works were tabulated.

1.5 Scope and Significance of the study

This study concerned with the parameters and analyzing their effect on the motorcycle helmet system. The parameters were impact velocities and impact angle during the motorcycle accidents. And the effects were identified from the response of the helmet system with respect to the load distribution or resistivity and energy absorption of the components of the helmet system.

Analyzing the effect of the parameters on the motorcycle helmet system determines the performance of that safety system. This indeed, helped as a user to limit and respect the range of activities accordingly in order to minimize the effect of accidents.

1.6 Limitations on the study

The first and the most challenging case was the experience on the tool for numerical analysis. The tool was Ansys Softeware – LS DYNA package. Using it was a preferable to extract outputs

of the analysis according to the identified problem. But to use this software, knowing about LsDyna Hyper-Mesh, LsDyna Keyword, LsDyna HyperView, LsDyna Program manager and LsDyna Ls-PrePost were mandatory. Taking trainings about the software was also not easy due the availability and time constraints. The other one was the need for high computing computers to run the long time taking numerical analysis.

1.7 Organization of the research

In chapter one, the background of the study followed by the problems that inspired to do this research, the objective, scope and significancy of the research were included. In chapter two, the list of related references and reviewed articles were presented. The research materials and various methodologies including 3D modeling, FE modeling, model validation and numerical analysis, were shown in chapter three. Chapter four, results of the analysis and discussions for those numerical results were included. The last chapter, chapter five, comprised the conclusion, recommendations and future work sections which explain about the results, the measure that can be taken based on the investigation and directions for the going research. At the last, the references and appendixes were included.

Chapter Two

2 Literature Review

2.1 Introduction

Researchers had looked at the performance of safety helmets in a variety of ways, from the ground-breaking to the most recent improved and advanced phases. In this section, the materials which used for the helmet components, the crushing effect in the motorcycle helmet, impactors and their effect were presented. So, below were a few recently published and reviewed research papers as per this work that provide information on motorcycle safety helmets.

According to ***Nasim et al., 2022*** [24], the goal of investigation was to develop a helmet made of a certain material that would cause as little head harm as feasible. The targets to be attained were the amount of dynamic compression in the system as well as the after-yield compressive stress-strain of hydrostatic pressure for plastic and uniaxial yield stress. The methods were FE modeling, proposed lattice linear, FE model validation following standard tests. As per the results, the linear impact error was within acceptable bounds with respect to the experimental value, however the peak acceleration error was a little overestimated. There were several conditions in the investigation, nevertheless, that require more research. The impact of the visor was not taken into account, stiffness and energy absorption were the only tests performed in the standard test, only ambient and hygrometric conditions were taken into account for the performance test, and lastly, the transition of polyamide 12 (PA12) from more ductile property to brittle with respect to temperature change was not taken into account.

The study's main goal by ***Levadnyi et al., 2018*** [25] was to predict the severity of traumatic brain injury brought on by head impact. Determining the size of the foam and shell of the helmet were the tasks taken into consideration in the study for that goal. Solidworks, CAD and ABAQUS software were used in that study's methodology to model the helmet. The analysis revealed that the degree of damage is influenced by impact velocity, mechanical characteristics, and orientation. The acceleration peak value on the protected head, with liner foam of thickness 10mm, was lowered by 57.7% as compared to the unprotected head. Among the helmets that

were subjected to 100% energy, 90% of which were absorbed by the system – approximately 72.5% of which by the foam and the remaining 27.5% of which by the helmet shell.

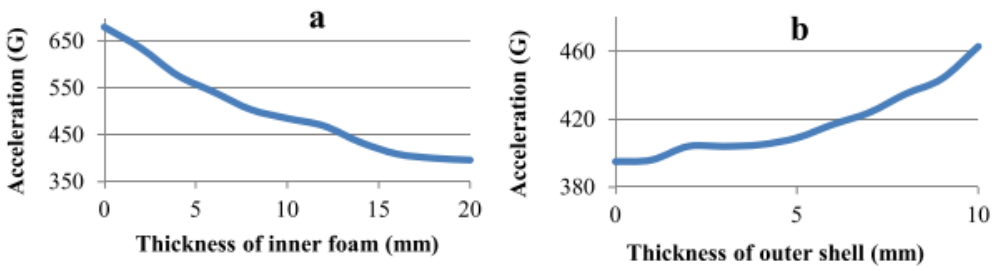

Source: (Levadnyi et al., 2018)

Figure 2.1. Variation of head acceleration with thickness of liner foam and outer shell.

The purpose of the study by ***Liu & Chen, 2017*** [15] was to model a motorcycle helmet with ventilation slits for comfort and safety. But here in this research the investigation about the simulated headform acceleration profile for each of the full-face, open-face, and half-face helmets with the given impact speed of 6 m/s was presented. A good general agreement exists between all three profiles as shown in the figure below. However, a close inspection reveals some differences between them – the half and open-face helmets have peak accelerations of 303g and 235g, respectively, whereas the full-face helmet has a much lower peak acceleration of 197g.

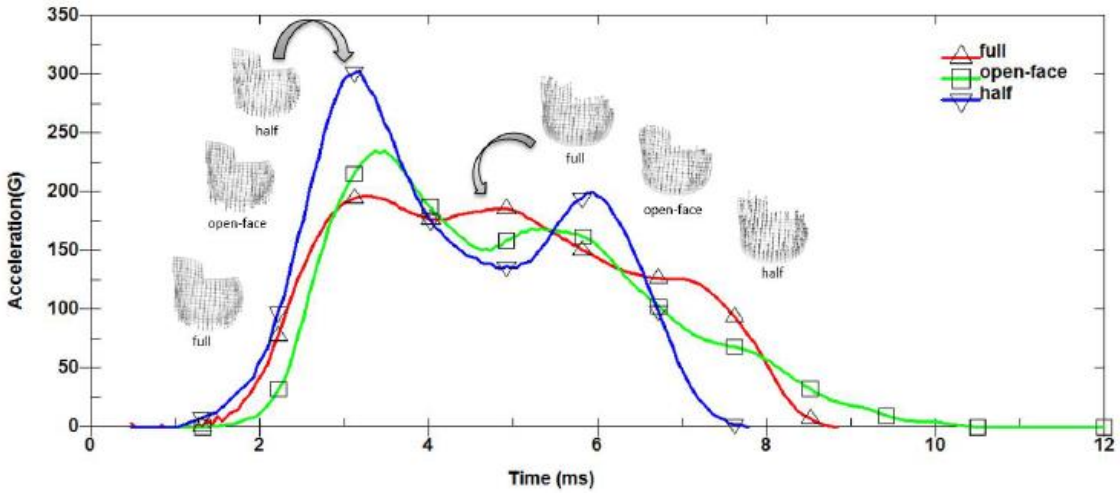

Source: (Liu & Chen, 2017)

Figure 2.2. Headform acceleration profiles for full-face, open-face, and half-face helmets.

The goal of the paper by ***Lie et al., 2021*** [26] was to establish a scientific framework for analyzing a new helmet by developing a methodology on the basis of kinematic and biomechanical head injury criterion. The analysis took into account the von-Mises reaction of the brain, the influence of the honeycomb filer in the helmet, and biomechanical factors. The simulation that followed was carried out by LS DYNA with the appropriate mass and element size of the models. The best novel helmet design was demonstrated by a 36.3%, 53.8%, 35.8%, and 46.1% reduction in A_{max}, HIC, ICP, and von-Mises stress, respectively. The shell thickness was 4mm; however, it is important to consider the effects of using more or less than the specified amount of shell thickness as well as the performance of replacing the bolt joints between the outer shell and the inner foam liner of the helmet with resins. It is also important to consider the effects of using a kerbstone anvil rather than a flat anvil for impact tests.

The goal of the study by ***Thai et al., 2021*** [14] was to develop motorcycle helmet system and investigating findings using numerical simulation while altering the liner foam's thickness in order to maximize the performance. Decrease on HIC, a standard indicator for predicting head injuries, a peak linear and rotational acceleration, and assessing the impact on internal energy were all taken into account. Solidworks and CAD design came first in the study's flow, then LS_Prepost modeling. On the chosen head shape of the Hybrid III, a drop test using the ECE R22.05 standard was conducted. The quantifiable values according to HIC, PLA, PRA as well as internal energy were within the range of threshold limits. Comparison was made and among the specification, the result tooled the type of helmet which can withstand the impact test more efficiently.

The study by ***Fernandes et al., 2020*** [27] was also focused on the objective of computationally evaluating the efficiency of the helmet that certified by the standards. The criteria for enhancing the standards already completed and utilized as a benchmark for simulation validation. The geometry of the component was completed using CATIA software and meshed with ABAQUS software; however, the FE model of the helmet was produced and validated by simulation based on guidelines for the assessment. As seen by the result data, the major stress fell within the anticipated range of the threshold, or between 0.1 and 0.4. Moreover, the range of the brain pressure threshold changed from 90 to 256 kPa to 100 to 500 kPa, indicating a significant risk of systemic damage. Due to the disagreements between the threshold value and the results of the

investigation, which caused severe brain damage, the system has to be improved or optimized in order to reduce the danger to the brain.

The study conducted by ***Kaczynski et al., 2019*** [28] aimed on merging desirable material properties for enhancing the performance and safety of the system. The approach used in the inquiry involved selecting materials from the literature, testing them under various temperature and impact stress conditions, and comparing the findings. Quantitative measurements of the greatest energy absorption at the lowest temperature and the minimum energy absorption at the highest temperature were made for various materials. And a comparison was done in order to choose the finest. Nevertheless, additional research is required to determine how the temperature will affect the chosen materials if the test is conducted outside of the specified range.

2.2 Motorcycle helmet materials

Under this sub-topic, the investigations related to the type of the materials for each component of motorcycle safety helmet and their effect on the performance of the helmet system had been reviewed as follow.

The goal of the study by ***Prasartthong & Carmai, 2022*** [29] was to analyze the effects of various parameters on linear and rotational accelerations using reduced order models by taking into account the impacts of material and its liner thickness, friction at interfaces, and other factors. In the investigation, different combination of the materials ABS, aluminum-foam (Al - F) & EPS were concerned. The study's methodology involved using a 3D scan surface model created with CAD software and an experimentally verified FE model. The analysis's findings indicate that, PLA reduced with an increasing liner thickness of EPS within the specified range but rose with coefficient of friction. Nevertheless, there was little difference in the thickness of ABS and Al-foam; additional research was needed to determine how well the helmet will absorb energy and resist penetration. Additionally, Using LS-DYNA codes, a full-face motorcycle helmet (AGV-K3) as stated by ***Xiao et al., 2022*** [30] was modelled to examine how well it protected against head injuries during crashes. The foam liner was manufactured of EPS, and the exterior shell was constructed of the thermoplastic material ABS, which has a thickness of 4 mm. LS-DYNA's piecewise linear plasticity model was used to define the outer shell's material. And a crushable foam material was used to model the EPS foam liner. Pursuant to the ECE R22.05

standard, the helmet was tested in a drop test against a flat steel anvil at various points while mounted on a headform weighing 4.8 kg. For the purpose of validating the FE model of helmet, the impact at sites specified in the ECE R22.05 standard was implemented. On the other hand, the study by ***Shankar et al., 2021*** [19] concerned with the performance analysis and identification of safety helmet specification using different materials basically five selective materials were investigated. The performance was then determined using total deformation, strain energy, and equivalent stress/energy for static and dynamic loads under various situations. For this experiment, FEA was done with ANSYS utilizing a model that was imported from CATIA software. When compared to the other materials that were chosen, ABS and PC have the highest deformation and strain energies, which can help to minimize system damage. But, the study by ***Fernandes et al., 2019*** [31] directed to the other type of material, which was cork agglomerate, for helmet paddings. This was accomplished by taking into account and evaluating the peak acceleration value while varying the component thickness and material type. With the use of the results' table, the numerical values for the peak acceleration were reported and compared. Peak acceleration with the maximum liner thickness (40 mm) was better, and at the same time, it was the maximum liner thickness for the study.

2.2.1 Helmet Shell Materials

As a summery for materials, the shell component of the helmet system, as stated by ***Aiello et al., 2007*** [21] & ***Leng et al., 2022*** [32], was mostly made of a thermoplastic material (acrylonitrile butadiene styrene - ABS), polycarbonate (PC) or composite materials like glass reinforced plastics (GRP) or Kevlars. The outer shell of the helmet as stated by ***Leng et al., 2022*** [32] serve to: - Distribute the impact load throughout the whole area of the system in order to reduce concentrated stress on the impact region; To avoid damage from a skull fracture and brain tissue penetration, the helmet must be protected against sharp things; Used as a framework for helmet liners to ensure that they won't be torn apart by penetration and to absorb the first shock as the first layer of protection.

As those mentioned points, different materials with different properties were used for that component. PC is a ductile material with the capacity to keep its mechanical properties under a variety of temperature variations. While keeping the constant modulus of elasticity in practice, the peak load and plastic component of crushing rise linearly with that of the energy content in

the tests. Nevertheless, based on the functions of the shell, acrylonitrile butadiene styrene (ABS) was chosen due to its properties and cost as the material employed as a shell component for this study. Table 2.1 below lists the material's characteristics. The physical size of the helmet model was assigned considering the revied papers [3] – from crown to bottom extreme it was 331.5 mm and from rear to front extreme it was 312.6 mm. Increasing the outer shell's thickness has a negative effect on the helmet's energy absorption capabilities. This happened as a result of ABS plastic's high density and stiffness but low damping capabilities. Due to the increased thickness of the outer shell, high density is characterized by an increase in the weight of the helmet as showed by ***Levadnyi et al., 2018*** [25]. But for this research, the size of the helmet shell was settled as 4 mm thickness, 294.65 mm from crown to bottom extreme, 272.09 mm from lateral to lateral (side to side) and 325.4 mm from rear to front extremes.

Table 2.1 Material properties of Acrylonitrile Butadiene Styrene (ABS).

Material	Density	Young's modulus	Poisson ratio	Yield strength
ABS	1200 kg/m^3	2 GPa	0.37	34.3 MPa

Source: (Lie et al., 2021)

2.2.2 Helmet Liner Foam Materials

The second important component of the helmet system is liner foam. Liner foam is the second important part of the helmet system. In most helmets, the inner foam is employed for energy management. The foam may be manufactured from a wide variety of materials. The availability, pricing, and qualities of the various materials influence the decision to use them, as stated by ***Shuaeib et al., 2007*** [33] expanded polypropylene (EPP) was one. Cork was another option for liner foam because of its strong energy absorption capabilities as stated by Kaczynski et al., 2019 [28]. But expanded polystyrene (EPS) is still the choice for most bike helmets. It is the most common due to that of cellular material with excellent shock absorption capacity, lightweight, relative low cost and desirable cost-benefit ratio, but poorer capacity after its first impact due to limited elastic recovery as stated by the researchers ***Kostopoulos et al., 2002*** [7] & ***Landro et al., 2002*** [34]. Expanded polystyrene (EPS) has allowed for increased deformation, lengthened impulse duration, and reduced peak forces in order to absorb as much impact energy as feasible during impact accidents as presented by ***Leng et al., 2022*** [32]. So, it was necessary to select

appropriate constitutive material models to simulate the mechanical behavior of each material in order to simulate the helmeted impacts. An elasto-plastic material was modeled as the EPS foam for such mechanical behavior investigation. But the crushable foam material model was also used to simulate plastic behavior and with 80 kg/m^3 was selected for this study. The model was designed to analyze crushable foams, which were frequently used as structures for energy absorption as shown by ***Fernandes et al., 2020*** [27]. Therefore, a stiff elastic material and on the other hand a soft EPS material were chosen for this research study to show the energy absorption behavior of the helmet system. The selection for EPS was due to its extremely effective energy absorption and dissipation capabilities along with low weight and inexpensive cost. Such materials are capable of absorbing between 30% and 50% of the entire energy delivered to the helmet system by irreversibly deforming themselves as stated by ***Kostopoulos et al., 2002*** [7].

As stated by ***Fernandes et al., 2020*** [27], the thickness of the expanded polystyrene (EPS) liners were ranged from 20 to 50mm. The thicker one, which covers the top of the head, was only slightly thinner at the low rear area and typically ranged between 40 and 50mm in thickness. The lateral ones, on the other hand, ranged in thickness from 20 to 40 mm, and they were also thinner at the low rear. On the other hand, its thickness was within the range of 12 mm to 20 mm as stated by ***Shuaeib et al., 2007*** [33]. As per the investigation by ***Levadnyi et al., 2018*** [25], the magnitude of the acceleration was reduced when the thickness of the foam layer was increased from 0 to 16 mm, but further increases in its thickness of the layer had no impact on the acceleration. Additionally, the HIC value indicated that using a helmet with 16 mm foam thickness reduced the HIC value.

Table 2.2. Mechanical properties of EPS foam with different densities.

Properties	Variation with density			
Density (kg/m^3)	30	50	70	80
Young's modulus (MPa)	15	25	39	20
Compressive strength (MPa)	0.224	0.328	0.510	0.58
Compressive stress at 10% relative deformation	0.244	0.344	0.540	---

Source: (Caserta et al., 2011)

2.2.3 Head-Form Materials

Numerous head finite element (FE) models have been created to study the kinematic and biomechanical characteristics under various loading conditions due to the rapid development of computational mechanics techniques. These well-known head models have been frequently used in conjunction with various helmet models. This was done to investigate the kinematics and biomechanical reactions of the helmeted head targeted to enhance helmet protection and lower the risk of head injuries as stated by ***Zheng et al., 2022*** [22]. Different head form models were used in different researches to investigate kinematic and biomechanical effects of head injury accidents. For the head form model, a rigid material model was used to investigate the effect of the accidents [22]. But in this research, instead of using those rigid materials a plastic kinematic material model was selected for the head form model. Then the stress propagation during the accidents can be simulated. ECE R22.05 requires that the mass of the head form be specified; a 4.7 kg head form must be used for a J-size helmet, and it is considered for this study. Figure 3.2 depicts the developed FE head form model along with its main inertial moments. The respective inertias for J-size are – I_{xx} =264 kg/cm^2, I_{yy} = 318.3 kg/cm^2 and I_{zz} = 193.1 kg/cm^2 [31].

2.3 Crushing effects in Motorcycle Helmet

As stated by ***Gao, Wang, et al., 2022*** [3], the purpose of the article was to construct and illustrate a helmeted headform and windshield glazing helmet system for modeling the impact interaction between those components. Based on that goal, factors such as the impact velocity, helmet pasture, and impact position on the windshield on head form reaction were taken into account. The process for achieving this resulted in simulation using LS-DYNA, ABAQUS, and validation using pertinent experimental data. The FE helmet model was used as the starting point. The key findings in the analysis; the impact velocities and HIC decrease was reported to be 11.1 m/s-40.3 and 13.9 m/s-74.4, respectively. On the other hand, the study's objective by ***Li et al., 2022*** [35] was to investigate the impact of various translational acceleration loadings on head response. The intracranial pressure, von-Mises stress, maximal main stress, HIC, and tissue level predictors were all examined in order to achieve the aim. To study the parameters, the 50th percentile male head model of THUMS was introduced. The investigation was conducted using a FE model and the LS_ DYNA code. For simulations, peak acceleration and duration ranges were also used. As

shown from the study, the head response would be affected by the loading curve shape, impact duration and peak magnitudes. Further the HIC and tissue-level predictor were analyzed. Six impacts with peak magnitudes between 100 and 350 g and durations between 6 and 14 milliseconds (ms) were chosen for the investigation. However, as per those papers, the rotational acceleration histories were considered and the result showed that lateral impacts produce the biggest peak value while crown impacts provide the smallest peak value. Moreover, impacts that occur closer to the supporter produce greater second peaks and HIC values. Yet there were only four variables—5.5 m/s, 8.3 m/s, 11.1 m/s, and 13.9 m/s—and the fluctuations in impact velocity were only around 2.8 m/s.

2.4 Impactors of motorcycle helmet system and their effects

Impactors which concerned in this research were the obstacles (Like flat anvil, kerbstone, footpath stage). But due to their variation and effect, initial impact velocity of the helmet system as integrated with the head of the rider during the accident and more on the impact angle of the helmet system also factors and were considered for the investigation. Here were investigations and findings from the reviewed papers regarding to the above considerations.

The objective of the study by ***Gao et al., 2022*** [20] was on the investigation of effect of oblique collision (i.e. impact angle during the accidents) accidents in the motorcycle helmet performance and on head injury. Effect of impact velocity, effect of foam mechanical properties, effect of impact angle, and effect of helmeted head form posture were the variables taken into account in the investigation to address the objective. In order to examine the consequences, the approach of constructing a FE model with LS DYNA was subsequently employed. There was also validation using data from previous experiments. According to the research, a higher impact velocity produces more internal energy, which results in more energy being used to repair damage. The higher the density of the foam liner, the higher the HIP value will be recorded because more damage dissipation energy is produced when the composite shell makes contact with the softer foam liner. As can be observed from the impact angle's effect, impacts with greater angles produce higher HIC and HIP values, indicating that those cases have a direct relationship to the impact angle's inclination value. Although, it appears that the position of the helmeted head has little bearing on how much energy is absorbed and how much is lost as damage in the composite

shell of the helmet. Only 30^0, 45^0, 60^0, and 75^0 oblique angles were taken into consideration in that study. On the other hand, anvil shape and impact site effects, impact velocity and angle effects, and a correlation analysis between head kinematics and biomechanics response were all taken into account during that investigation as stated by ***Zheng et al., 2022*** [22]. The method's flow was based on those parameters, and model validation using standards and experiment values was done using a FE model (LS_ DYNA for parameters and simulations) on the helmet and head. Then impact time 5.2 ms (milliseconds) for peak acceleration transmitted to the head, 5.8 ms for peak contact force between helmet and head, 6.8 ms for peak strain in helmet liner were recorded. As showed by ***Miralbes et al., 2019*** [36], as compared with the standard which was 60^0-60 km/h, the results on the cases 15^0-100 km/h, 30^0-70 km/h, 45^0-40 km/h and 45^0-50 km/h of impact angle and velocity correlation in the inquiry were maximum. The purpose of the work by ***Kongwar et al., 2022*** [23] was to investigate the structural performance of commercial motorcycle helmets using LS_ DYNA. According to the goal, the characteristics that were to be studied included effects from different speeds, effects from different impact angles, structural strength due to energy absorption, HIC, and AIS. The study's workflow involved using the 3D modeling software Solidworks, meshing with hypermesh, and then performing material modeling with LS_DYNA to arrive at the final conclusions. TIS 369-2557 was used to validate the helmet structural model, and the greatest acceleration error was 4.8%.

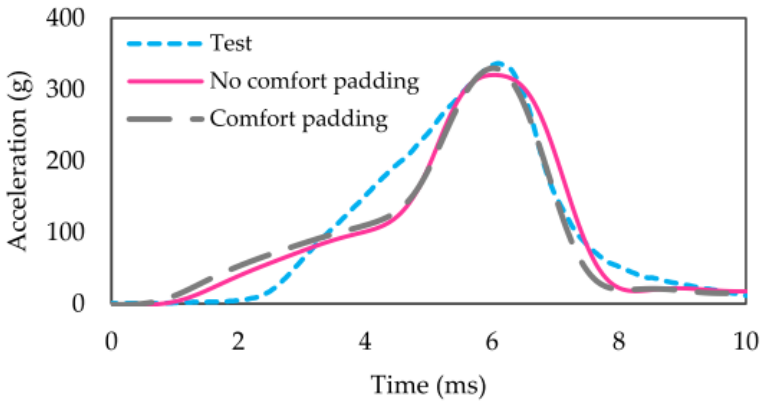

Source: (Kongwat et al., 2022)

Figure 2.3. Relationship between comfort padding and those without comfort padding helmets.

The analysis revealed that comfort padding was used more for the wearer's comfort than for harm prevention. According to this study, the investigated safest impact angle for sharp corners

was 45^0, and at the same time, foam's ability to absorb energy declines as the contact angle of the headform rises. The parameters that were used to investigate the necessary findings were still in range. So, it requires more research on figuring out the consequences of a continuous investigation which can be carried out over a short period of time.

2.5 Research Gaps

Generally, several efforts had been made to explore how to enhance the performance of helmet systems by determining the determinant elements and behavior under the given condition. For instance, as demonstrated in this review part, the effectiveness of the helmet under various material types, impact height, velocity, and crushing conditions had been studied. The impact of material from various size optimization, impact velocity (beyond the stipulated extreme values – for example, the maximum velocity considered was 50 km/h [3]), impact height, and impact angle, however, require further considerations in accordance with the procedures and guidelines for each relevant paper. For the subsequent of those reviewed researches, the gaps which considered in this research were determining the effect of impact velocities up to 60 km/h as per the permitted urban speed limit for light weight vehicle in Ethiopia and the effect of impact angles on the helmet system with in different anvil types using that maximum allowable speed limit.

Chapter Three

3 Materials and Methods

3.1 Materials

As previously noted from literatures, the essential parts from motorcycle safety helmet are its outer shell and inner liner foam. The material types for those components were summarized in the literature section. Then the materials which were used for this research were high computing computers from rail way centers. Since the analysis was numerical, here were the computational tools which were used for the numerical analysis – for the modelling purpose, Solidworks 2022 SP1 30.1.0.82 software; and for the numerical analysis, ANSYS – LS DYNA (HyperMesh 2019.1 – LsDyna (Keyword971_R10.1)) software. For graphing purpose, the Excel also integrated with.

3.2 Methods

The following chart had illustrated the progression of the tasks which were taken into account in this study to investigate the numerical analysis and to in reach the final results.

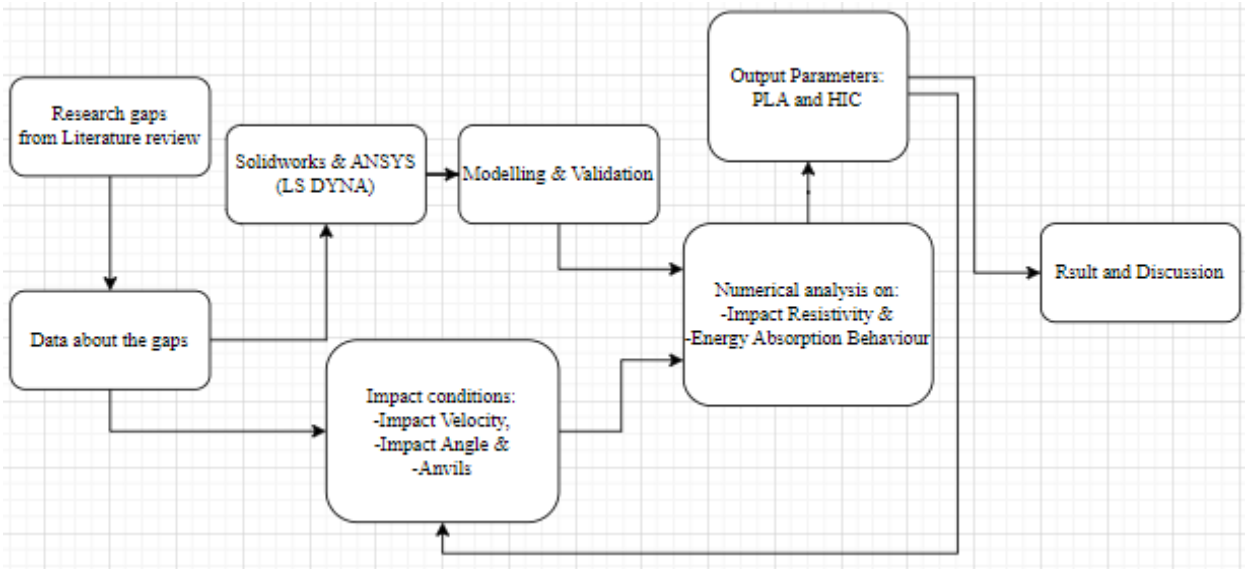

Figure 3.1. Methodological flow of the section.

The selection for standards was depend on the parameters and the responses that considered during the analysis. According to studies on motorcycle helmets, one or more of the standards used to control how well the system works across the world [6]. But for this study endeavor, the ECE 22.05 standard specifications were chosen to look at the defined parameters connected to the standards. This was because the ECE 22.05 standard specification provides the most accurate method for estimating the HIC and assessing the severity of head injuries in case of linear impact [22], [37]. Head Injury Criterion (HIC) is the most criterion for predicting the risk on the riders' head during accidents [26]. Modeling the helmet system in accordance with the selected standard, and then validating the model was followed. The models for the helmet and headform were constructed with the help of Solidworks Software to the desired model and then exported to Ansys Software for further analysis. There were some challenges to select the better one between the following two softwares. Although ABAQUS has it all incorporated, ANSYS depends on its alliance with DYNA for explicit analysis. For novices, ANSYS WB is simpler, but it might be challenging to create meshes that are truly excellent. With the aid of the central difference approach and sophisticated software called LS-DYNA, dynamic analysis of a nonlinear explicit issue may be carried out. Moreover, LS-DYNA offers a selection of material models for modeling, which is appropriate for a helmet structure made up of several materials [23]. And due to its accuracy and capacity to analyze both metallic and non-metallic structures, the FE technique (LS DYNA, ANSYS Software) was here chosen [5], [33]. Here then, the processing of the finite element modeling was follow-up using Ansys 2023 R1 - Ansys LS_DYNA Student in this research study.

For this work, the numerical analyses were done in a dynamic system and an explicit dynamic analysis was considered. That was because the explicit dynamic analysis is considered to extremely short period of impact load action on the system during the accident. Time is the primary distinction between static and dynamic analysis. All we need is static analysis if the load is delivered sufficiently slowly that inertia effects won't be an issue. Vibrations as well as collisions and other rapid occurring circumstances are handled via dynamic analysis (which happens in time). Impact analysis obviously calls for a dynamic strategy. Real dynamic issues may be solved using implicit and explicit methods. There isn't a single one that is better; both are fine. If our analysis involves very slow-moving events, the implicit solver is particularly useful; i.e., when the analysis lasts longer than one second and that nothing jarring happens during that

period. Yet fewer FEA products have an explicit solver. It works well for quickly occurring events (can say faster than 0.1s). The time increment in this case cannot be explicitly defined by the solver; it is set by default. And here the impact load type and mean applied time of the load are the causes of the selection of explicit solver.

Then after numerical analysis were proceed to determine the effect of the impact velocity and angle variation. This is determined on the crashing and deformation response of the shell, the deformation response of the liner foam, the stress distribution on the components, and on the responses of the head (on the bases of head injury criterion-HIC and peak linear acceleration-PLA).

3.2.1 Independent variables (input parameters)

The independent variables which were consider in this research were the impact velocities and impact angles. The impact velocities ranges from 7.5 m/s to 17.5 m/s. Why the minimum value for the impact velocity was 7.5 m/s was due to the specification from standard ECE R22.05 for validation. And also, the maximum value was for including the maximum speed limit of the light weight vehicles in Ethiopia which is 16.67m/s. The range for the impact angle was 0^0 to 90^0. Regarding to the impact velocities, the following speed limit regulations are applied for deriving vehicles in Ethiopia. The specification as indicated in the following table are based on the weight of the vehicle, and related to driving places – urban and/or out-side urban. The vehicle weight which considered in this research was under light weight vehicles. And for this research work, urban with a maximum speed limit of around 16.5 m/s was considered for some investigations.

Table 3.1. Ethiopian Speed Limit for Vehicles

Vehicle Weight	Urban Speed Limit	Out of Urban speed limit
Up to 3.5 tons	60 km/h	100 km/h
3.5 – 7.5 tons	40 km/h	80 km/h
7.5 tons and above	30 km/h	70 km/h

Source: From Ethiopian speed limit law of Art 84 (1) of Regulation No. 208/2011

3.2.2 Dependent variables (Output parameters)

The parameters due the effect of the independent variables are dependent variables. For this research, those dependent variables were the resultant linear acceleration, head injury criterion, and the internal energy which developed with in the helmet system due to the impact load. The other were the positions for the peak linear acceleration and the t_1 and t_2 interval (the interval on which the head injury criterion value recorded) variation due to variable input parameters also showed.

3.2.3 Governing Equations and Metrics for head injury

In the case of the helmet system, the energy conservation during accidents expressed using the internal absorbed energy due to compression, kinetic energy due to motion and shear energy due to sliding of the system on the surface gives the total energy absorbed by the system and dissipated from the system as follow [22]:

$$E_t = E_i + E_k + E_s \quad \text{.....3.1.}$$

In the study by ***Zheng et al., 2022*** [22], in order to evaluate the likelihood of head injuries in various impact situations, a number of kinematics- and biomechanics-based metrics have been developed. Many key head injury metrics are briefly discussed in this section. However, as evidenced by the experiments, the Hybrid III model can only provide kinematic head responses, but the THUMS head model can produce both kinematic and biomechanical head responses. Thus, it is suggested that the THUMS model be employed in research projects to identify brain injuries based on those two measures.

a) Kinematics-based metrics

The head injury may be evaluated using the basic kinematic parameters by utilizing the maximum values of the resulting velocity and acceleration defined as:

$$Z_m = \max\{|Z(t)|\} \quad \text{.....3.2.}$$

Where: the kinematic parameter $Z(t)$ denotes angular velocity $\omega(t)$, translational acceleration $a(t)$ and angular acceleration $\alpha(t)$; and the Z_m is the maximum value of these kinematic parameters.

Following an acceleration-time tolerance curve, also known as the Wayne state tolerance curve (WSTC), the Gadd severity index (GSI) was initially developed in 1966 defined as:

$$GSI = \int a(t)^{2.5} dt \quad \text{.....3.3.}$$

Where $a(t)$ is the resultant acceleration in terms of g's (g = 9.81 m/s^2).

Head Injury Criteria (HIC) and Peak Linear Acceleration values be obtained from the head-form are used to evaluate the protective capabilities of the helmet, but only when the impact load is linear. Head Injury Criterion (HIC) is the most criterion for determining whether motorcyclists may sustain the head injuries or not during accidents. It is most widely used injury criteria where the human head is taken into consideration as the impacted mass for measuring the severity of injury into the skull or brain. The equation 3.4 below is used to calculate HIC based on the highest acceleration experienced during the chosen time interval [23].

And the maximal acceleration that the head form's center of gravity may experience during impact is known as Peak Linear Acceleration (PLA). It is a criterion used to assess if a rider had a head injury in an accident. It has different specification or reference value for different standards. As PLA stands for permissible acceleration of the head form's center of gravity during impact, it is stated by using the multiplication of the gravitational constant g [15].

The dynamic behavior of the protective helmet was greatly influenced by the mechanical characteristics of the shell and foam as well as the impact's velocity [38].

In order to further take into account a temporal average effect during impacts, the GSI developed the HIC (as specified in equation 3.3 above) in 1971. We can calculate the value of the head damage criteria by calculating the linear acceleration of the model's head shape. The HIC's formulation in terms of linear acceleration defined as:

$$HIC = (t_2 - t_1)\left[\frac{1}{t_2 - t_1}\int_{t_1}^{t_2} a_{res}(t)dt\right]^{2.5} \quad \text{.....3.4.}$$

And similarly [39], determining the rotational acceleration to the RIC with in intervals of the time hence RIC, with respect to rotational acceleration, was formulated similarly to HIC by replacing the linear acceleration term with angular acceleration, defined as follows:

$$RIC = (t_2 - t_1)\left[\frac{1}{t_2 - t_1}\int_{t_1}^{t_2} \alpha_{res}(t)dt\right]^{2.5} \quad \text{.....3.5.}$$

The effects of both translational and rotational kinematics were combined in the development of the generalized acceleration model for brain injury threshold (GAMBIT) in 1986, as seen in the following equation:

$$G(t) = \max\{[\left(\frac{a(t)}{a_c}\right)^n + \left(\frac{\alpha(t)}{\alpha_c}\right)^m]^{1/s}\} \quad \text{.....3.6.}$$

where $a(t)$ and $\alpha(t)$ denotes the translational and angular accelerations expressed in g's and rad/s^2, respectively; n, m, and S are empirical constants, a_c and α_c are the limits for a net translational and net angular acceleration, respectively. In line with reference, $n = m = S = 2$, $a_c = 250$ g and $\alpha_c = 25,000$ rad/s^2.

The head injury power (HIP), which takes into account the combined effects of translational and angular acceleration on brain damage, was also proposed in 2000. The HIP with respect to the mass, head-form's moment of inertia and accelerations respectively be given as:

$$HIP = \sum m\, a_i(t) \int a_i(t)dt + \sum I_{ii}\, \alpha_i(t) \int \alpha_i(t)dt \; ; (i = x, y, z) \quad \text{.....3.7.}$$

Where the M is the mass of the head, I_{ii} denotes the principal moments of inertia of the head, and subscript i denotes the anatomical axes ($i = x, y, z$).

The head angular velocities were used to suggest the brain injury criteria (BrIC), which stated in 2013, as shown below:

$$BrIC = [(\frac{\omega_x}{\omega_{xc}})^2 + (\frac{\omega_y}{\omega_{yc}})^2 + (\frac{\omega_z}{\omega_{zc}})^2]^{1/2} \quad \text{.....3.8.}$$

Where ω_x, ω_y and ω_z are the head angular velocities in three orthogonal directions, and ω_{xc}, ω_{yc} and ω_{zc} are the corresponding directionally dependent critical values.

b) Biomechanics-based metrics

The basic measures used as biomechanical metrics for head injury prediction typically include major principal strain (ε_p), shear strain (ε_s), von Mises stress (σ_{vm}), and intracranial pressure (ICP) in the brain. The head FE models were also used to propose a number of component-level injury measurements, including the cumulative strain damage measure (CSDM), dilatation damage measure (DDM), and relative motion damage measure (RMDM). It should be highlighted that FE simulations may be used to determine the basic biomechanical parameters.

But here in this study the kinematics-based metrics of PLA and HIC were considered for the investigations. The following table illustrates the specifications of the models and the threshold parameters which supports for the analysis. As showed in the selected standard, the kinematic based metrics which was considered in this research work were presented in the following table.

Table 3.2. Summary of kinematic based metrics.

Standards	Head form sizes	Assembly weight	Criteria and range
ECE 22.05	A	3.1	$t_2 - t_1 \leq 36$ ms;
	E	4.1	
	J	4.7	PLA $\leq$ 275g;
	M	5.6	
	O	6	HIC $\leq$ 2400

Source: (Nations & Committee, 2020)

3.3 Modeling

In researches, the method of modeling determined by different ways. As one, optical measurement system with a three-dimensional (3D) capability was used to scan helmets that were purchased from a commercial vendor in Taiwan [14]. In order to create a 3D model of each helmet, eight scans were conducted at 45^0 intervals. Using Geomagic Studio software, eight scans were combined into a single 3D model. Using SolidWorks software, the dimensions of the helmet and solid components in the 3D model were established. Finally, ABAQUS software was used to convert the 3D model to a finite element (FE) format. Since they act as stress raisers and thus affect the mechanical response of the helmet, the small holes in the inner and outer surfaces of the helmet (such as those used for visor or chin strap attachment purposes) were left in the models. To make the modeling process simpler, features like air vents and plate surfaces that are only used for aerodynamics and styling were left out.

For this research work, the models of the helmet and headform were adopted from CAD (computer aided design [24]) files and resized using Solidworks Software with respect to ECE

standards. Then it was imported to ANSYS software for validation and further analysis. For each headform type the minimum size was specified on figure 3.2 [40] and the details are presented in Appendix 2 (Table one and two).

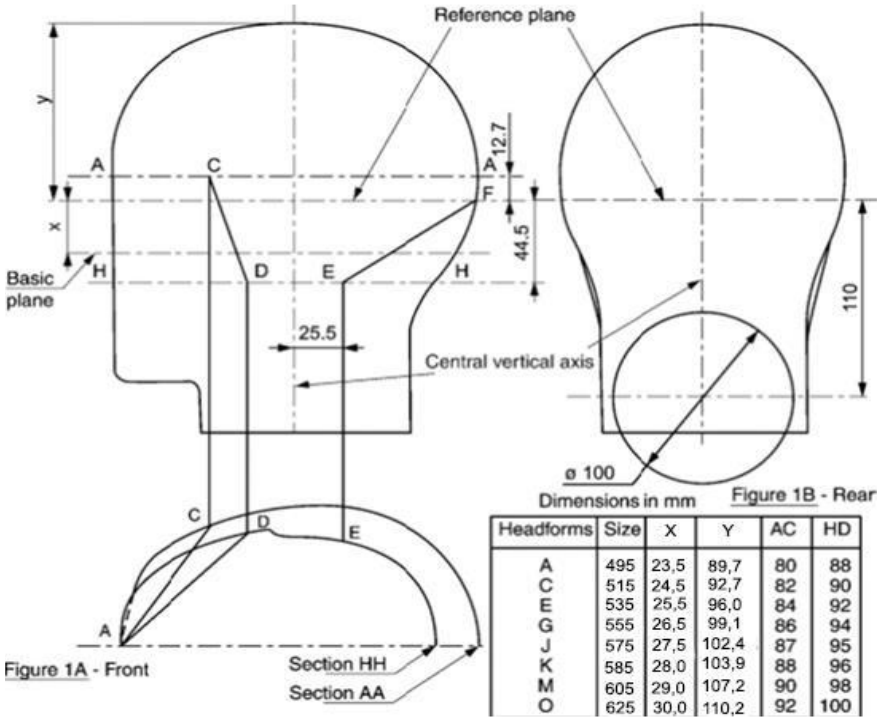

Headforms	Size	X	Y	AC	HD
A	495	23,5	89,7	80	88
C	515	24,5	92,7	82	90
E	535	25,5	96,0	84	92
G	555	26,5	99,1	86	94
J	575	27,5	102,4	87	95
K	585	28,0	103,9	88	96
M	605	29,0	107,2	90	98
O	625	30,0	110,2	92	100

Source: (Nations & Committee, 2020)

Figure 3.2. Diagram and minimum size of the headform.

3.3.1 Finite Element Modelling

As stated before, an exterior impact load distributing shell, an energy-absorbing lining, a chin pad, and a chin strap make up the helmet model [39]. But for this research, only the two, impact resistive and energy absorbing parts, which are the shell and liner foam, were considered. But the face shield and comfort pads of the helmet were not taken into account in this study as their negligible effect on the energy absorption of the helmet system during accidents [26]. And therefore, the analysis was done on the headform as integrated with those selected helmet components. Figure 3.3 below shows the positions of impacts which were considered in the analysis – front (B), crown (P), rear (R) and lateral (S/X) [21].

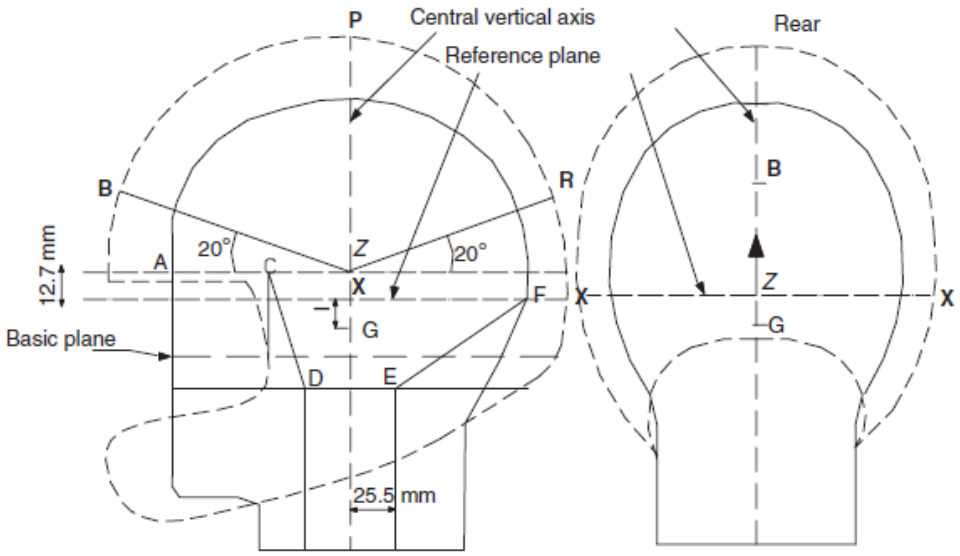

Source: (Aiello et al., 2007)

Figure 3.3. Identification of impact points.

There were also considerations on the directions of the motion in addition to impact positions to determine the effect of impact angle variation on the helmet system as shown in figure 3.4 [23].

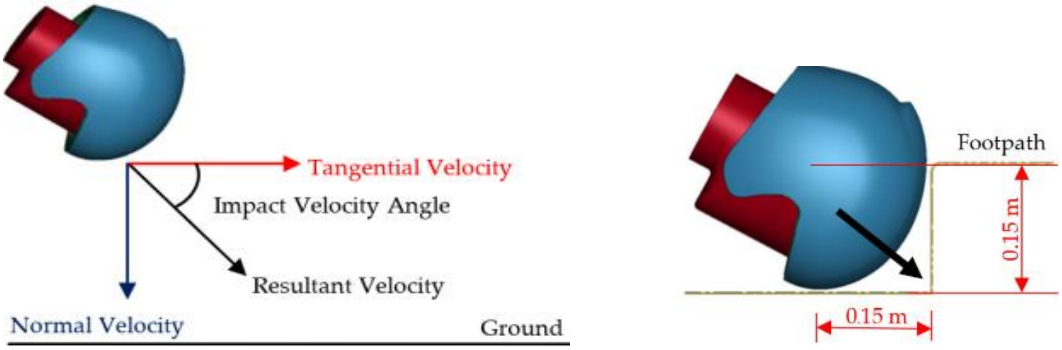

Source: (Kongwat et al., 2022)

a b

Figure 3.4. Impact angel variation when collusion with flat anvil (a) and with footpath (b).

Accidents may happen everywhere by any time; the place where the helmet fall on is an impactor or anvil. The geometry of the impactors for flat anvil and kerbstone were shown in figure 3.5 below [21].

Source: (Aiello et al., 2007)

Figure 3.5. Geometries of the Impactors.

The models for this research, which were the headform, liner foam, helmet shell, and their assemblies considering the respective impact positions, were presented in the Appendixes (Appendix 1) of this document.

3.3.2 Numerical Procedures in Hypermesh Ls – Dyna Software

The model was imported in the IGES file format from the Solidworks software following the load, boundary condition specification and numerical analysis with help of ***Hypermesh 2019.1 – LsDyna (Keyword971_R10.1)*** software.

Conditions that considered in the analysis

Materials were assigned for each component; in the case of boundary conditions - lower part of the anvil was fixed, and surface contact of upper surface of anvil with external surface of helmet (contact automatic surface to surface), internal surface of helmet with outer surface of liner foam (contact tie nodes to surface), inner surface of liner foam with head form (contact automatic surface to surface) with the static and dynamic frictional coefficients of 0.3 and 0.2 respectively were applied for the analysis [22]. The loading system for the investigations were impact angles and impact velocity during accidents.

Contact Conditions

General automated contact type components were used to implement the contact surfaces of the helmet types. There were multipoint, tie, and contact limitations in the 3D dynamic FE models.

Moreover, only a parallel motion may occur between the contact surfaces. And also, interpenetration was avoided by using automated surface-to-surface contact choices between the EPS foam liner and the ABS shell, between the foam and the headform model as well as between the shell and the anvil. Between the outer shell and the foam liner as well as between the foam liner and the headform, a static and dynamic friction coefficient of 0.3 & 0.2 respectively were assigned [15].

The contact conditions that considered in this simulation - one is *CONTACT_ AUTOMATIC_ SURFACE_ TO_ SURFACE for the component head form to the inner surface of the component liner foam and also the outer surface of the component helmet shell to the flat anvil. The reason for the selection of this type of contact was that there be surface contact gap between the respective components before the deformation due the accidents.

And the second was *CONTACT_ TIED_ NODES_ TO_ SURFACE for the outer surface of the component liner foam to that of the inner surface of the component helmet shell. This was because of the initial tie contact construction between the liner foam and the helmet shell components in the motorcycle helmet system.

3.3.3 Mesh convergence test

Mesh convergence profile of the model was done by considering the peak linear acceleration on the components during the impact simulation. The trend was made by starting some value of element size which was relatively coarse (maximum value of 15 mm) to relatively fine element size (minimum value of 4 mm) as shown in Table 3.3.

Table 3.3. Change in Peak Linear Acceleration value with element size.

Element Size (mm)	*Number of Nodes*	*Number of Elements*	*Peak Linear Acceleration*
15	7355	29452	487
14	8698	35443	474
13	10539	43391	397
12	12454	51714	418
11	15163	62437	387
10	17407	72804	391
9	21560	91010	389
8	29157	121260	351
7	32513	163189	338
6	***47142***	***204363***	***334***
5	71178	313364	329
4	122391	551749	334

But as shown in the following figure, the profile of the graph became relatively constant after the element size with value of 7 mm and below. So, for each of the remaining analysis, the minimum number of elements was considered were 204,363; and the maximum element size was 6 mm.

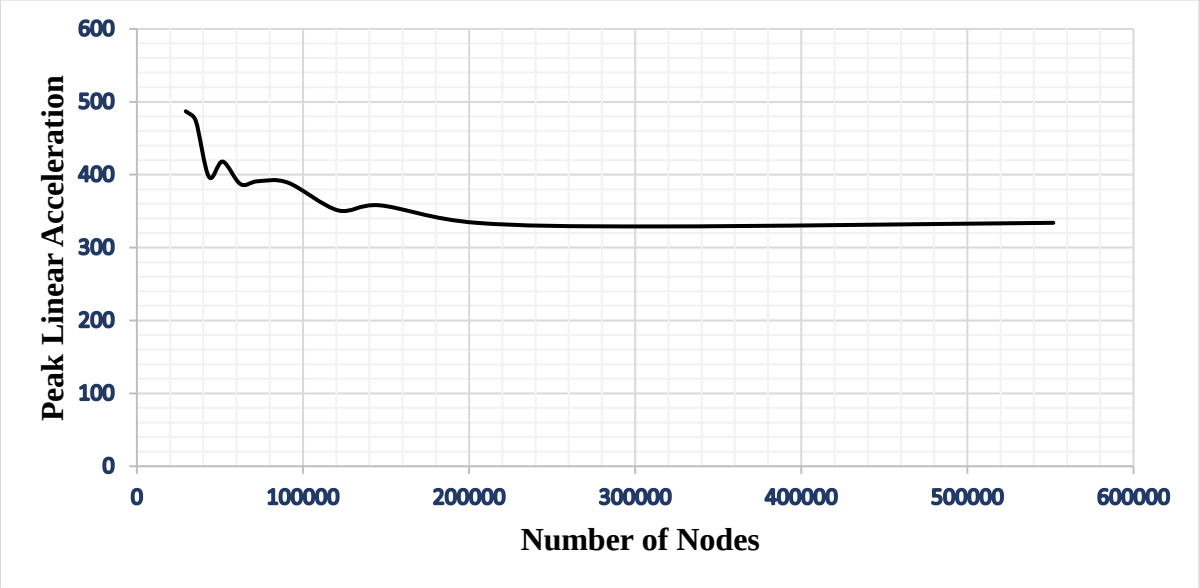

Figure 3.6. Mesh Convergence Profile.

- Stress distribution on the components of the helmet system

To disperse most of the penetrating impact load to the helmet system, the shell (figure 3.7a) component of the helmet system is constructed from stiffer materials. On the other hand, materials with a high capacity to absorb most of the impact energy during an accident are used to make the liner foam (figure 3.7b) [10], [11]. And then the stress load which in reach in the head form (figure 3.7c), as much as the performance of the two components, are minimized [12].

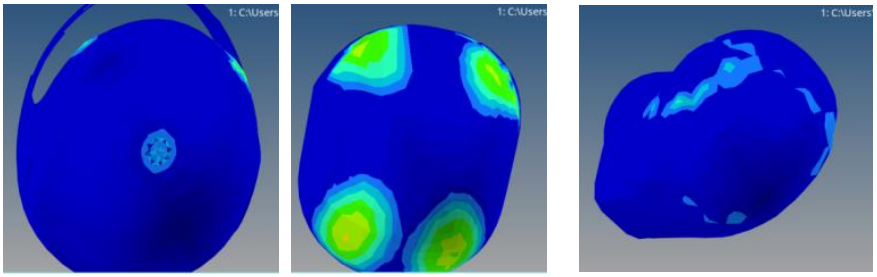

a b c

Figure 3.7. Stress load distribution on the components.

As shown in figure 3.8, at the starting time of the impact the energy was only the kinetic energy (the energy that a body possesses because it is in motion) and then during the initial impact it starts to decreased to a minimum of 16.5J with in the duration of about 0.57 milliseconds which was the compression interval. The maximum amount of the kinetic energy converted to internal energy and some of the rest, but minimum amount, converted to interface (the energy created between two sliding surfaces) and hourglass energies during that compression time. After the maximum peak value of the internal energy of the system, the rebounce of the system started and the kinetic energy came back in some range. Those energies are reported using *DATABASE_ GLSTATE.

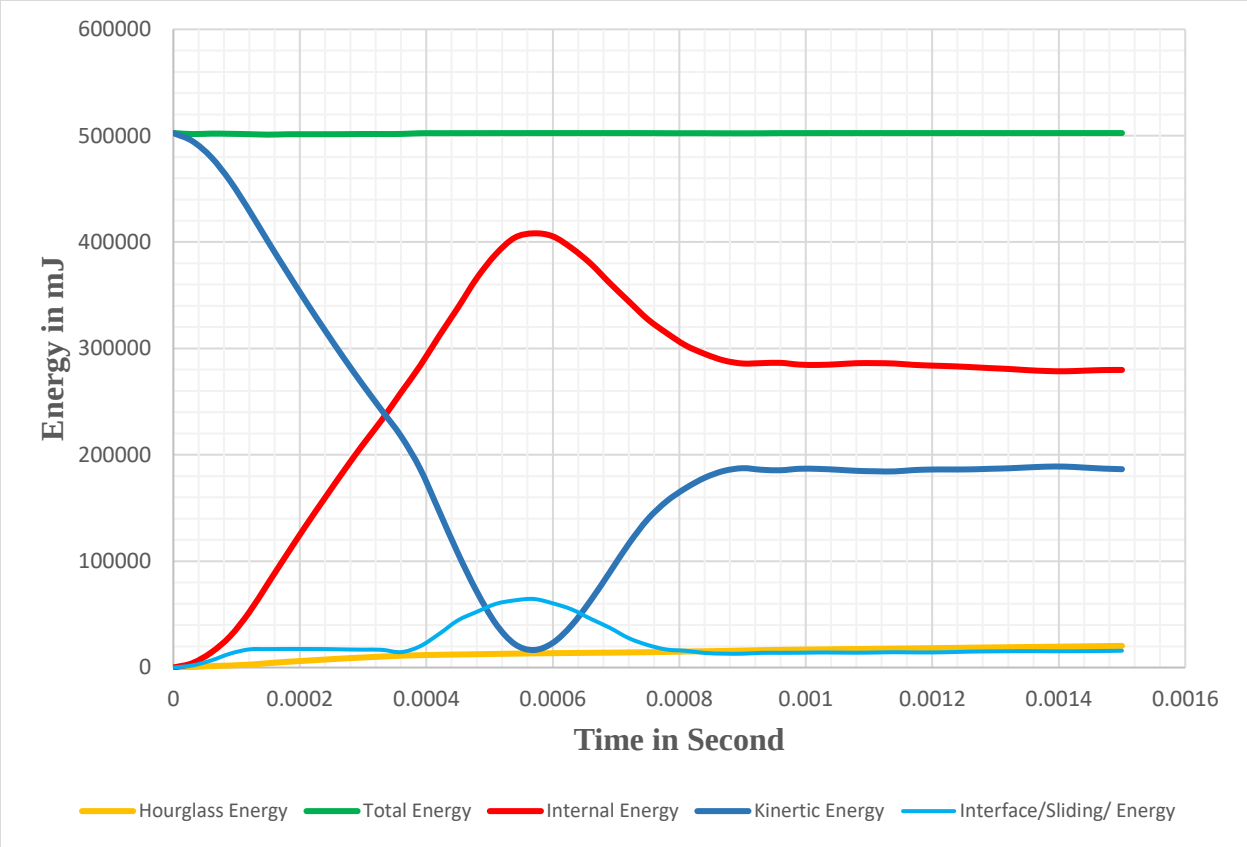

Figure 3.8. Energy balance of the helmet system.

3.4 Validation of the Model System

For validation, the value of accelerations transmitted to the head and HIC values that were simulated using numerical analysis and experimental investigations were considered. There were expectations on degrees of agreement between all generated acceleration curves and HIC values with their corresponding experimental findings. The helmet model models were be validated against the standard drop impact tests before they were used for further studies. By following ECE 22.05, five different impact points, located at the front (B), rear (R), crown (P) and lateral (left and right, both in S) positions, were defined to crash onto different rigid anvils to assess the helmet performance.

In this study, two standard drop tests (i.e., front/rear impact to flat anvil) at an initial impact velocity of 7.5 m/s were carried out to validate the accuracy of the helmet and helmeted head models [22]. As per the previous studies, the head model was a rigid Hybrid III and it was

developed by Livermore Technology Corporation. The model consists the skin and skull layers. But in this study, the model was solid and done by the help of Solidworks Software as stated in the modeling section.

Meanwhile, the model for this study was symmetrical. So, there was a need to use symmetrical sections to reduce the computing time during numerical analysis. The headform and helmet's symmetry plane were where the impact velocity assigned on. On the symmetry plane of the headform, both the headform and the helmet have the same initial velocity (as discussed above). The anvil's top surface and the inclinations of the impact velocity were what determine the impact angle, which was set to be for the simulation [20]. Depending on the selected impact positions and the reaction analysis, the results were recorded in Table 3.4. Those of investigated peak linear acceleration and head injury criteria values were exhibiting a reasonably good agreement with the corresponding values of previously made experimental and numerical analysis counterparts. The model was validated hence the percent error value were not more than the acceptable limit. For more, both the peak linear acceleration (PLA) and Head Injury Criterion (HIC) were summarized in Table 3.4.

Table 3.4 Peak Linear Acceleration and Head Injury Criteria of drop impacts.

Drop impact tests	Metrics	Experiment	Model Simulation	Error (%)
Front impact effect on flat anvil as stated by ***Zheng et al., 2022*** [22]*)*	PLA	219g	217g	-0.91
	HIC	1989	2146	7.89
From the investigation of this work	*PLA*	*...*	*199g*	*-9.1*
	HIC		*1927*	*-3.11*
Rear impact effect on flat anvil as stated by ***Zheng et al., 2022*** [22])	PLA	236g	242g	2.54
	HIC	2236	2299	2.95
From the investigation of this work	*PLA*	*...*	*251g*	*6.35%*
	HIC		*2416*	*8.01%*

Chapter Four

4 Result and Discussion

4.1 Results

4.1.1 Results of effects of impact velocities

In this sub-section, the results due to the variation of impact velocities were presented. The material for the liner component of the helmet was elastic material.

A. Effect of impact velocities on position B (front position)

Here were results of the numerical investigations for front impact position (B) – Stress distribution (MPa) and Resultant Linear Acceleration (RLA) in m/s^2 when using elastic material type as a liner foam.

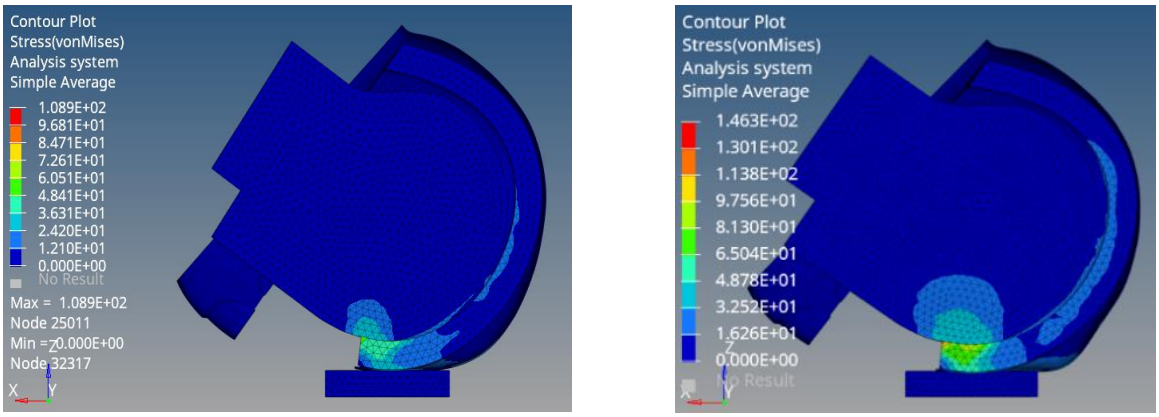

a b

Figure 4.1. Stress distribution on the system at 7.5 m/s (a) and 17.5 m/s (b) respectively.

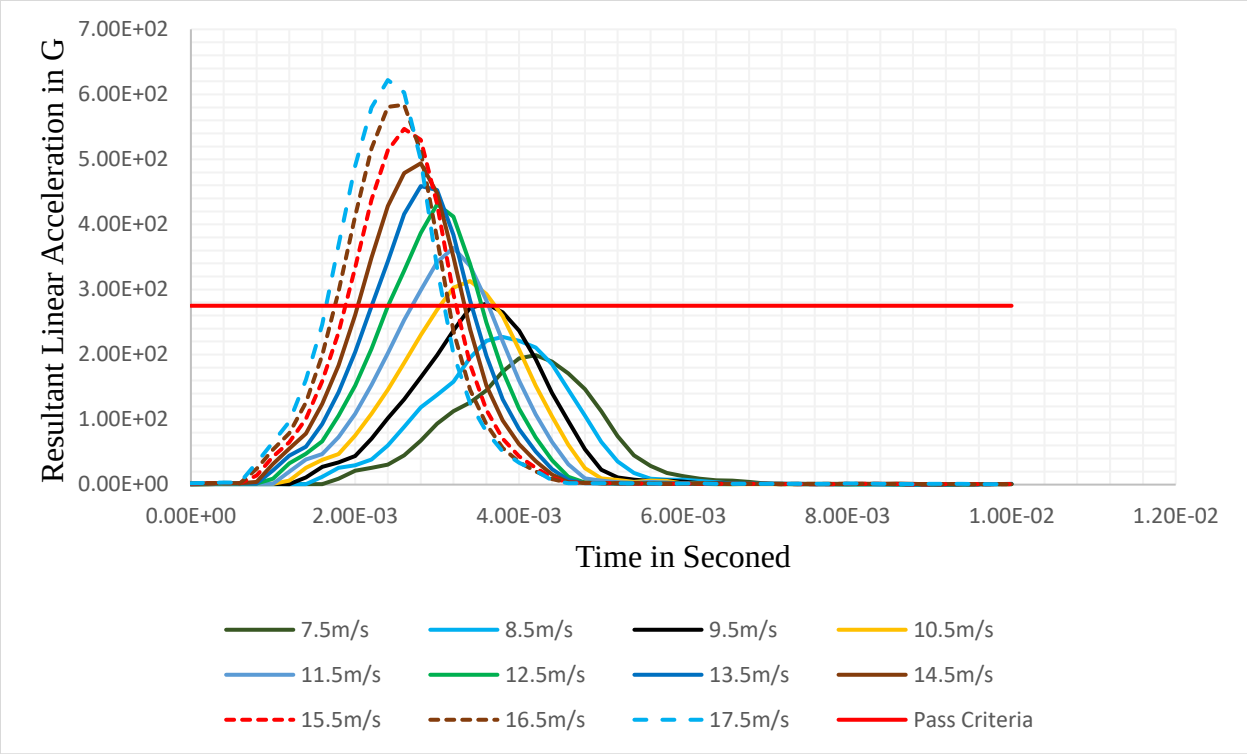

Figure 4.2. RLA on front impact at different impact velocities.

B. Effect of impact velocity on position R

Here were result values of stress distribution (MPa), and RLA (m/s^2) of motorcycle helmet system for rear impact position (R). The results for RLA (m/s^2) for different velocities were also presented in figure 4.4 below.

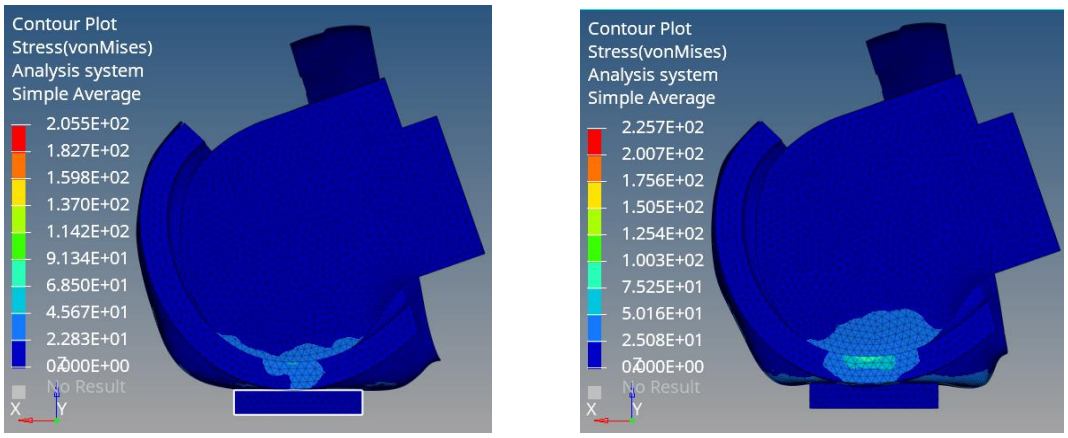

a b

Figure 4.3. Stress distribution values at 7.5 m/s (a) and 17.5 m/s (b) respectively.

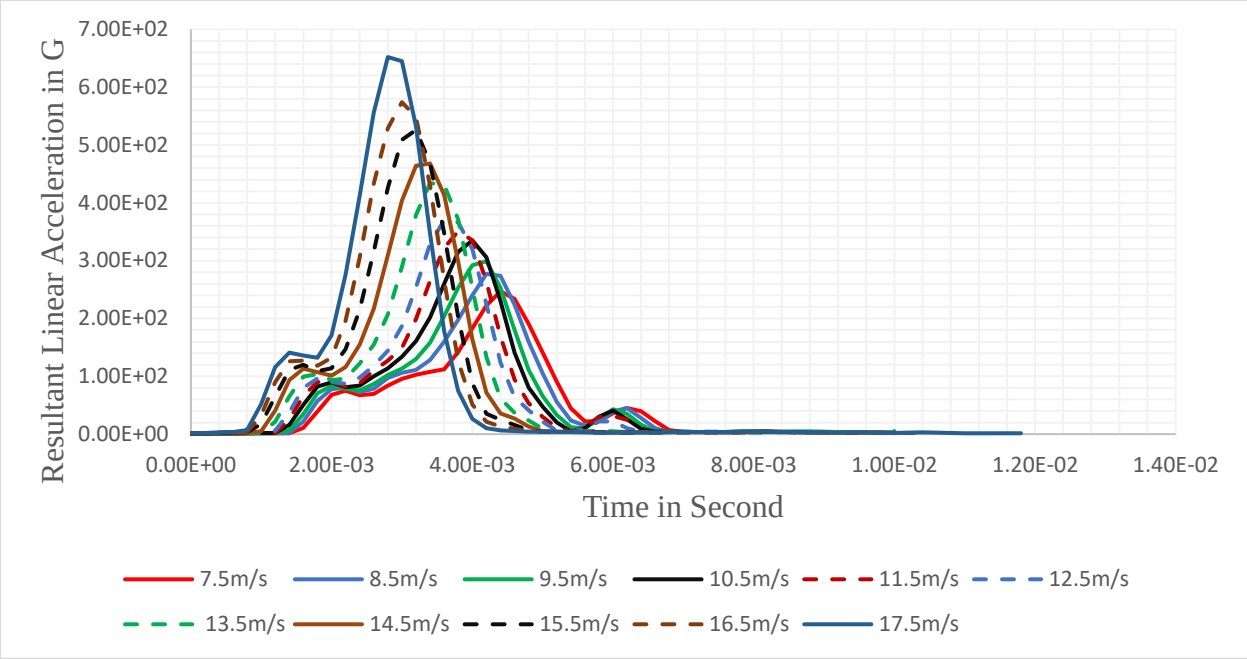

Figure 4.4. RLA values for rear impact position at different impact velocities.

C. Effect of impact velocity on impact position P

Here were result values of stress distribution (MPa), and RLA (m/s^2) of motorcycle helmet system for crown impact position (P). The results for RLA (m/s^2) of crown impact position for different velocities were also presented below.

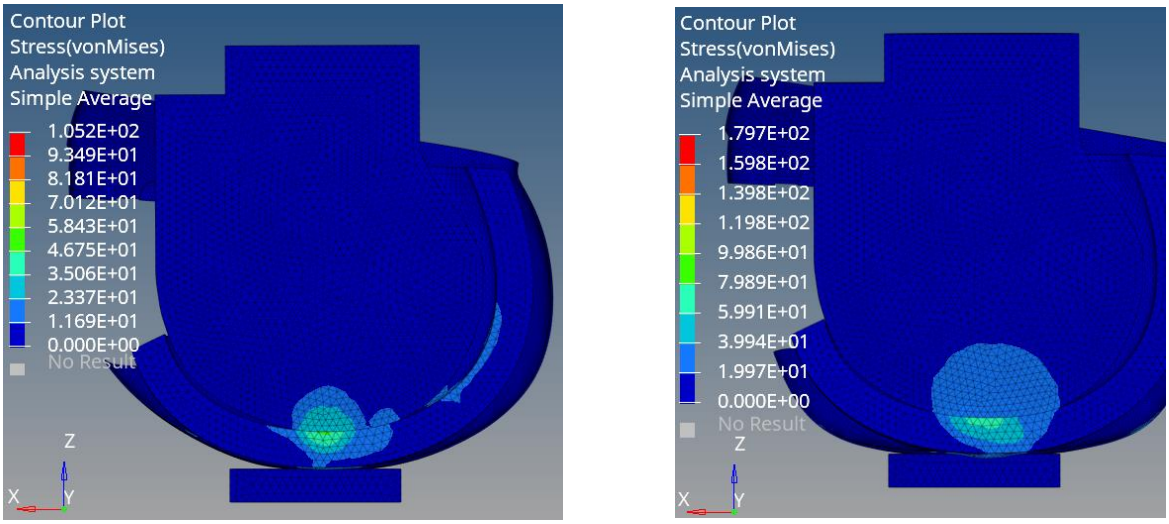

a b

Figure 4.5. Stress distribution values at 7.5 m/s (a) and 17.5 m/s (b) respectively.

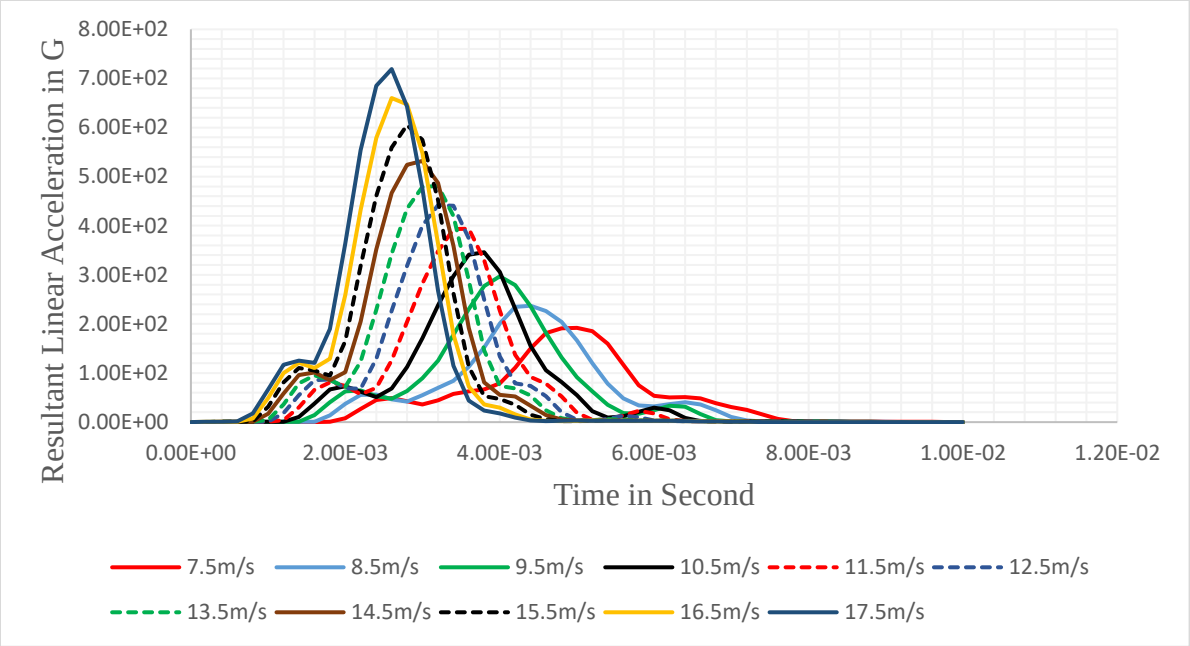

Figure 4.6. RLA values for crown impact position at different impact velocities.

D. Effect of impact velocity on impact position S

Here were result values of stress distribution (MPa), and RLA (m/s^2) of motorcycle helmet system for lateral impact position (S). The results for RLA (m/s^2) for different impact velocities on lateral position were also presented in figure 4.8 below.

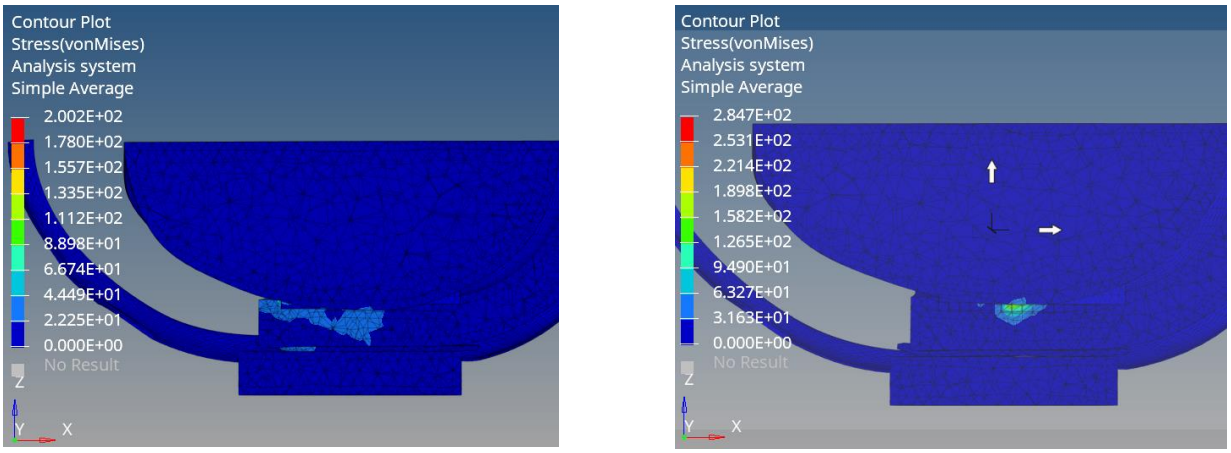

a b

Figure 4.7. Stress distribution values at 7.5 m/s (a) and 17.5 m/s (b) respectively.

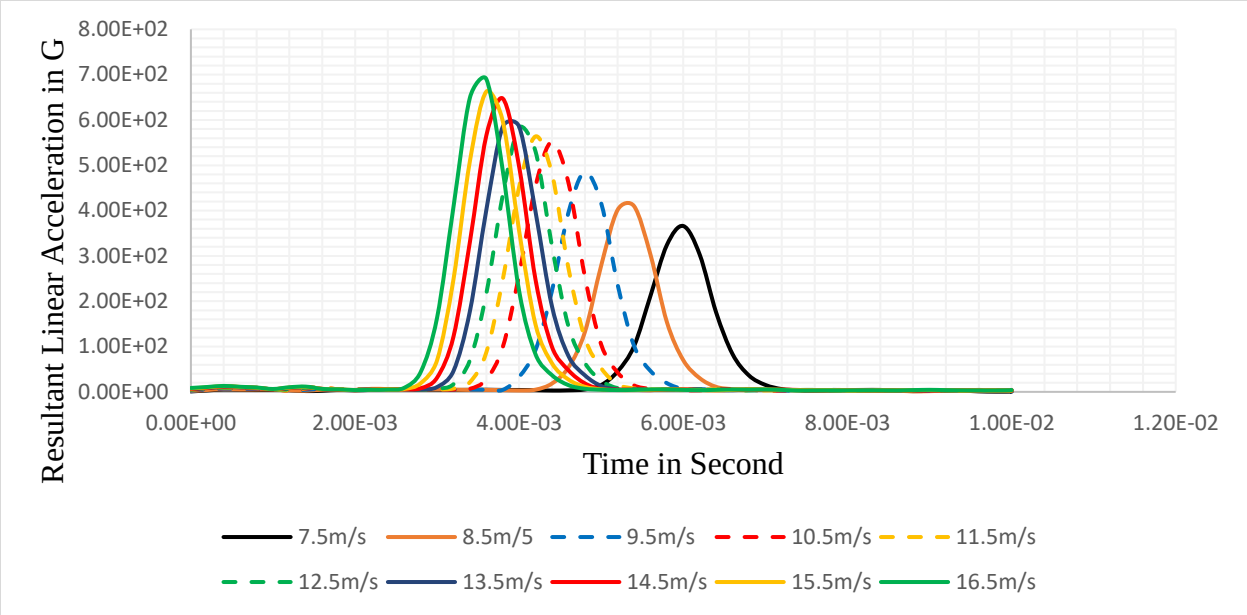

Figure 4.8. RLA values for lateral impact position at different impact velocities.

In the following figure (figure 4.9), comparisons between effect of impact velocity at 16.5 m/s for those of four impact positions were displayed.

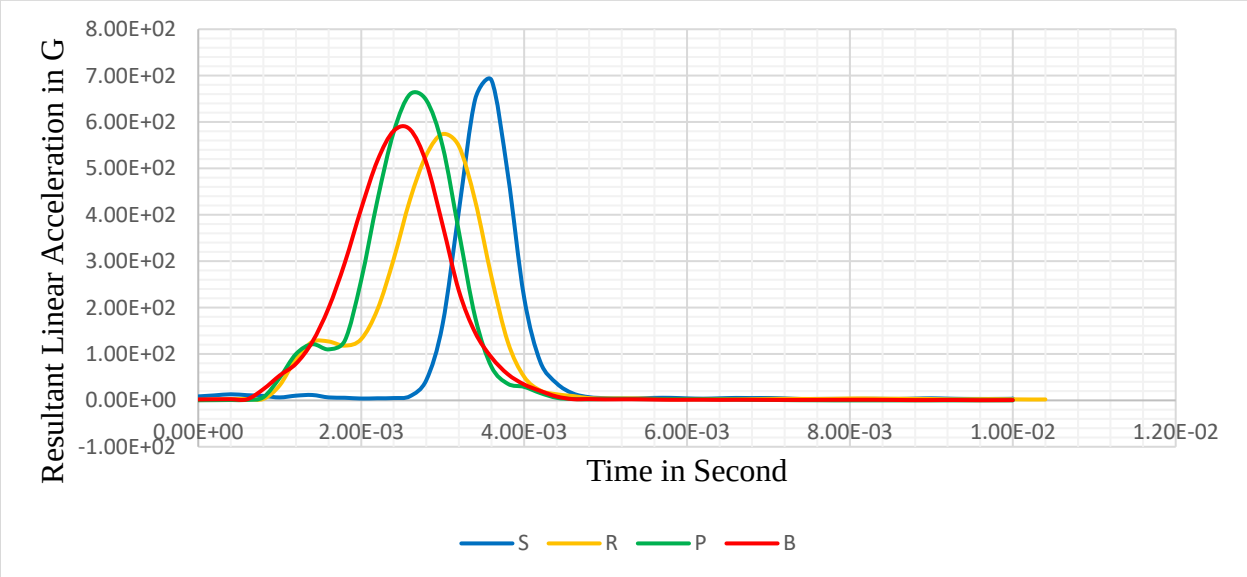

Figure 4.9. RLA difference between lateral, rear, crown and front impact positions.

4.1.2 Energy absorption of the helmet system

Here were results of internal energies from the investigation considering the elastic liner foam material for the liner component of the helmet system. The results were extracted from each of the given impact positions at different impact velocities as shown from figure 4.10 to figure 4.13.

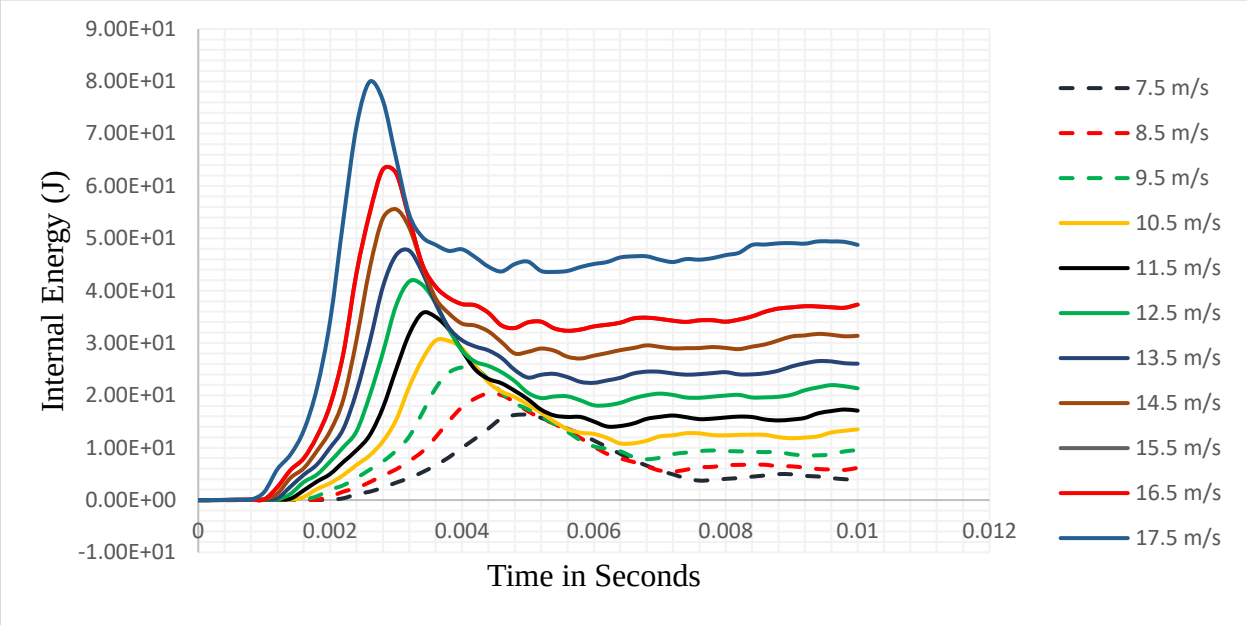

Figure 4.10. Internal energy values for crown impact position at different impact velocities.

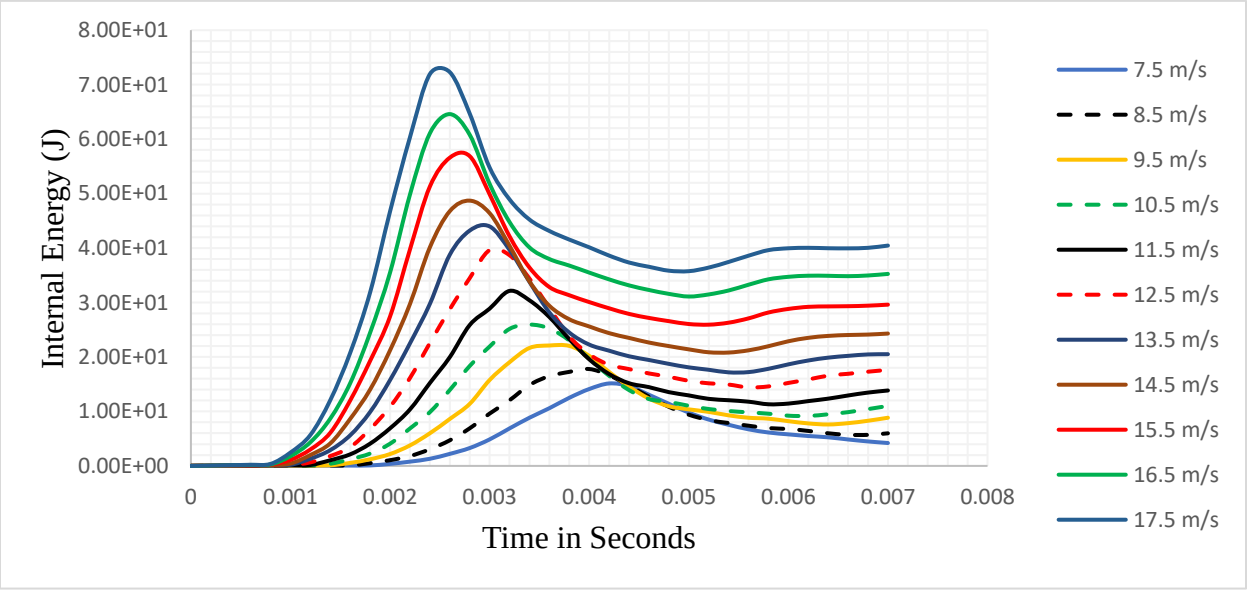

Figure 4.11. Internal energy values for front impact position at different impact velocities.

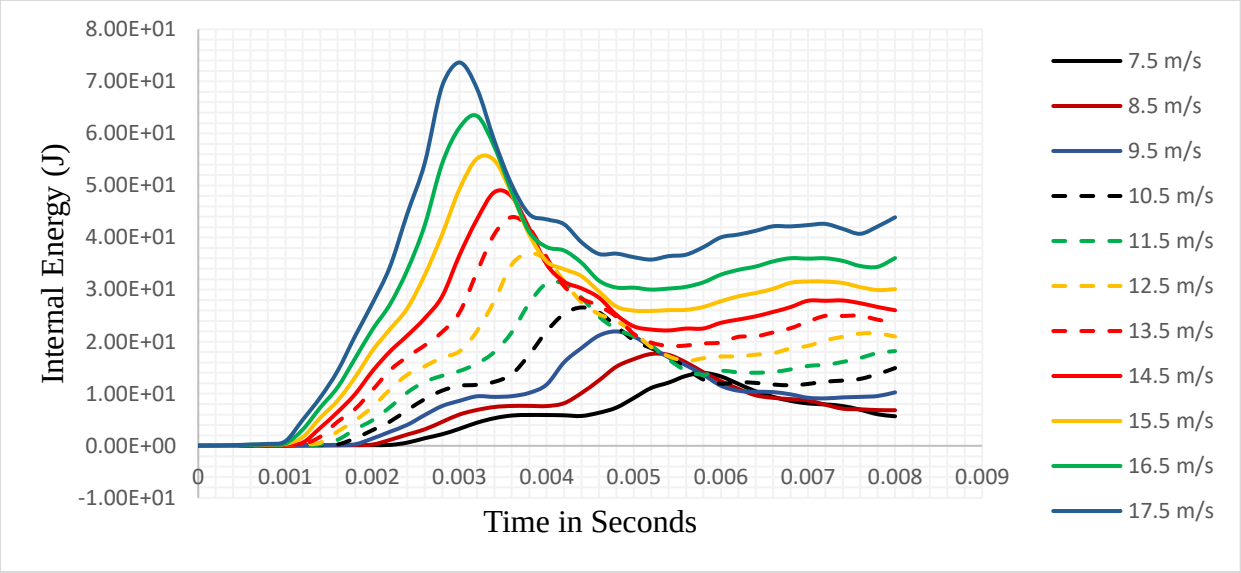

Figure 4.12. Internal energy values for rear impact position at different impact velocities.

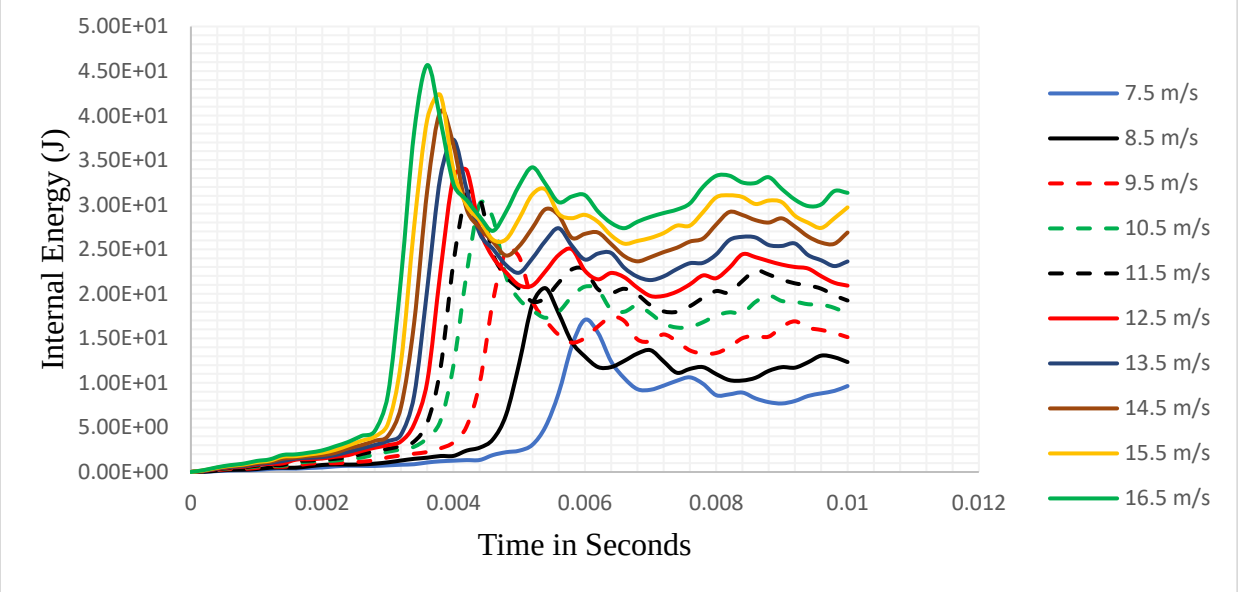

Figure 4.13. Internal energy values for lateral impact position at different impact velocities.

The comparison for those of the internal energies which developed in the helmet system regarding with the impact positions at the impact velocity of 16.5 m/s were presented on figure 4.14 below.

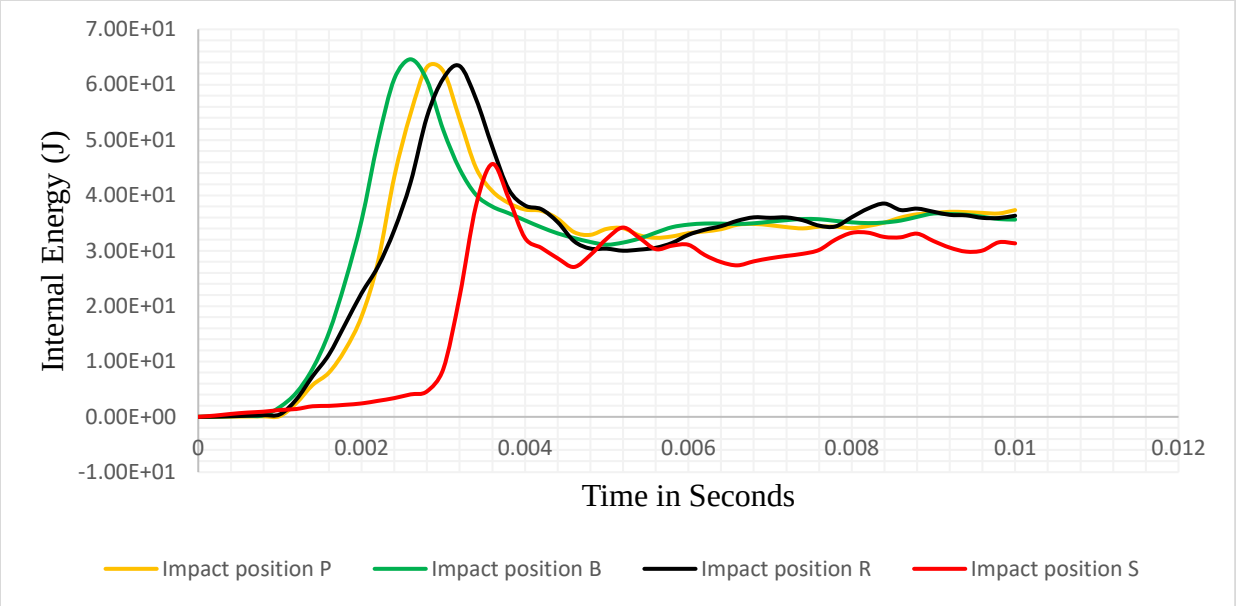

Figure 4.14. Internal energy difference impact positions at 16.5 m/s.

4.1.3 Results from elastic and crushable liner foam materials

The following figures (figure 4.15 – figure 4.18) show the differences of peak linear acceleration values between using elastic material and crushable foam material for liner helmet components. And the pass criterion which is 275G also presented.

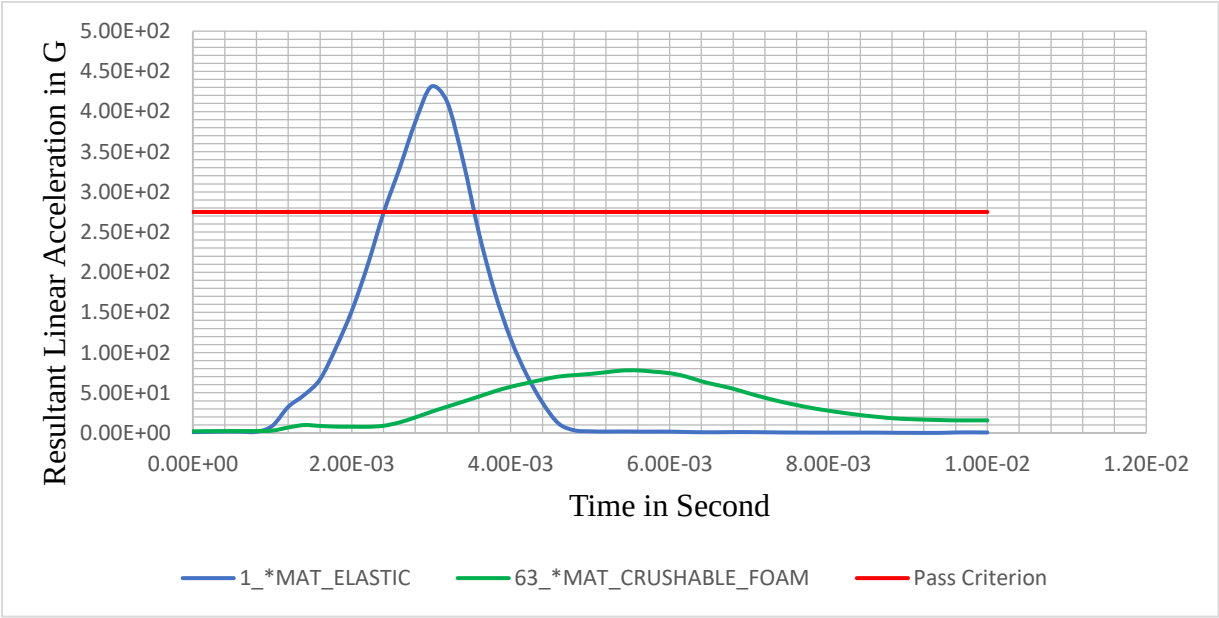

Figure 4.15. For front (B) impact position at 12.5 m/s.

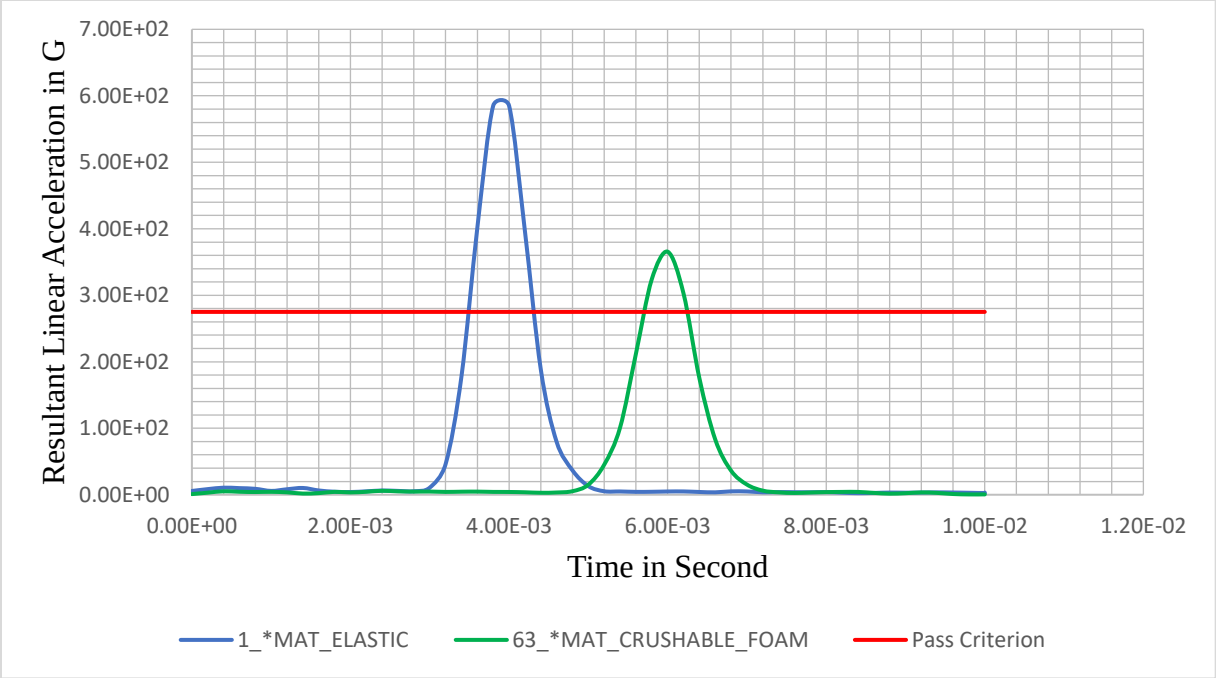

Figure 4.16. For lateral (S) impact position at 13.5 m/s.

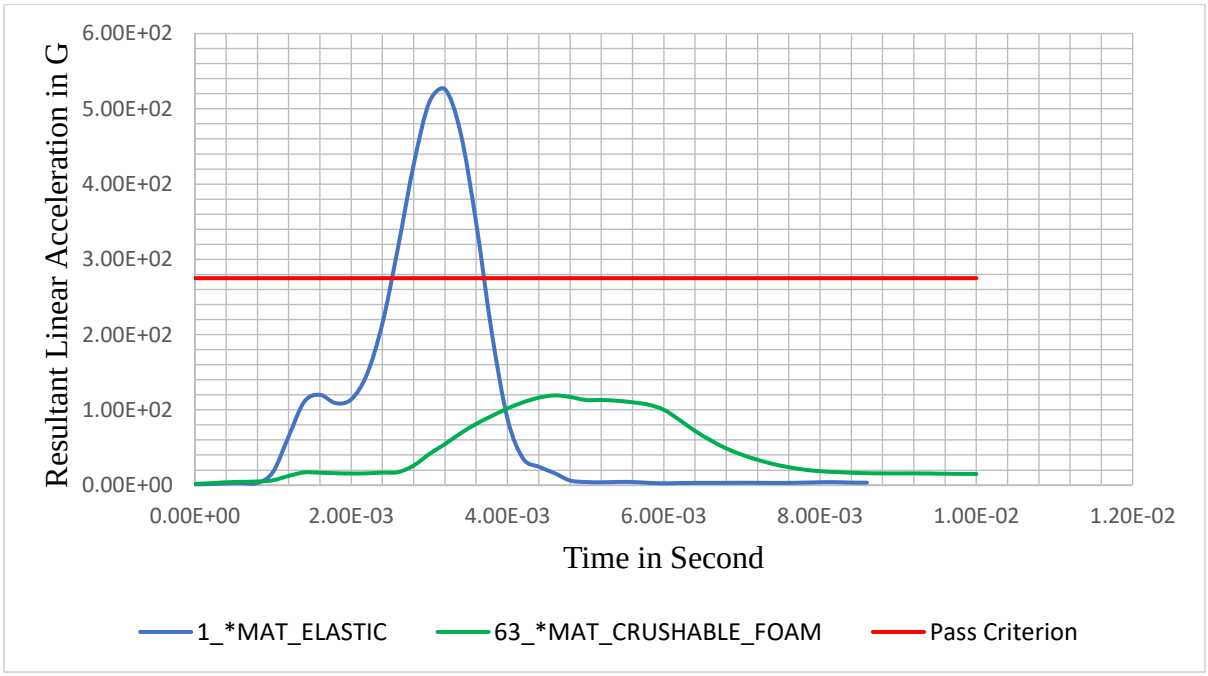

Figure 4.17. For rear (R) impact position at 15.5 m/s.

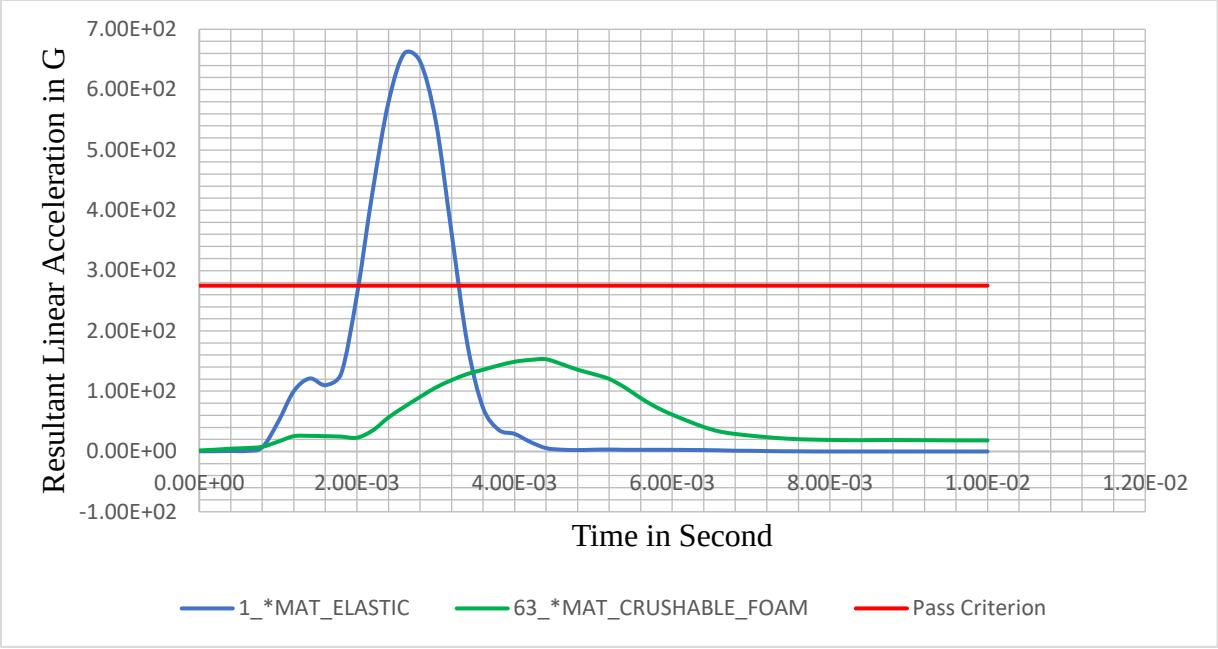

Figure 4.18. For crown (P) impact position at 16.5 m/s.

The following figures, figure 4.19a and figure 4.19b show the extent of deformation at 3 ms and figure 4.19c shows the differences of energy distribution values between using elastic material and crushable foam material for liner helmet components. The results were investigated considering the crown impact position at 16.5 m/s.

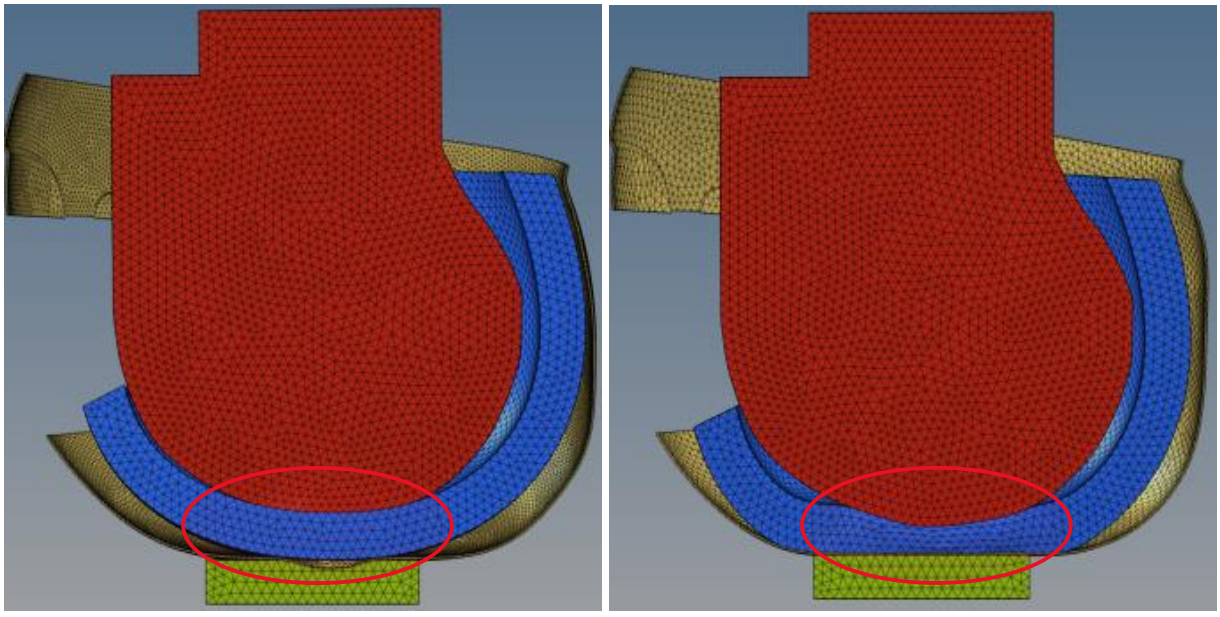

a. Elastic Liner Foam

b. Crushable Liner Foam

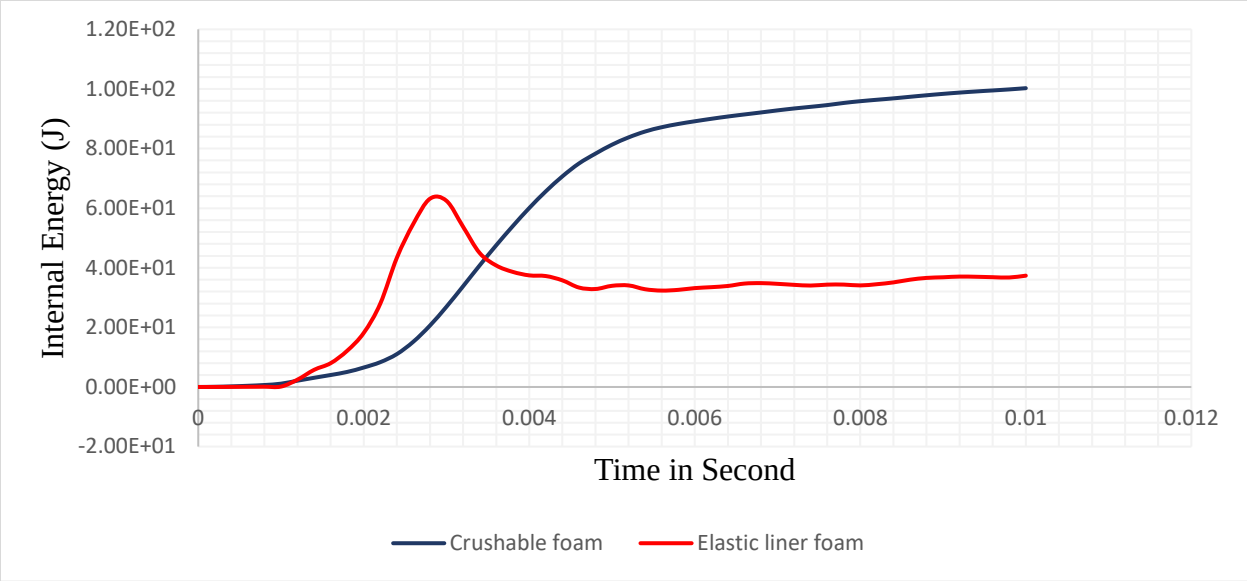

c.

Figure 4.19. Energy absorption capacity of materials for crown impact position at 16.5 m/s.

4.1.4 Results from thickness difference of crushable liner foam

The following result represents the extent of the value change in the output parameters with respect to the change in the liner thickness for the lateral impact position.

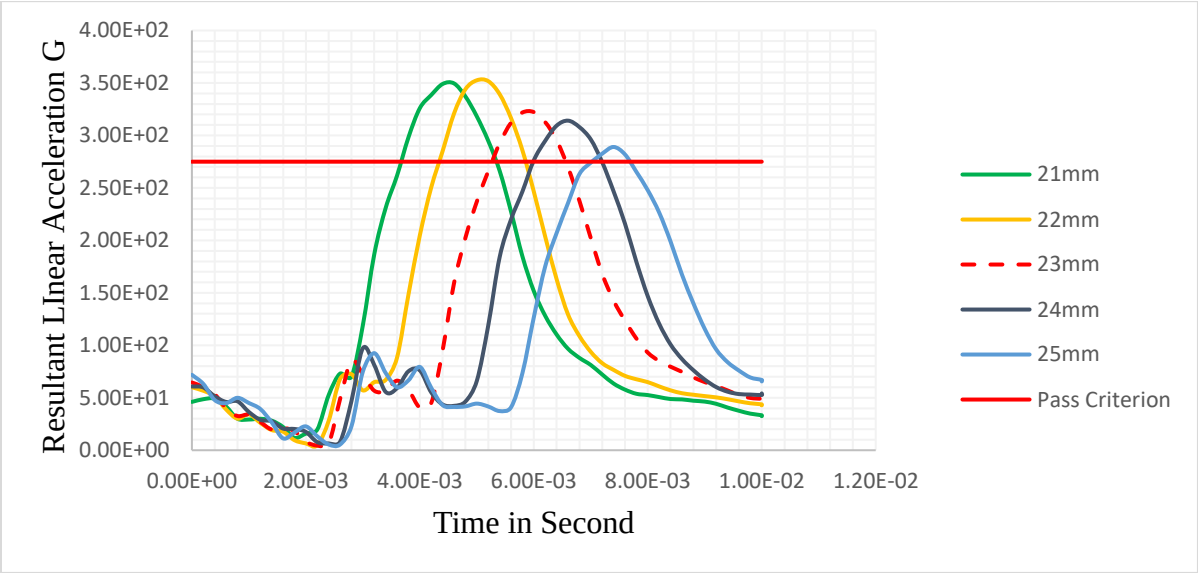

Figure 4.20. Effects of liner thickness of crushable foam at 13.5 m/s on lateral impact position.

4.1.5 Effect of liner thickness difference for energy absorption

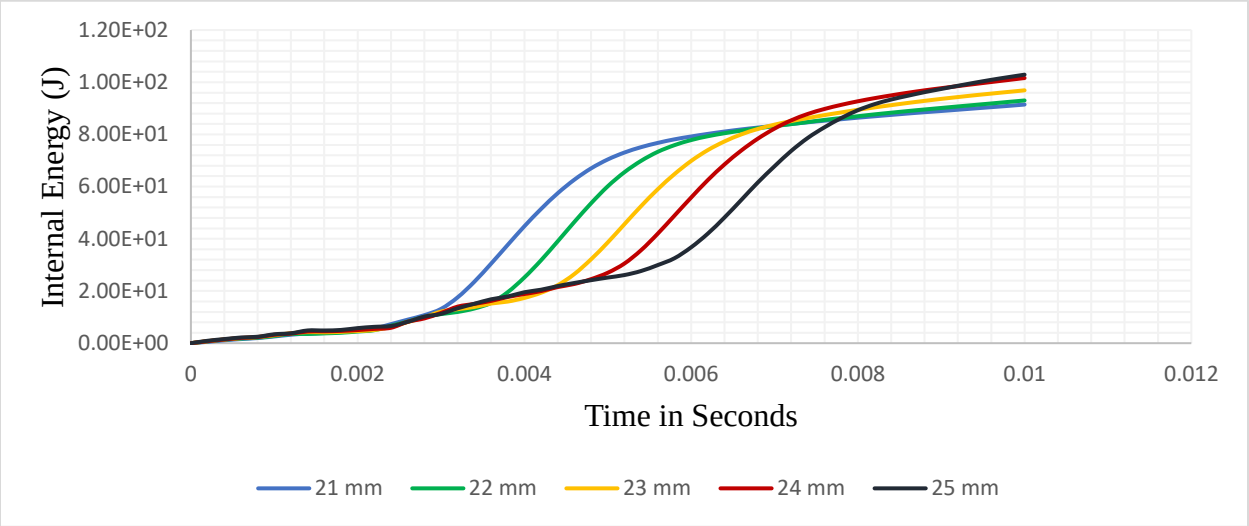

Figure 4.21. Liner thickness of crushable foam at 13.5 m/s on lateral impact position.

4.1.6 Results of impact angles' effect on flat anvil impactor

The following results, from figure 4.22 to figure 4.25, were presented on the effect of impact angle considering crushable foam as a liner foam and the impactor as a flat anvil impactor.

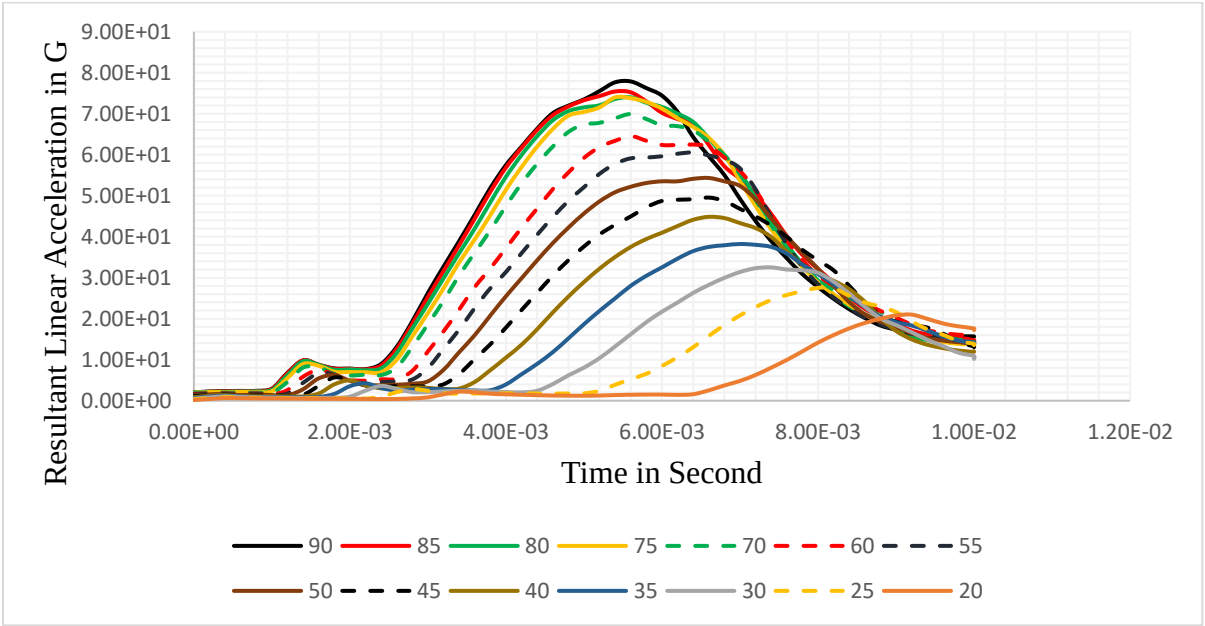

Figure 4.22. Effects of impact angles from 90^0 to 20^0 at 12.5 m/s on front impact position.

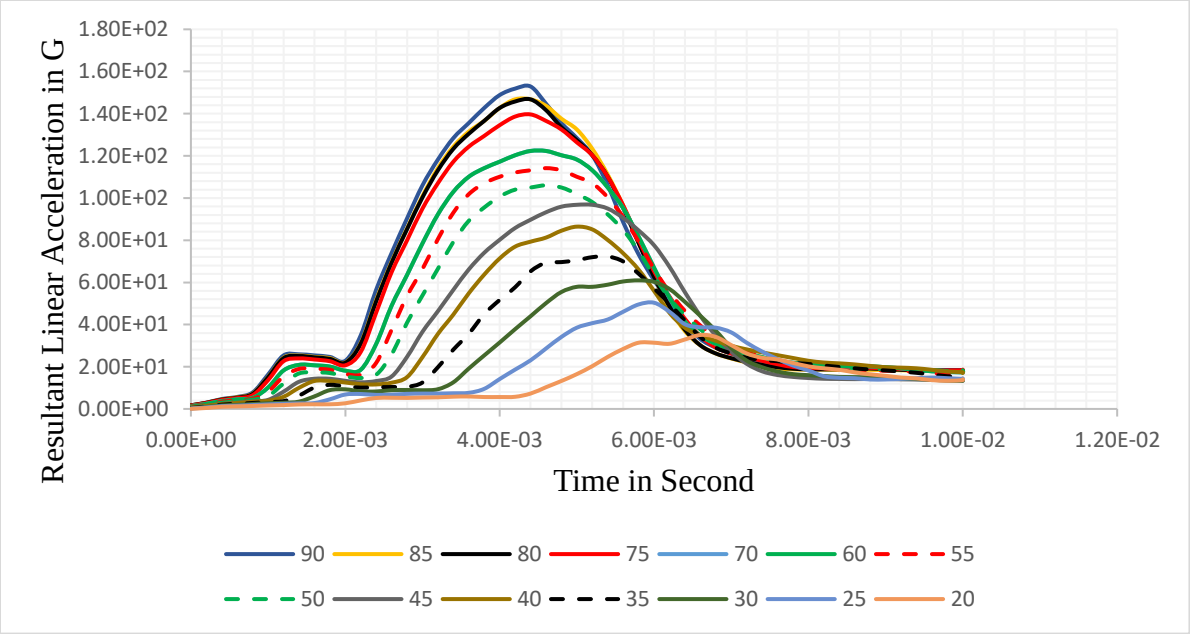

Figure 4.23. Effects of impact angles from 90^0 to 20^0 at 16.5 m/s on crown impact position.

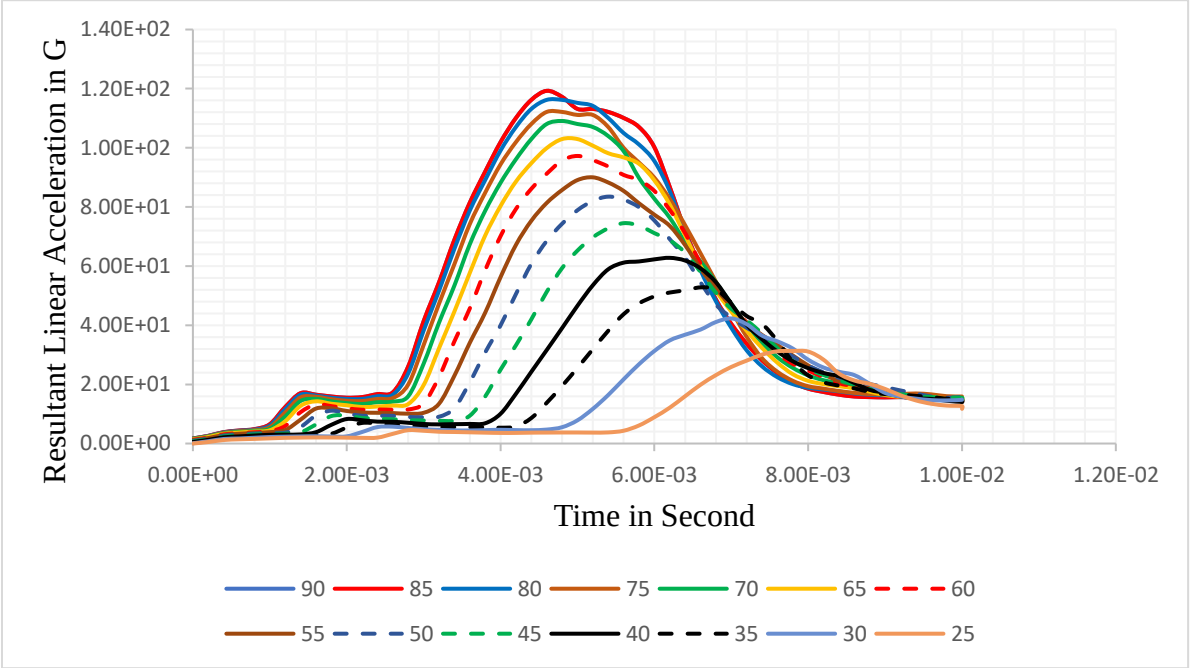

Figure 4.24. Effects of impact angles from 90^0 to 25^0 at 15.5 m/s on rear impact position.

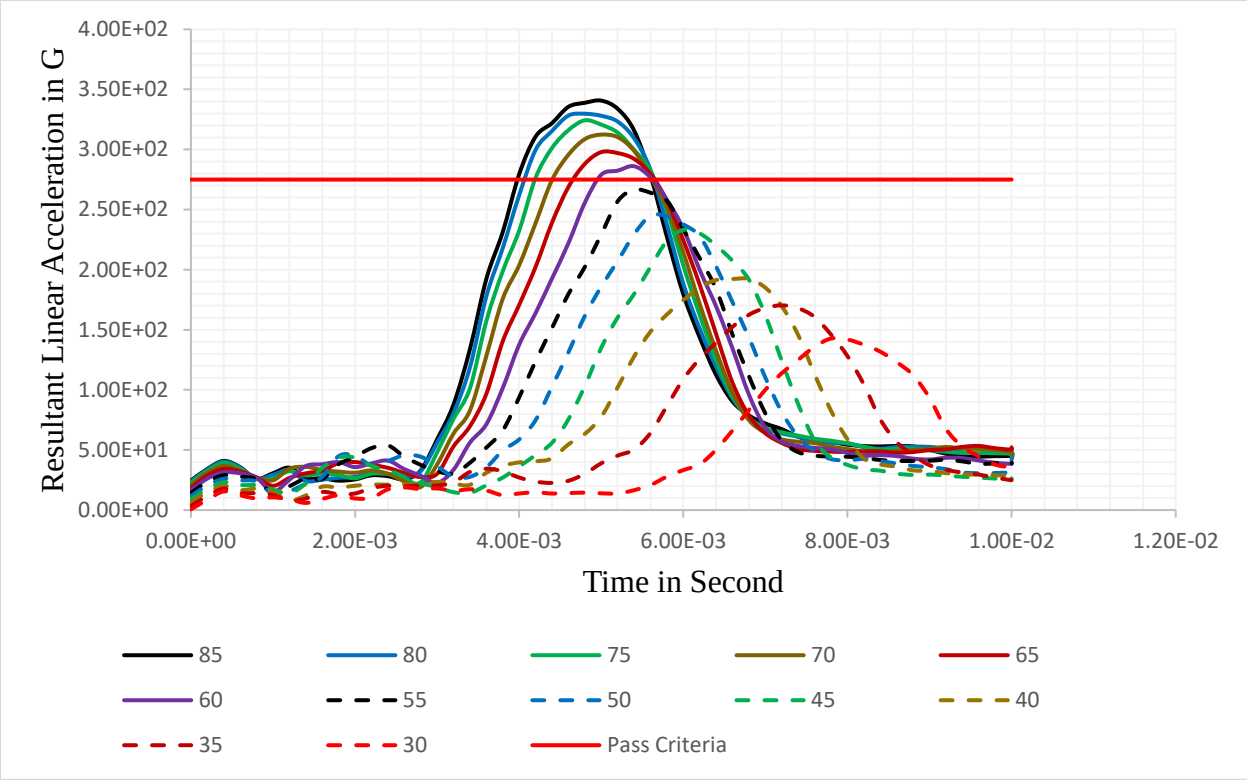

Figure 4.25. Effects of impact angles from 90^0 to 30^0 at 13.5 m/s on lateral impact position.

4.1.7 Energy absorption of crushable liner foam

Here were results of the energies distribution (total energies, internal energies and kinetic energies) from the investigation considering the crushable liner foam material for the liner component of the helmet system. The results were extracted from each of the given impact positions at different impact velocities as shown from figure 4.26 to figure 4.29.

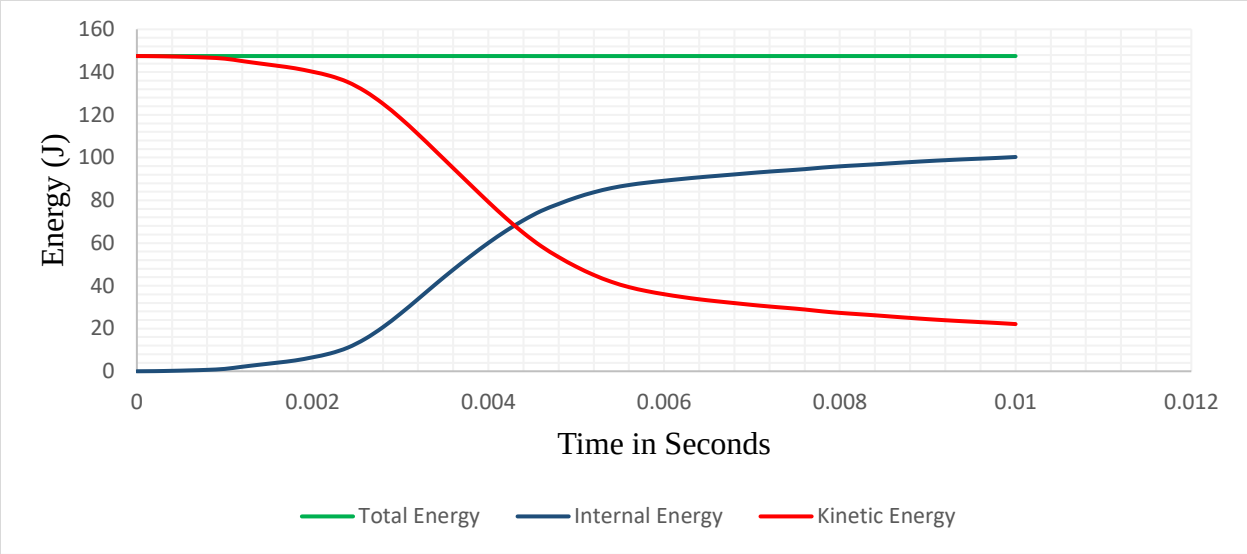

Figure 4.26. Energy distribution at 16.5 m/s on crown impact position.

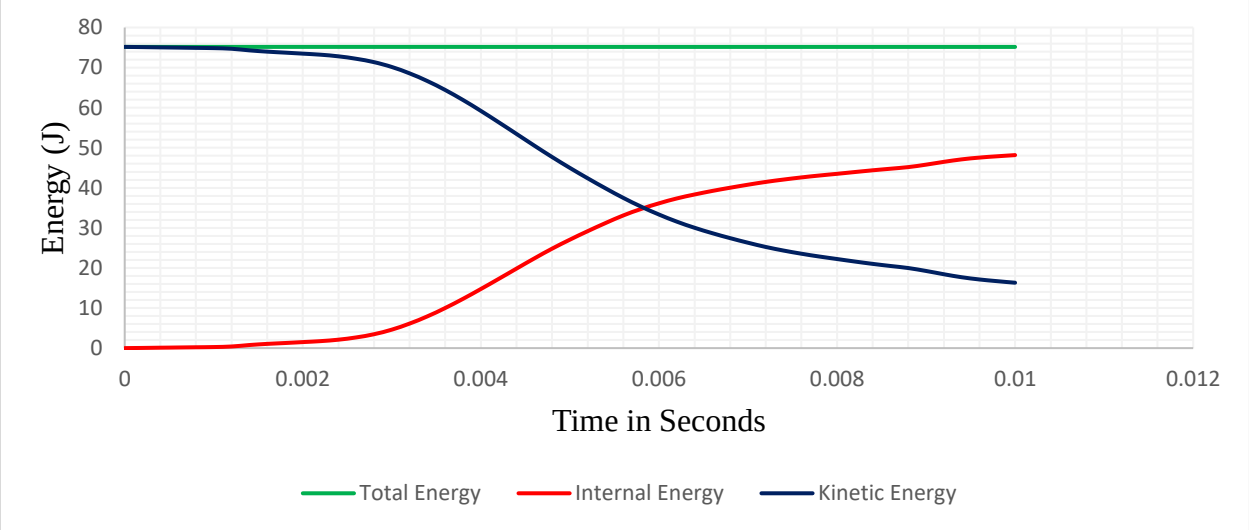

Figure 4.27. Energy distribution at 12.5 m/s on front impact position.

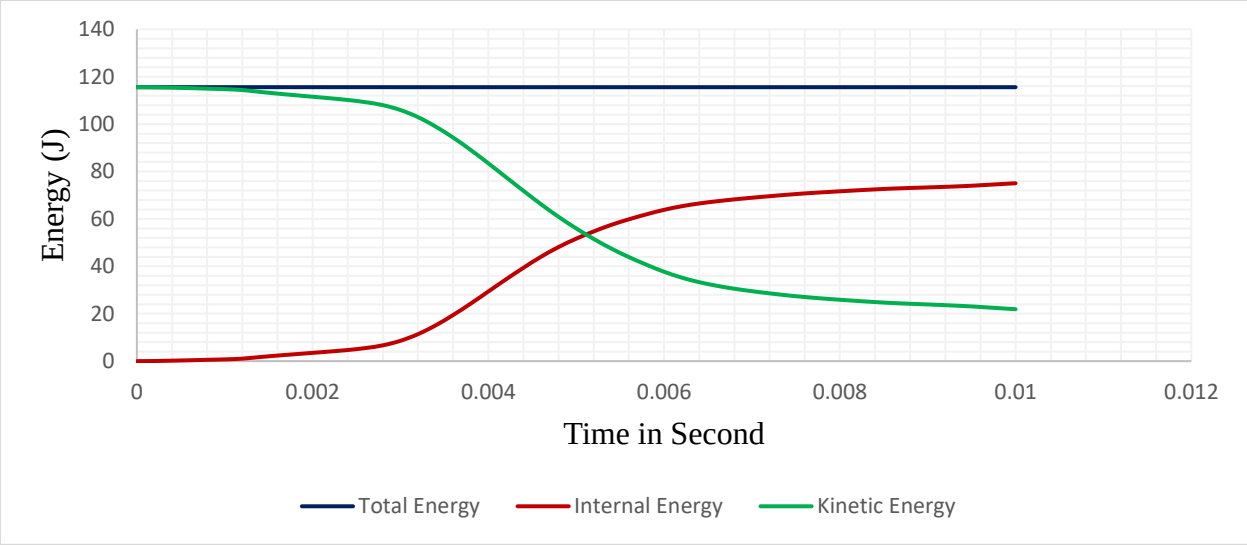

Figure 4.28. Energy distribution at 15.5 m/s on rear impact position.

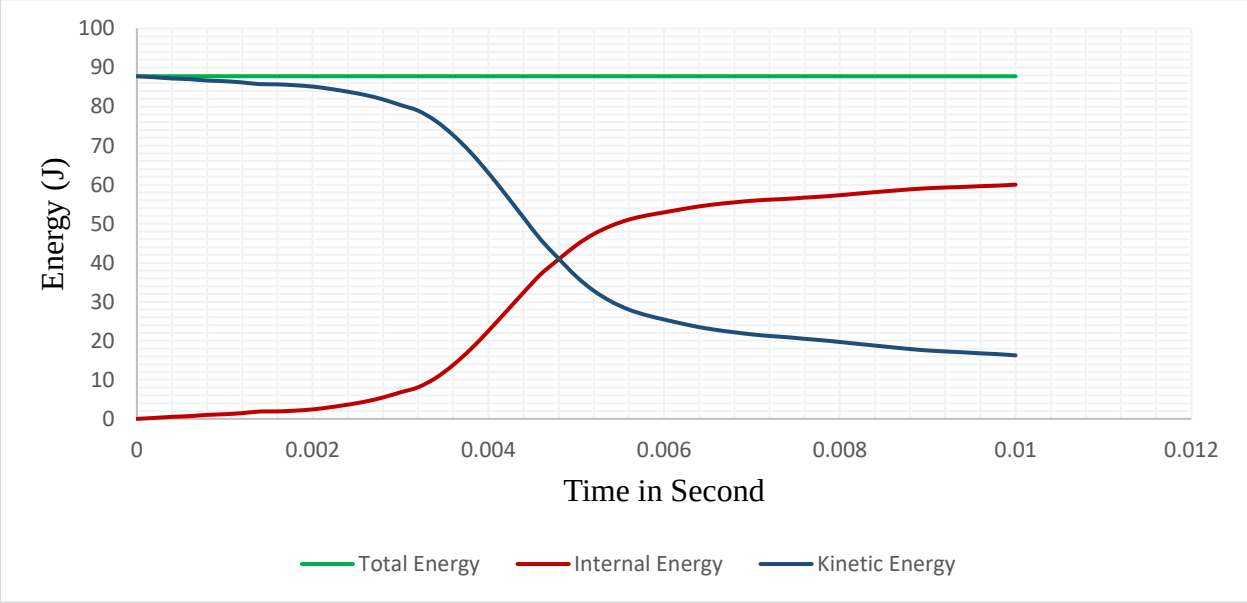

Figure 4.29. Energy distribution at 13.5 m/s on lateral impact position.

Here were results of internal energies from the investigation considering the crushable liner foam material for the liner component of the helmet system. The results were extracted from the crown impact positions at different impact velocities as shown from figure 4.30 below.

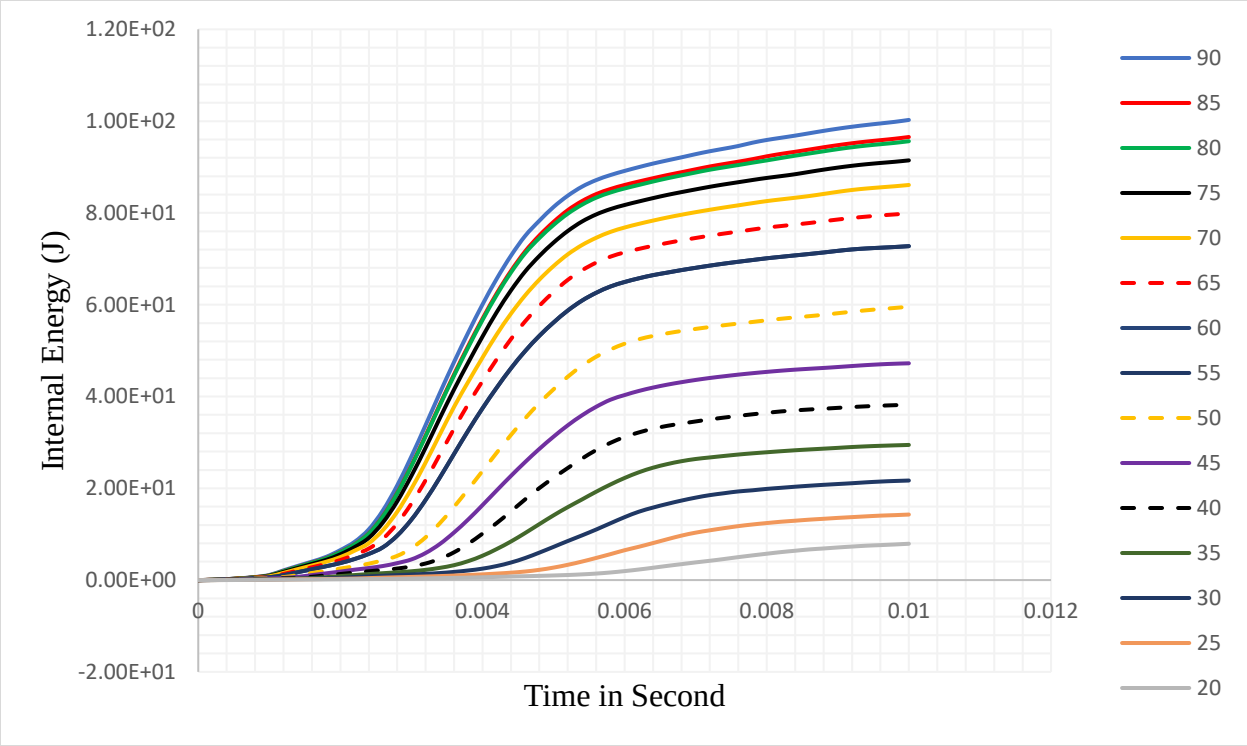

Figure 4.30. Effects of impact angles on internal energy distribution (90^0 to 20^0) at 16.5 m/s on crown (P) impact position.

4.1.8 Results of effect of impact angel and footpath curve

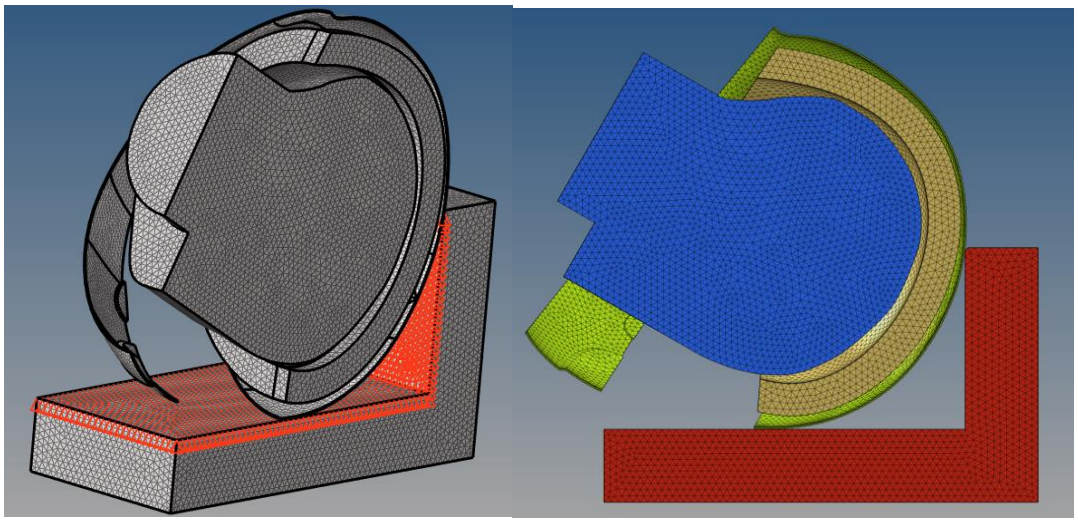

Figure 4.31. Footpath curve accident model presentation.

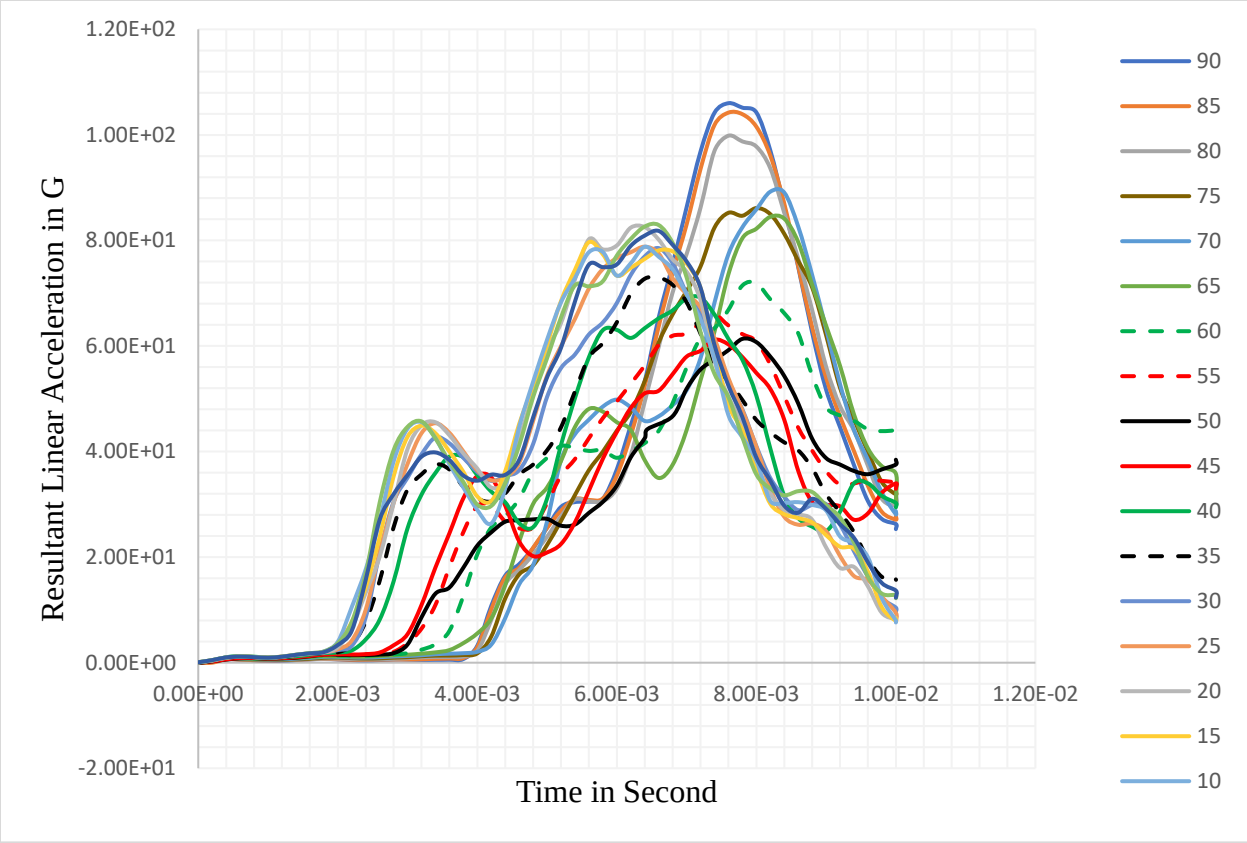

Figure 4.32. The effect of footpath curve with resultant velocity directed from normal (90^0) to transversal (0^0) directions.

4.2 Discussion

Numerous factors, including Head Injury Criterion (HIC), Head Impact Injury (HIP), Cranial Stress intracranial pressure, Primary Shear Stress of the Brain Cumulative Stress Damage (CSDM), and Amplified Damage (DDM) measurements, must be taken into account when studying the effects of head injuries. But in this study, numerical analyses were done for the determination of PLA, HIC and internal energy dissipation values.

The findings in the result section of this chapter were investigated based on different considerations – impact velocity, liner foam material type, liner foam thickness, impact angle variations, and anvil types. The results were also presented regarding with the impact resistivity and energy absorption parameters.

4.2.1 Effect of impact velocity with stiff elastic liner

In this section the results which obtained from the impact velocity of 7.5 m/s and 17.5 m/s were discussed - since the effect of the others were in between those selected velocities – the minimum and maximum extreme values. The PLA and HIC values due the rest velocity variations were presented in Appendix 3.

A. Discussions for results on impact position B

The stress distribution indicated at figure 4.1a was investigated with the impact velocity of 7.5 m/s. Under this much linear impact velocity, the head form suffered the maximum of 36.31 MPa as compared with the liner foam which suffered for about a maximum stress of 48.41 MPa. But as the linear impact velocity becomes maximize, the stress distribution on each component also maximized, which was indicated by figure 4.1b and that was investigated at the velocity of 17.5 m/s. For such linear impact velocity value, the recorded stresses were – for the head form which was a maximum of 48.78 MPa and for the liner foam which was also a maximum of 130.1 MPa.

The investigation also gave us the following results on the basis of the Peak Linear Acceleration (PLA) in G's (PLA per Gravity) and Head Injury Criteria which were developed due to different linear impact velocities. Those recorded values were – for the velocity of 7.5 m/s as shown in figure 0.3, 199G/1927, but increased with velocity and at 17.5 m/s as shown in figure 0.13, it became 622G/23900. As stated above, when the value of impact velocity increased, the peak value of linear acceleration also increased, but its position shifts to the left as shown in figure 4.2. As showed from the results, the values which cross the pass criterion line were out of the safe mode regarding with the standards.

Summary about front impact position – B

As shown in the results, when the linear impact velocity became maximized, the stress distribution on each component also maximized. It was also concluded that as the impact velocity increased, both of PLA and HIC of the system maximized – as shown from figure 0.3 on which 199G PLA and 1927 HIC value to 622G of PLA and 23900 of HIC value as recorded in figure 0.13. Those values indicate that when the value of the input increased, then the output variable crosses the threshold value indicated. So, the suggested liner foam component has a

minimum performance on the basis of energy absorbance. This was due to the material properties, the material with stiff mechanical property has less absorbance of energy [3].

As the investigation showed that most of the time, the value of the intervals between t_1 and t_2 (which were the intervals on which the HIC values were recorded/analyzed) was minimized as the impact velocity increased from 7.5 m/s to 17.5 m/s as shown figure 4.2.

B. Discussions for results on impact position R

The stress distribution indicated at figure 4.3a which investigated with the impact velocity of 7.5 m/s was – on the head form a maximum of 22.83 MPa and on the liner foam about a maximum stress of 68.5 MPa. But as the linear impact velocity became maximized, the stress distribution on each component also maximized as indicated in figure 4.3b that was investigated at the velocity of 17.5 m/s. For such linear impact velocity value, the recorded stresses were – on the head form a maximum of 50.16 MPa and on the liner foam a maximum of 100.3 MPa.

From the investigation of rear impact position, the following results were also recorded on the basis of the PLA in G's (per Gravity) and HIC which were developed due to different linear impact velocities. The values as per the analysis were – for the velocity of 7.5 m/s in figure 0.14, it was 250G/2416, for the velocity of 17.5 m/s in figure 0.23, it was 645G/23160.

Summary about rear impact position – R

As shown in the results, as the linear impact velocity become maximized, the stress distribution on each component also maximized. This was indicated by figure 0.14 which investigated at the velocity of 7.5 m/s and then maximized to the indicated values in figure 0-23 that was investigated at the velocity of 17.5 m/s.

With similar manner of investigations for front impact position, the value of PLA and HIC increased with the increment of impact velocity – as showed from figure 0.14 which were 250G PLA and 2416 HIC maximized to the values of 645G of PLA and 23160 of HIC as recorded in figure 0.23. The reason why this was also the material property of the liner foam as stated above with in the front impact condition case.

And also, the investigation showed that most of the time, the value of the interval between t_1 and t_2 is minimized as the impact velocity increased from 7.5 m/s to 17.5 m/s as shown in figures 4.4. Higher impact velocities also result in higher energy levels [41].

C. Discussions for results on impact position P

The stress distribution indicated at figure 4.5a was investigated with the minimum impact velocity 7.5 m/s, and the head form suffers the maximum of 35.06 MPa but the liner foam suffers about a maximum stress of 46.75 MPa. But the stress distribution on each component as the linear impact velocity became maximized, which were indicated by figure 4.5b that was investigated at 17.5 m/s, and the recorded stresses were – for the head form a maximum of 39.94 MPa and for the liner foam a maximum of 79.89 MPa.

The investigation also gave us the following results on the basis of the PLA in G's and HIC. Those recorded values were – at 7.5 m/s as shown in figure 0.24, 166G/1690, but increased with velocity and at 17.5 m/s as shown in figure 0.34, it became 719G/30270. Similarly with front and rear impact position analyses, when the value of impact velocity increased, then peak value of linear acceleration also increases, but its position shifts to the left as shown in figure 4.6.

Summary about crown impact position – P

As shown in the results, when the linear impact velocity became maximized, the stress distribution on each component also maximized. This was indicated by figure 4.5a, which was investigated at the velocity of 7.5 m/s, to figure 4.5b, which was investigated at the velocity of 17.5 m/s. It was also summarized that as the impact velocity increases, both of PLA and HIC of the system maximized – as shown from figure 0.24 on which 185G PLA and 1690 HIC value to 719G of PLA and 30270 of HIC value as recorded in figure 0.34. Those values indicated that when the value of the impact velocity during accidents increases, then the output variable crosses the threshold value. The reason behind also similar with the front and rear impact investigations as the same liner material type was used for the analysis.

As shown in figure 4.6, the value of the intervals between t_1 and t_2 was minimized as the impact velocity increased from 7.5 m/s to 17.5 m/s.

D. Discussions for results on impact position S

The stress distribution indicated at figure 4.7a was investigated with the impact velocity of 7.5 m/s, and a maximum of 44.5 MPa developed on the head form and 66.74 MPa on the liner foam. In a similar manner for the other impact position analysis, as the linear impact velocity became maximized, the stress distribution on each component also maximized.

As the recorded values, the PLA/HIC at the velocity of 7.5 m/s as shown in figure 0.35 was 366G/3831, and increased with velocity – at 16.5 m/s as shown in figure 0.44, it became 690G/16800.

Summary about lateral impact position – S

In a similar way of the above discussed impact positions, the stress distribution varies with velocity. This was shown on figure 4.7a which was investigated at 7.5 m/s and figure 4.7b, which was investigated at the velocity of 16.5 m/s.

And also, as the impact velocity increased, both of PLA and HIC of the system maximized – as shown from figure 0.35 on which 366G of PLA and 3831 of HIC value to 690G of PLA and 16800 of HIC value as recorded in figure 0.44. But those of the PLA and HIC values crosse the threshold value. The value of the intervals between t_1 and t_2 was decreased as the impact velocity increased from 7.5 m/s to 16.5 m/s as shown figure 4.10.

Generally, using 1 _*MAT ELASTIC, which is an elastic material, to liner component of the helmet system supports to analysis the mechanical properties of the helmet system. But as shown from the results, for maximum velocities the values of PLA and HIC were out of the safe mode range (the result crosses the threshold values of each respective parameters – PLA/HIC values of 275G/2400) which stated by ECE 22.05. The reason is that elastic material are stiff materials; and stiff materials have high density and less energy absorption capacity relative to soft materials [25].

The front, crown, and rear impacts typically produced small peak values as shown in figure 4.9, while the lateral impact frequently produced large in this investigation. As indicated by that figure, figure 4.9, the PLA values of the impact positions at 16.5 m/s were 548G for R, 584G for B, 647G for P and 690G for S; which all were above 275G. The reason could be that the stiffer foam causes the foam liners to absorb relatively less energy under impact loads as a whole impact analysis [3]. But, as the result indicated by that figure, the lateral position as compared with the other was more sever for the given impact velocity [35]. The reason was that the thickness of the liner component is relatively minimum (20.64 mm) as compared to the other positions. And the second sever impact position was the crown position of the helmet system; it was considered as a reference to make the rest of the two-impact position in safe mode range

(maximum or threshold values of 275G/2400 for PLA/HIC). The thickness how it affects the output parameters were presented on figure 4.20.

4.2.2 Effect of impact velocity on energy absorption

As showed from the results, the value of internal energies affected by the impact velocity. The results were extracted from each of the given impact positions at different impact velocities as shown from figure 4.10 to figure 4.13. Then from the investigation considering the elastic liner foam material for the liner component of the helmet system, the maximum energy which absorbed by the system shifted to left. The energy absorption for each the shell component and liner foam were studied; and the value of the shell as compared with the liner foam component was small. Which indicates that the energy absorption performance of the foam was maximum [3]. With a similar fashion as showed in figure 4.14, the lateral impact positions with less impact resistivity – i.e., maximum value results with peak linear acceleration and head injury criterion – had less energy absorption performance [23].

The reasons behind were the mechanical properties of the materials which used for the liner foam component as a whole system, and also the thickness of the liner foam on the lateral impact position made the lest energy absorption performance on the lateral impact positions.

In order to minimize those unsafe mode results and less energy absorption performance of the helmet system, crushable foam – 63_*MAT CRUSHABLE FOAM – a soft material, was used and the results on the basis of PLA which investigated at different impact velocities from the two liner materials were compared as shown in the figures from figure 4.15 to figure 4.18. And also, on the basis of energy absorption, the comparison was done as showed on figure 4.19 considering the crown impact position at 16.5 m/s; how it is better to use crushable foam liner was defined.

As shown from figure 4.19c, the maximum energy absorption for the elastic liner foam was recorded around 3 ms and then starts to re-bounce. The maximum energy absorbed by that liner foam was 62.4 J. As compared to the elastic liner foam with in the same input parameters and conditions, the crushable liner foam delay the compression time up to 10 ms and maximize the energy to be absorbed by the system – up to 100 J as shown in figure 4.19c. This was done by the deformation of the liner foam as shown in figure 4.19b as compared with figure 4.19a.

To effectively act as the impact energy absorber and lower the risk of skull fracture and head injury, crushable foam (EPS) is therefore recommended for this motorcycle helmet liners model [8]; the findings show that crushable foam can absorb impact energy, and the HIC value is less than that of stiff material – and even less than the standard limit.

The thickness of liner foam in this study was not uniform and ranges from 20.64mm to 29.82mm. The minimum thickness of the liner was on the lateral position of the component. Using this liner thickness size makes the value of PLA on position P 153G which was less than the standard value of 275G. But for lateral impact position, which had minimum thickness relative to the other impact positions, was still greater than the allowable maximum PLA value when using crushable foam material as a liner. Even at 13.5m/s the PLA value of impact position S was 366G, 33.1% greater than that of the maximum allowable standard value as shown in figure 4.16. This could be solved by increasing the thickness value of the liner foam at the lateral position as shown in figure 4.20. From the analysis, the PLA values were 350G, 352G, 322G, 314G, and 282G for the thicknesses of 21 mm, 22 mm, 23 mm, 24 mm and 25 mm respectively. The trend shows that the values of the peak linear acceleration were decreased when increasing the liner foam thickness. The recorded values were still greater than the maximum allowable PLA value of 275G. Maximizing the liner foam thickness may give a safe mode range result, but the limitation here was that due to the increased thickness of the component, the weight of the helmet will be affected [25]. And also, there must be consideration on the oversized thickness of the liner foam as it may be penetrated by the head form [42].The energy absorption capacities of the component with different liner thickness were also investigated as showed on figure 4.21 – the absorption performance maximized with thickness.

4.2.3 Effect of impact angle with soft crushable foam liner

4.2.3.1 Considering Flat Anvil

The effects of impact angles were investigated on flat anvils and results were recorded. As shown in figure 4.23 of crown impact position, the values of PLA were recorded at 16.5 m/s for different impact angles. A PLA of 153G was recorded at impact angle of 90^0. But when the value of the angle decreased, PLA values also continuously decreased – at the impact angle 20^0, PLA became 34.1G. The HIC value of the system was maximum of 1708 which was in the allowable

range, and decreased with the angles. The position of the peak values also continuously shifted to right when impact angles decreased. Despite of the values, the trend of the other impact condition results (as shown from figures figure 4.22, figure 4.24 & figure 4.25) also similar response for different impact angles.

As shown in figure 4.22 of front impact position, the values of PLA were recorded at 12.5m/s for different impact angles. A PLA of 77.7G was recorded at impact angle of 90^0. But when the value of the angle decreased, PLA values also continuously decreased – and at the impact angle 20^0, PLA became 20.8G. The HIC value of the system, a maximum of 400 which was in the allowable range, and decreased with the angles. The position of the peak values also continuously shifted to right when impact angles decreased.

In figure 4.24, results for rear impact position, the values of PLA were recorded at 15.5 m/s for different impact angles. A PLA of 116G was recorded at impact angle of 85^0. But when the value of the angle decreased, PLA values also continuously decreased – at the impact angle 30^0, PLA became 32.1G. The maximum value of HIC as recorded in this impact position was 1078, which was in the allowable range, and decreased with the angles as previous impact results. Here also the position of the peak values was continuously shifted to right when impact angles shifted from 85^0 to 30^0.

The displayed results in figure 4.25 of lateral impact position were recorded at 13.5 m/s for different impact angles. A PLA of 304G was recorded at impact angle of 85^0. But when the value of the angle minimized, PLA values also continuously decreased – at the impact angle 30^0, PLA became 143G. The maximum value of HIC as recorded in this impact position was 725.2, and decreased with the angles as previous impact results. The position of the peak values also continuously shifted to right when impact angles decreased.

There were also results of the energy distribution (total energies, internal energies and kinetic energies) from the investigation considering the crushable liner foam material for the liner component of the helmet system. The results were showed from figure 4.26 to figure 4.29. From the results, the maximum energy was absorbed within the system – around 100J (66.67% of the coming impact load) as shown on figure 4.26 [25]. The effect of impact angles on the energy absorption also summarized on figure 4.30 – as the impact angle decreased the value of the energy dissipated also decreased. This was because of the relation with the decrement of the normal component of the impact load on the system during accidents.

4.2.3.2 Considering Footpath Curve

Footpath curve also considered to determine the effect of impact angles as shown in figure 4.31 in the modeling section, and the results for the curve of the resultant linear acceleration at the given impact velocity were displayed in figure 4.32. There are different peaks in the graph. Which are due to the effect developed on each component of the system with respect to the time variance [38], [43]. As shown in that figure, the value of the acceleration was maximum when one of the components of the resultant velocity was maximum (either it tended to 0^0 on which the transversal (longitudinal) component was maximum or it tended to 90^0 on which the normal component of the resultant impact velocity was maximum). But the need to investigate on this condition was to analyze the optimum value of the angles on which the risks were minimized. So, as shown from the result, the peak value of the curve decreased to a relative minimum value as the angle gone from the two extreme values to the middle. Finally, the most minimum value from the peaks was recorded at the angles around 45^0 [23]. Here the result showed that the extent of the risk minimized as the inclination of the resultant impact velocity was about 45^0 for the given specified impact velocities; this was because the impact load decomposed towards the two impact points as the same time, there effect was minimized.

Chapter Five

5 Conclusion and Recommendation

5.1 Conclusion

In this study, the kinematic properties under various impact scenarios were examined using head models and a representative motorcycle helmet. This developed numerical investigation was supported by earlier executed experimental tests. Based on the validated helmeted head model, numerical analyses of the structural behaviors of the helmet and responses of the head, as well as parametric studies on the effects of various impact conditions, were carried out. Then the following conclusions were drawn given the investigations of the study.

- Impact velocities related with the material types which used for the components defines the helmet performance. As shown from figure 4.15 to figure 4.18, when using the material crushable foam as a liner component, 81.1%, 77.4%, 76.4% and 37.4% reductions were recorded considering the peak linear acceleration; on the other hand, as regard to energy absorption, 37.6% to 62.7% were recorded on the crown impact position at 16.5 m/s as shown in figure 4.19.
- When the thickness for the lateral impact position as shown in figure 4.21, using 25 mm thickness relatively maximize the impact resistivity (17.2% reduction of PLA) and energy absorption (10.3% maximization).
- When impact velocity and impact angle increases, the value of PLA and HIC also increase which indicates that the severity of the accidents were direct relations with driving speed and the angle of impact during accidents. But using crushable material, and the probably of the accident happened on a minimum impact angle reduce the severity of the accidents.
- The investigation showed that the output parameters had direct relation with the impact angle and impact velocity; however, the time intervals between t_1 and t_2 decreased and the points of PLA for each analysis changed to left with respect to increasing input parameters – impact velocities and impact angles. Which was because for the relative maximum impact load there

would small change of compression time. Therefore, duration of time on which the accidents may happen affected by the impact load conditions.

- From the investigation, the maximum resultant impact velocity that make the analysis out of the safe mode during normal impact may came to safe range when it happens with in small impact angles [22]. Due to the longitudinal component of the impact velocity had no any effect on the system and its magnitude increased as the impact angle decreased.
- From the investigated impact position considering the footpath curve, the relative sever conditions of the accidents were recorded if the resultant impact velocity was directed to either in the longitudinal direction when the angle was 0^0 or in the transverse direction (normal to the curve) when the angle was 90^0. But the minimum values of PLA were recorded at the angles around 45^0. This was because the impact curve acted as the impact load decomposer and the impact load decomposed towards the two impact curve planes.

5.2 Recommendation

The aforementioned findings allowed for some recommendations as per this helmet model system.

- In order to minimize the effect of impactors during accidents, this model of helmet system – despite of the comfort parts – may be used;
- To enhance the performance of the helmet system, the thickness of the lateral position be 25 mm. Above this much thickness of the liner foam may cause biomechanical effect due to its weight;
- The investigation was done considering most probably on flat surface accidents. So, using this model for sharp edge spiking accidents may not sufficient;
- The usage of the model above the specified maximum urban speed limit also not be recommended.

5.3 Future Works

As seen after the flow of this research work and investigated results, the following suggestions were tabulated to add some improvement on future works:

- The method for this research was a numerical analysis; an experimental investigation be recommended on the future works as it supports more for the real impact accident scenario;
- The investigation here was concerned in linear kinematic based parameters only. In real accident scenarios, the rotational as well as the biomechanical based parameters are there. Therefore, for the future works, those of the rotational and biomechanical based parameters will be incorporated for further investigations.

Reference

[1] M. Bottlang, G. Digiacomo, S. Tsai, and S. Madey, “Heliyon Effect of helmet design on impact performance of industrial safety helmets,” *Heliyon*, vol. 8, no. April, p. e09962, 2022, doi: 10.1016/j.heliyon.2022.e09962.

[2] R. Silva, K. Aires, T. Santos, K. Abdala, R. Veras, and A. Soares, “Automatic detection of motorcyclists without helmet,” in *2013 XXXIX Latin American Computing Conference (CLEI)*, Oct. 2013, pp. 1–7. doi: 10.1109/CLEI.2013.6670613.

[3] W. Gao, J. Wang, X. He, Y. T. Feng, S. Chen, and C. Wang, “Modeling the mechanical behavior of a helmeted headform impacted with a laminated windshield with consideration of composite failure,” *Compos. Struct.*, vol. 279, no. August 2021, p. 114787, 2022, doi: 10.1016/j.compstruct.2021.114787.

[4] C. E. Lopes Albuquerque *et al.*, “How Safe Is Your Motorcycle Helmet?,” *J. Oral Maxillofac. Surg.*, vol. 72, no. 3, pp. 542–549, Mar. 2014, doi: 10.1016/j.joms.2013.10.017.

[5] S. M. Montgomery, H. Hilborn, C. M. Hamel, X. Kuang, K. N. Long, and H. J. Qi, “The 3D printing and modeling of functionally graded Kelvin foams for controlling crushing performance,” *Extrem. Mech. Lett.*, vol. 46, p. 101323, Jul. 2021, doi: 10.1016/j.eml.2021.101323.

[6] A. Mcintosh, “Motorcycle Helmet Standards – Harmonisation and Specialisation ?,” no. October, 2015.

[7] V. Kostopoulos, Y. P. Markopoulos, G. Giannopoulos, and D. E. Vlachos, “Finite element analysis of impact damage response of composite motorcycle safety helmets,” vol. 33, no. B, pp. 99–107, 2002.

[8] N. Rahmanifar, F. Eskandari, and M. Shafieian, “Mechanical Characterization of Expanded Polystyrene (EPS) as a Liner Foam in Motorcycle Helmets,” in *2020 27th National and 5th International Iranian Conference on Biomedical Engineering (ICBME)*, Nov. 2020, no. Icbme, pp. 79–82. doi: 10.1109/ICBME51989.2020.9319446.

[9] F. A. O. Fernandes and R. J. Alves de Sousa, “Motorcycle helmets—A state of the art

review," *Accid. Anal. Prev.*, vol. 56, pp. 1–21, Jul. 2013, doi: 10.1016/j.aap.2013.03.011.

[10] S. K. Bhudolia, G. Gohel, E. S. B. Subramanyam, K. F. Leong, and P. Gerard, "Enhanced impact energy absorption and failure characteristics of novel fully thermoplastic and hybrid composite bicycle helmet shells," *Mater. Des.*, vol. 209, p. 110003, Nov. 2021, doi: 10.1016/j.matdes.2021.110003.

[11] M. Dymek, M. Ptak, and F. A. O. Fernandes, "Design and Virtual Testing of American Football Helmets–A Review," *Arch. Comput. Methods Eng.*, vol. 29, no. 2, pp. 1277–1289, 2022, doi: 10.1007/s11831-021-09621-7.

[12] A. Gilchrist and N. J. Mills, "Modelling of the impact response of motorcycle helmets," *Int. J. Impact Eng.*, vol. 15, no. 3, pp. 201–218, 1994, doi: 10.1016/S0734-743X(05)80013-2.

[13] M. Tabary, S. Ahmadi, and M. H. Amirzade-iranaq, "The effectiveness of different types of motorcycle helmets – A scoping review," *Accid. Anal. Prev.*, vol. 154, no. September 2020, p. 106065, 2021, doi: 10.1016/j.aap.2021.106065.

[14] T. Q. Thai, H. A. Ly, C. B. Vo, H. T. Do, and P. T. L. Nguyen, "Design and modeling motorcycle helmets using numerical simulation," in *AIP Conference Proceedings*, 2021, vol. 2420, no. November, p. 020006. doi: 10.1063/5.0068424.

[15] D. Liu and Y. Chen, "A Finite Element Investigation into the Impact Performance of an Open-Face Motorcycle Helmet with Ventilation Slots," *Appl. Sci.*, vol. 7, no. 3, p. 279, Mar. 2017, doi: 10.3390/app7030279.

[16] F. M. Shuaeib, A. M. S. Hamouda, M. M. Hamdan, R. S. Radin Umar, and M. S. J. Hashmi, "Motorcycle helmet," *J. Mater. Process. Technol.*, vol. 123, no. 3, pp. 422–431, May 2002, doi: 10.1016/S0924-0136(02)00047-X.

[17] S. F. Khosroshahi, S. A. Tsampas, and U. Galvanetto, "Feasibility study on the use of a hierarchical lattice architecture for helmet liners," *Mater. Today Commun.*, vol. 14, pp. 312–323, Mar. 2018, doi: 10.1016/j.mtcomm.2018.02.002.

[18] D. Liu, C. Chang, C. Fan, and S. Hsu, "Influence of environmental factors on energy absorption degradation of polystyrene foam in protective helmets," *Eng. Fail. Anal.*, vol.

10, no. 5, pp. 581–591, Oct. 2003, doi: 10.1016/S1350-6307(03)00040-2.

[19] S. Shankar, R. Nithyaprakash, S. Praveen, S. Sathish Kumar, and A. M. Sriram, “Analysis of motor cycle helmet under static and dynamic conditions considering different materials,” *Mater. Today Proc.*, vol. 43, no. xxxx, pp. 1098–1102, 2021, doi: 10.1016/j.matpr.2020.08.327.

[20] W. Gao, X. He, J. Wang, Y. T. Feng, and C. Wang, “Numerical investigation of oblique impact behavior of a helmeted headform on a windshield considering failure,” *Thin-Walled Struct.*, vol. 171, no. August 2021, p. 108722, 2022, doi: 10.1016/j.tws.2021.108722.

[21] M. Aiello, U. Galvanetto, and L. Iannucci, “Numerical simulations of motorcycle helmet impact tests,” *Int. J. Crashworthiness*, vol. 12, no. 1, pp. 1–7, Jan. 2007, doi: 10.1533/ijcr.2006.0134.

[22] G. Zheng, X. Zhang, S. Li, T. Pang, Q. Li, and G. Sun, “Correlation between kinematics and biomechanics of helmeted head under different impact conditions,” *Compos. Struct.*, vol. 291, no. October 2021, p. 115514, 2022, doi: 10.1016/j.compstruct.2022.115514.

[23] S. Kongwat, T. Nueanim, and H. Hasegawa, “FE Analysis of Motorcycle Helmet Performance under Severe Accidents,” *Appl. Sci.*, vol. 12, no. 11, p. 5676, Jun. 2022, doi: 10.3390/app12115676.

[24] M. Nasim, M. J. Hasan, and U. Galvanetto, “Impact behavior of energy absorbing helmet liners with PA12 lattice structures: A computational study,” *Int. J. Mech. Sci.*, vol. 233, no. April, p. 107673, 2022, doi: 10.1016/j.ijmecsci.2022.107673.

[25] I. Levadnyi, J. Awrejcewicz, Y. Zhang, M. F. Goethel, and Y. Gu, “Finite Element Analysis of Impact for Helmeted and Non-helmeted Head,” *J. Med. Biol. Eng.*, vol. 38, no. 4, pp. 587–595, Aug. 2018, doi: 10.1007/s40846-017-0324-3.

[26] S. Li, Z. Xiao, Y. Zhang, and Q. M. Li, “Impact analysis of a honeycomb-filled motorcycle helmet based on coupled head-helmet modelling,” *Int. J. Mech. Sci.*, vol. 199, no. January, p. 106406, Jun. 2021, doi: 10.1016/j.ijmecsci.2021.106406.

[27] F. A. O. Fernandes, R. J. Alves de Sousa, M. Ptak, and J. Wilhelm, “Certified Motorcycle

Helmets: Computational Evaluation of the Efficacy of Standard Requirements with Finite Element Models," *Math. Comput. Appl.*, vol. 25, no. 1, p. 12, 2020, doi: 10.3390/mca25010012.

[28] P. Kaczyński, M. Ptak, F. A. O. Fernandes, L. Chybowski, J. Wilhelm, and R. J. Alves de Sousa, "Development and Testing of Advanced Cork Composite Sandwiches for Energy-Absorbing Structures," *Materials (Basel).*, vol. 12, no. 5, p. 697, Feb. 2019, doi: 10.3390/ma12050697.

[29] N. Prasartthong and J. Carmai, "Investigation of the Effect of Child Helmet Design Parameters on Head and Brain Injuries Using Reduced-Order Modelling," *Appl. Sci.*, vol. 12, no. 16, p. 8016, Aug. 2022, doi: 10.3390/app12168016.

[30] Z. Xiao, L. Wang, Y. Zhang, and C. Yang, "A study on motorcyclist head reponses during impact against front end of vehicle," *Int. J. Crashworthiness*, vol. 27, no. 1, pp. 147–159, 2022, doi: 10.1080/13588265.2020.1779457.

[31] F. Fernandes, R. Alves de Sousa, M. Ptak, and G. Migueis, "Helmet Design Based on the Optimization of Biocomposite Energy-Absorbing Liners under Multi-Impact Loading," *Appl. Sci.*, vol. 9, no. 4, p. 735, Feb. 2019, doi: 10.3390/app9040735.

[32] B. Leng, D. Ruan, and K. M. Tse, "International Journal of Impact Engineering Recent bicycle helmet designs and directions for future research : A comprehensive review from material and structural mechanics aspects," *Int. J. Impact Eng.*, vol. 168, no. December 2021, p. 104317, 2022, doi: 10.1016/j.ijimpeng.2022.104317.

[33] F. M. Shuaeib, A. M. S. Hamouda, S. V. Wong, R. S. R. Umar, and M. M. H. M. Ahmed, "A new motorcycle helmet liner material: The finite element simulation and design of experiment optimization," *Mater. Des.*, vol. 28, no. 1, pp. 182–195, Jan. 2007, doi: 10.1016/j.matdes.2005.04.015.

[34] L. Di Landro, G. Sala, and D. Olivieri, "Deformation mechanisms and energy absorption of polystyrene foams for protective helmets," vol. 21, pp. 217–228, 2002.

[35] S. Li and Q. M. Li, "Head responses subjected to frontal translational acceleration loads," *Int. J. Mech. Sci.*, vol. 231, no. July, p. 107598, Oct. 2022, doi: 10.1016/j.ijmecsci.2022.107598.

[36] R. Miralbes, D. Ranz, and J. Peña, “Study of the influence of impact velocity and angle of impact against a motorcyclists´ protection systems design and neural damage sustained using numerical methods,” *Int. J. Crashworthiness*, vol. 24, no. 2, pp. 171–183, Mar. 2019, doi: 10.1080/13588265.2018.1424297.

[37] G. D. Caserta, L. Iannucci, and U. Galvanetto, “Shock absorption performance of a motorbike helmet with honeycomb reinforced liner,” *Compos. Struct.*, vol. 93, no. 11, pp. 2748–2759, 2011, doi: 10.1016/j.compstruct.2011.05.029.

[38] S. K. Bhudolia, G. Gohel, E. S. B. Subramanyam, K. F. Leong, and P. Gerard, “Enhanced impact energy absorption and failure characteristics of novel fully thermoplastic and hybrid composite bicycle helmet shells,” *Mater. Des.*, vol. 209, p. 110003, Nov. 2021, doi: 10.1016/j.matdes.2021.110003.

[39] A. Bracali and N. Baldanzini, “Estimation of Head Accelerations in Crashes Using Neural Networks and Sensors Embedded in the Protective Helmet,” *Sensors*, vol. 22, no. 15, p. 5592, Jul. 2022, doi: 10.3390/s22155592.

[40] U. Nations and I. T. Committee, “Economic and Social Council,” vol. 2020, no. June, 2020.

[41] M. Ptak, P. Kaczynski, F. A. O. Fernandes, and R. J. A. de Sousa, “Assessing impact velocity and temperature effects on crashworthiness properties of cork material,” *Int. J. Impact Eng.*, vol. 106, pp. 238–248, Aug. 2017, doi: 10.1016/j.ijimpeng.2017.04.014.

[42] S. J. Bonin, J. C. Gardiner, A. Onar-Thomas, S. S. Asfour, and G. P. Siegmund, “The effect of motorcycle helmet fit on estimating head impact kinematics from residual liner crush,” *Accid. Anal. Prev.*, vol. 106, no. June, pp. 315–326, 2017, doi: 10.1016/j.aap.2017.06.015.

[43] G. Gohel, S. K. Bhudolia, S. B. S. Elisetty, K. F. Leong, and P. Gerard, “Development and impact characterization of acrylic thermoplastic composite bicycle helmet shell with improved safety and performance,” *Compos. Part B Eng.*, vol. 221, no. May, p. 109008, 2021, doi: 10.1016/j.compositesb.2021.109008.

Appendixes

Appendix 1:

The models, part drawings and assembly drawings integrated with the anvil shown as follow. Here the following are the models for the components of head form, liner foam and the helmet shell of the helmet system respectively.

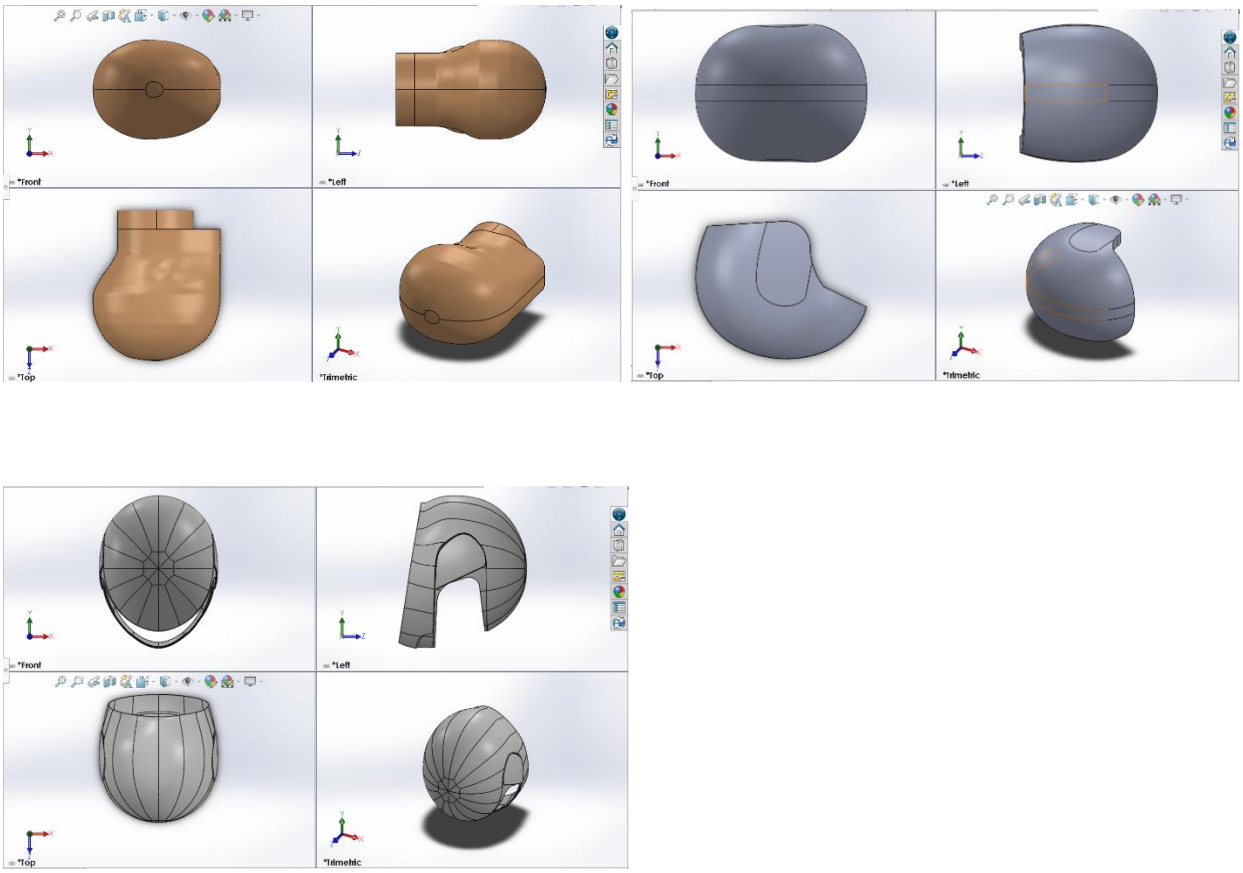

Figure 0.1. Part drawings of the helmet system.

The following figures are also the assembly of the helmet system which integrated with the head form and flat anvil impactor. The figures represented the most representative positions of the impacts that may happen during the accidents.

Impact position B

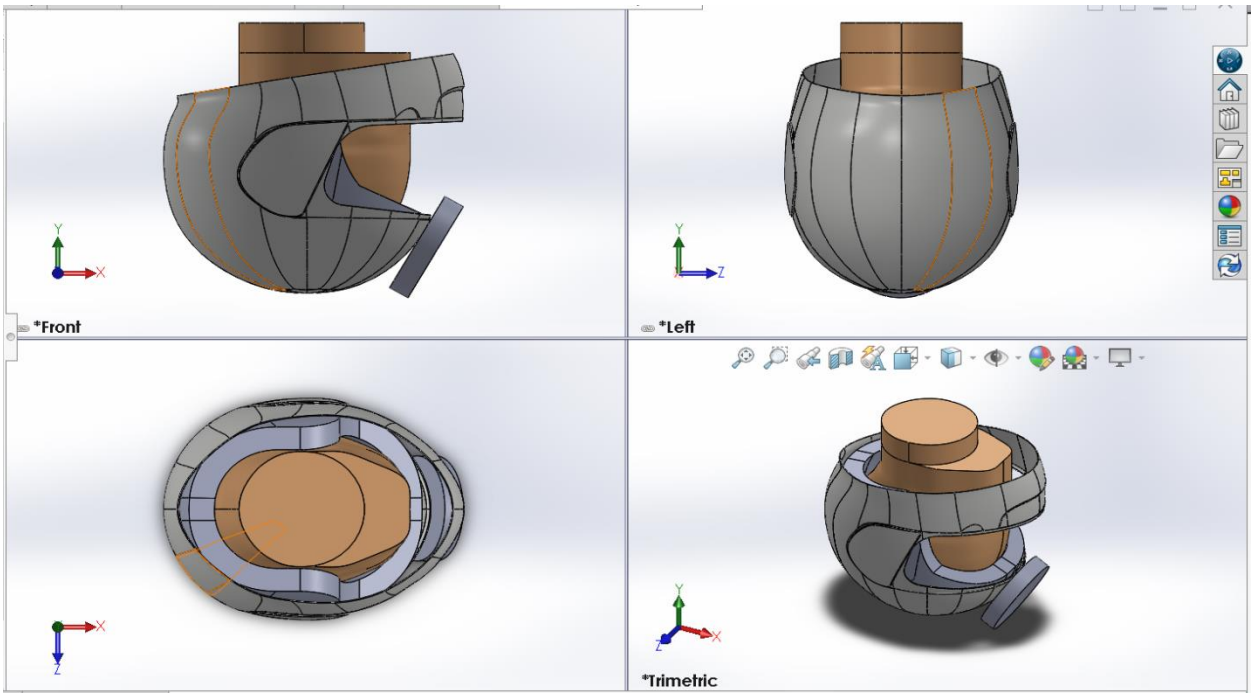

Impact position P

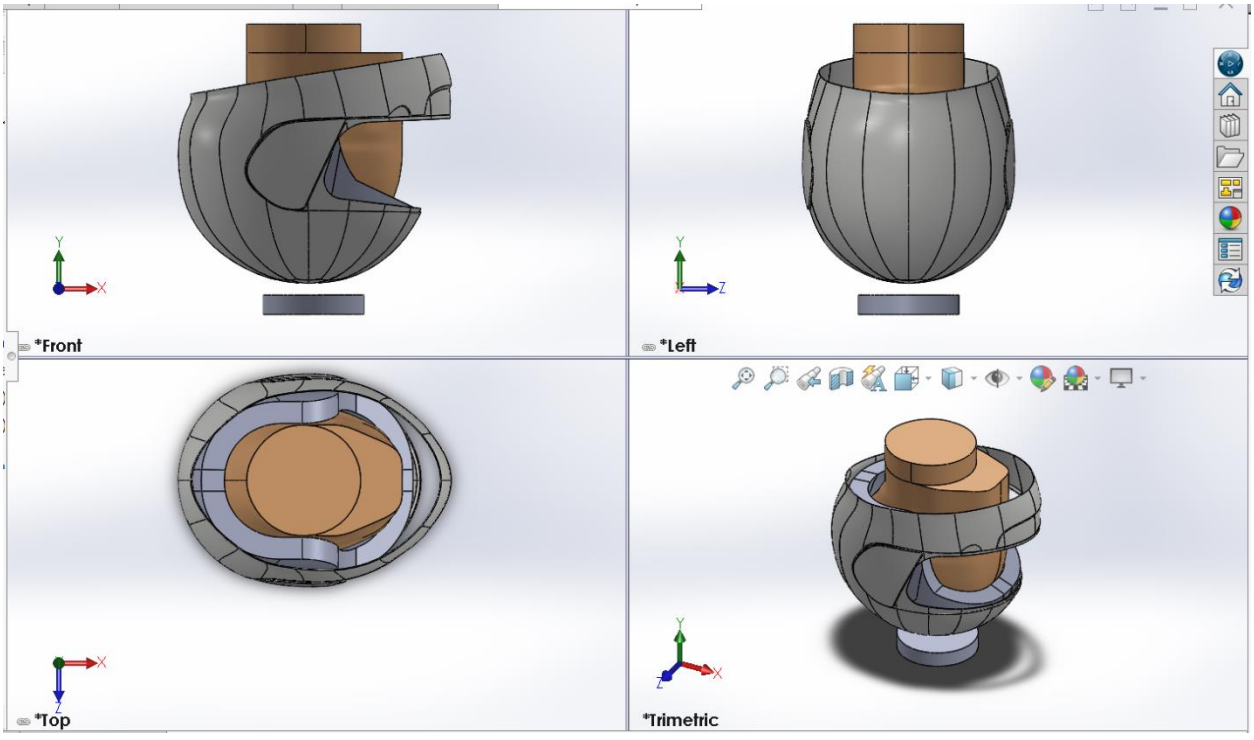

Impact position C

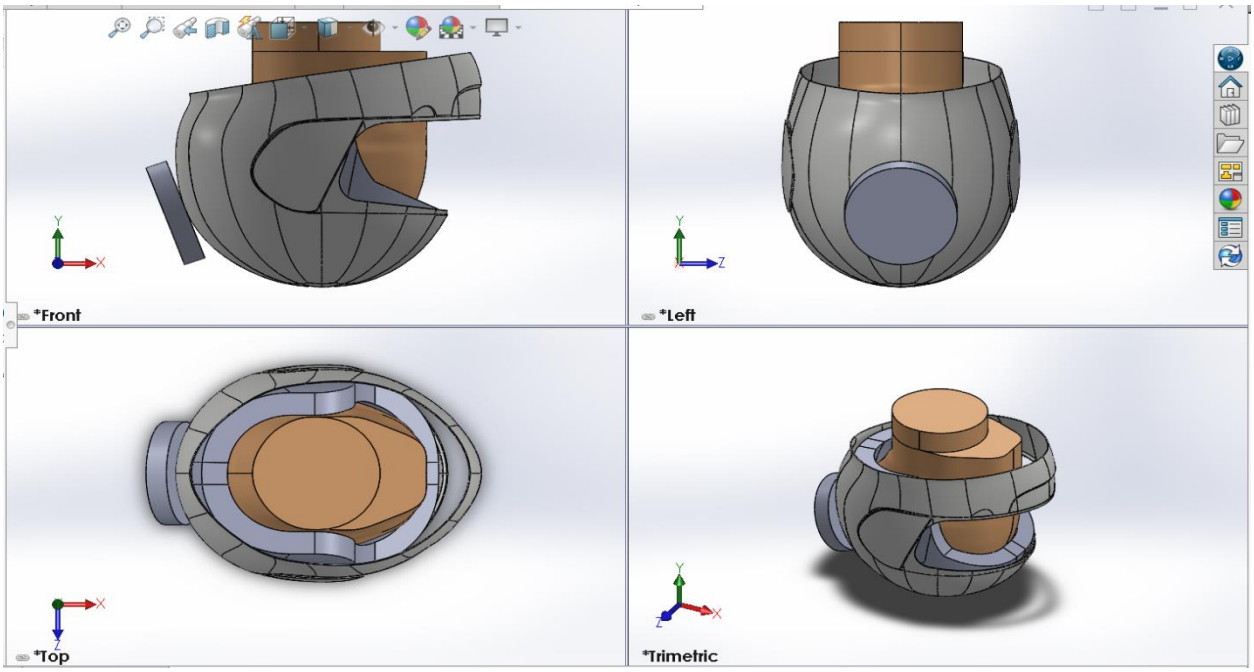

Impact position S

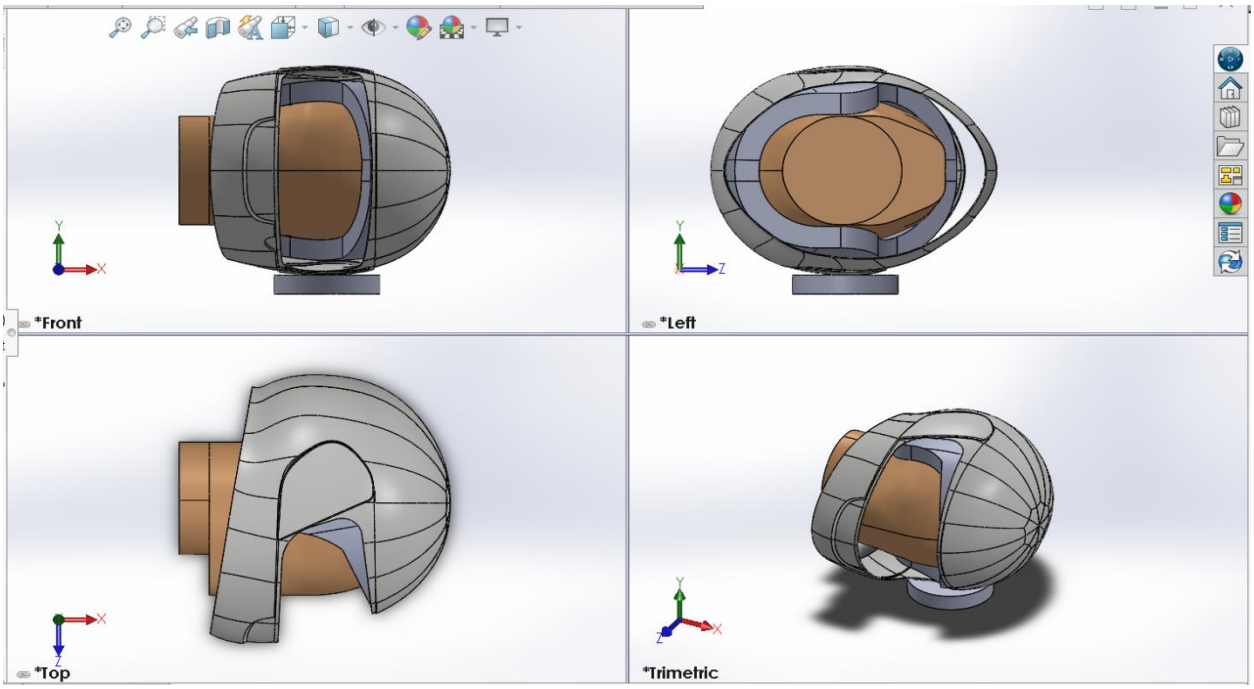

Figure 0.2. Assembly drawings for the helmet system.

Appendix 2.

Table 0.1. Dimension and mass of headforms.

Size designation	*h (mm)*	*x(mm)*	*y(mm)*	*Mass (g)*
445	108,5	21,0	81,7	
455	110,6	21,5	83,3	1 970 ± 75
465	112,7	22,0	84,8	
475	114,8	22,5	86,4	
485	116,9	23,0	88,0	
495	119,0	23,5	89,7	3 100 ± 100
505	121,1	24,0	91,2	
515	123,2	24,5	92,7	
525	125,3	25,0	94,5	
535	127,4	25,5	96,0	4 100 ± 120
545	129,5	26,0	97,5	
555	131,6	26,5	99,1	
565	133,7	27,0	100,8	
575	135,8	27,5	102,4	4 700± 140
585	137,9	28,0	103,9	
595	140,0	28,5	105,4	
605	142,1	29,0	107,2	5 600 ± 160
615	144,2	29,5	108,7	
625	146,3	30,0	110,2	6 100 ± 180
635	148,4	30,5	111,8	
645	150,5	31,0	113,5	

Source: (Nations & Committee, 2020)

The headform inertia matrix of reference for the homologation is according to Table one (principal directions only, with regards to the center of gravity).

The general characteristics of the test headforms to be used shall be as follows:

Table 0.2. Properties of the headform.

Headform denominatio n	*Circumference [mm)*	*Mass [Kg)*	*lxx [Kg cm"] (± 5%)*	*lyy [Kgcm") (± 5%)*	*lzz [Kg cm2") (± 5%)*
A	495·	3.1 (± 0.10)	142.2	166.6	95.0
C	515'	36 (± 0.10)	172.6	203.3	113.2
E	535·	4.1 (± 0.12)	202.9	238.6	141.3
J	575·	4 7 (± 0.14)	264.0	318.3	193.1
M	605'	5 6 (± 0.16)	337.4	402.7	252.7
0	625'	6.1 (± 0.18)	383.6	461.1	293.5

Source: (Nations & Committee, 2020)

Tolerances according to UN 960:2006. The coefficient of friction (μ) shall be 0.3 ± 0.05 between the outer surface of the head form and the common fabric used in the comfort padding of the helmet.

Appendix 3.

NOTE**:* - For each the following graphs, there are labels: - ***label A – represents the resultant acceleration curve per gravitational acceleration (*RLA/9.81 in mm/s*^{2}) and ***label B*** – represents the area on which the head injury criteria (*HIC*) determined on. All RLA values in the following figures are in mm/s^2 (or multiply each value with 10^{-3} to express in m/s^2) and to get the corresponding HIC values use the multiplication coefficient of 10^{-7} which is form the coefficient of RLA and the exponent 2.5 from equation 3.4 ($10^{-3*2.5} = 10^{-7}$).

➢ The following figures are the representation of the results for the front impact position.

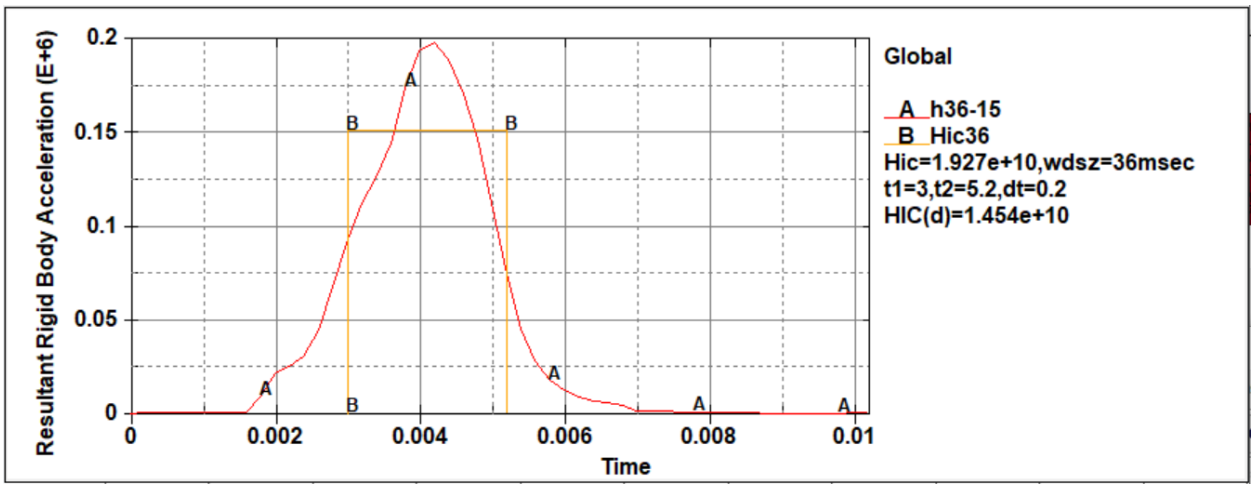

Figure 0.3. RLA distribution and HIC values at 7.5 m/s.

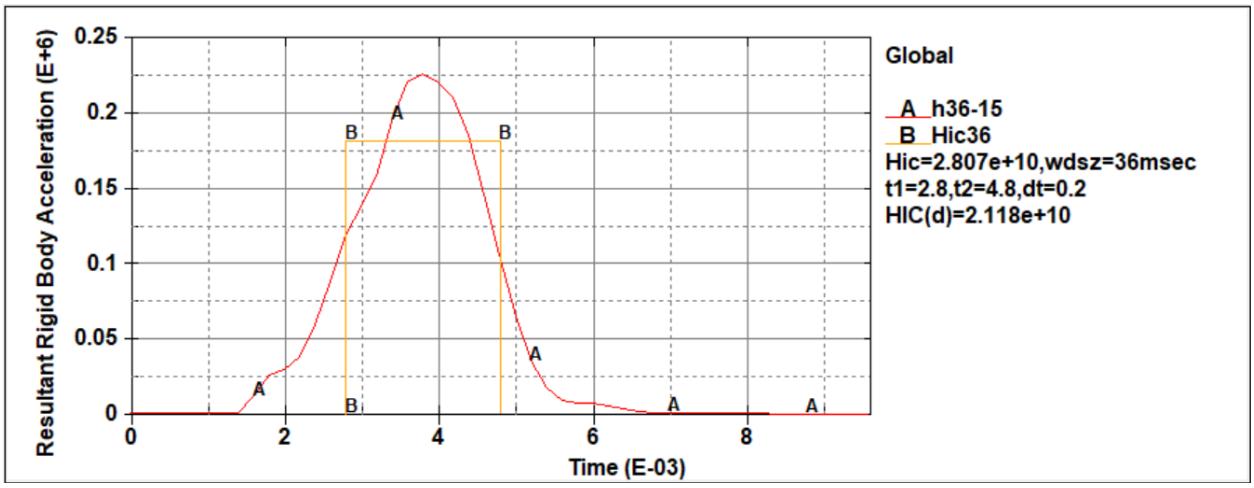

Figure 0.4. RLA distribution and HIC values at 8.5 m/s.

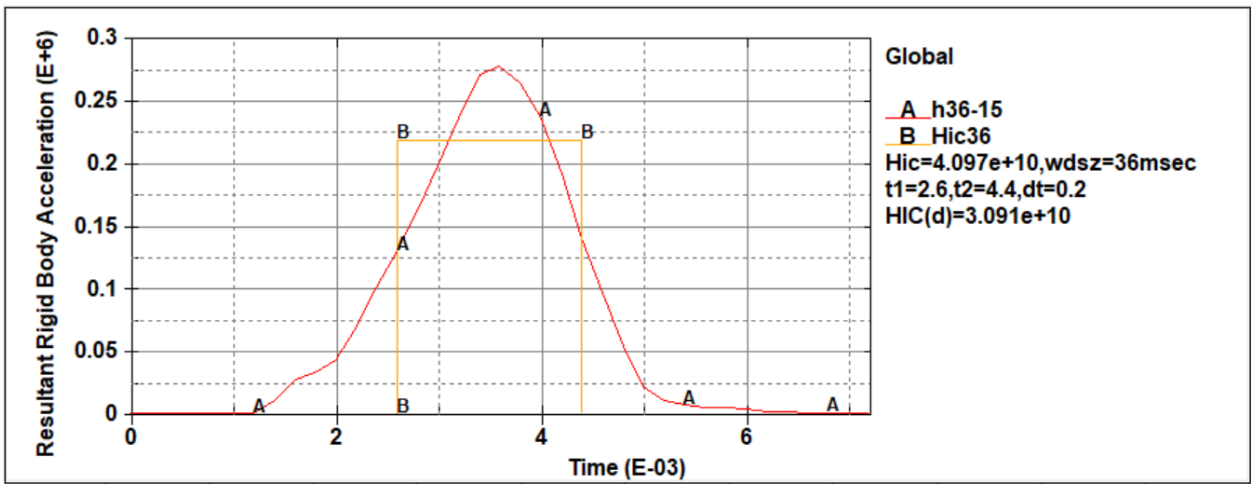

Figure 0.5. RLA distribution and HIC values at 9.5 m/s.

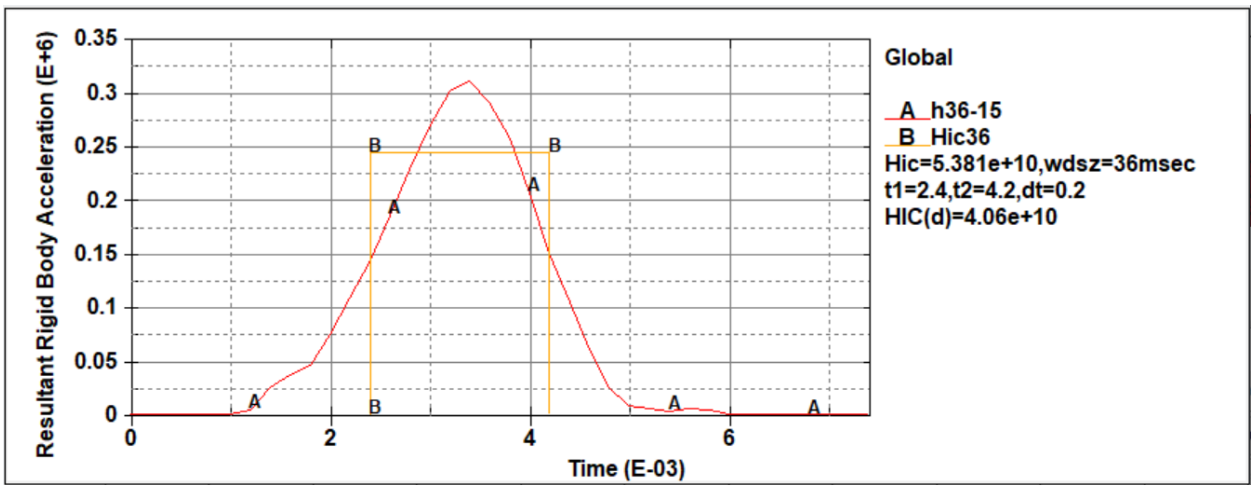

Figure 0.6. RLA distribution and HIC values at 10.5 m/s.

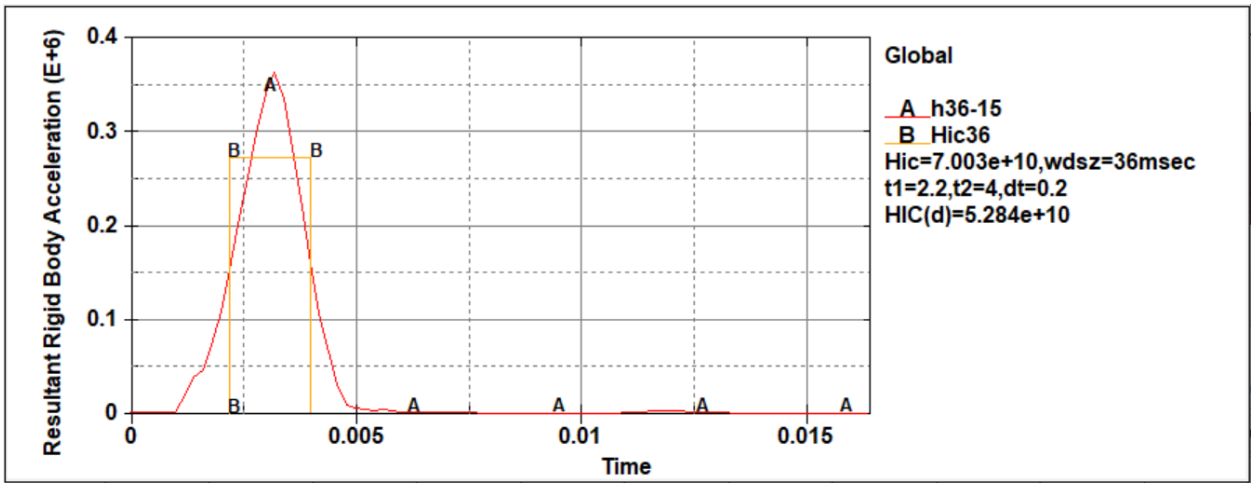

Figure 0.7. RLA distribution and HIC values at 11.5 m/s.

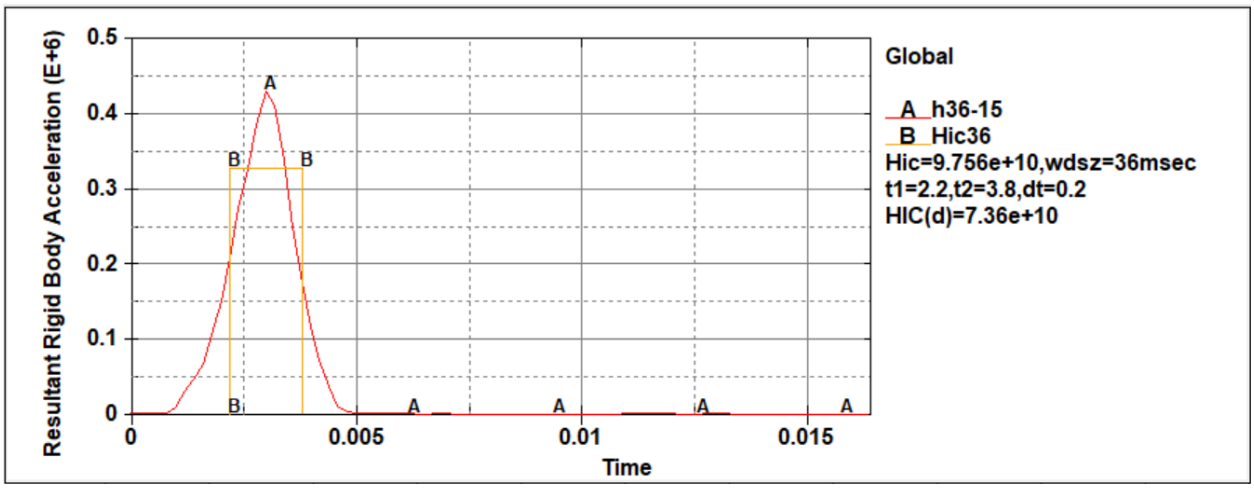

Figure 0.8. RLA distribution and HIC values at 12.5 m/s.

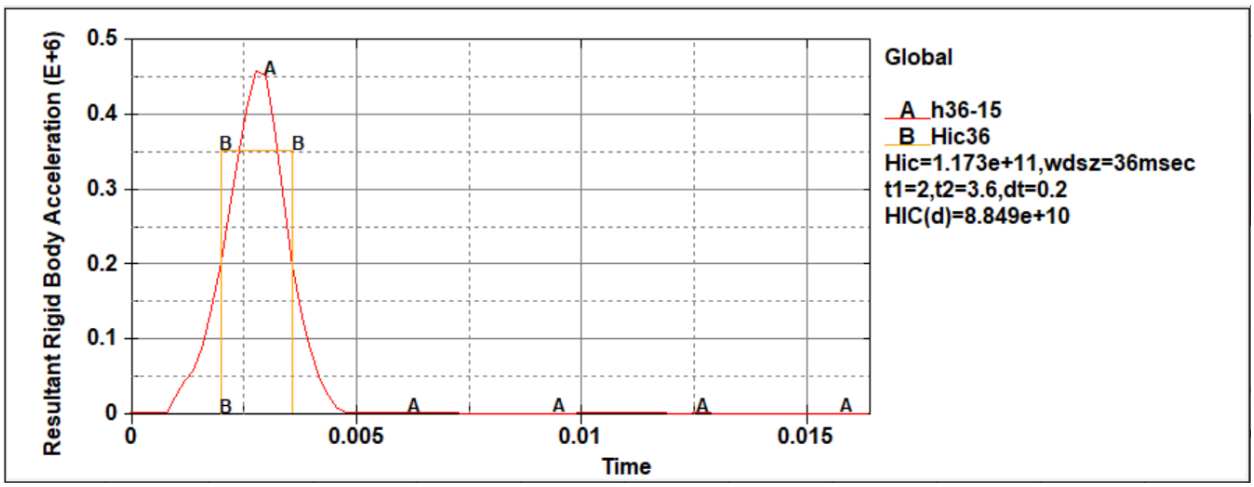

Figure 0.9. RLA distribution and HIC values at 13.5 m/s.

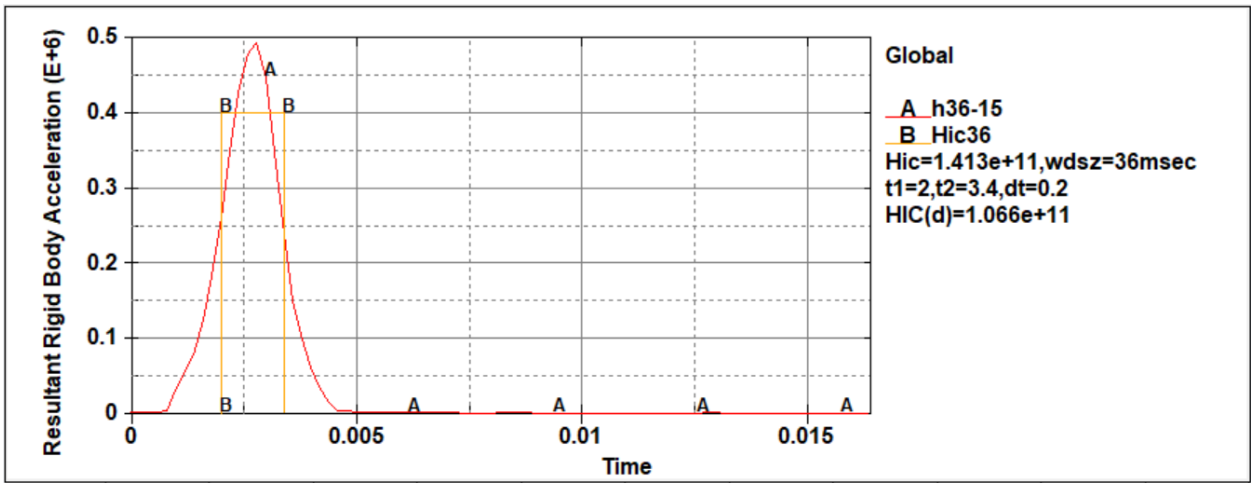

Figure 0.10. RLA distribution and HIC values at 14.5 m/s.

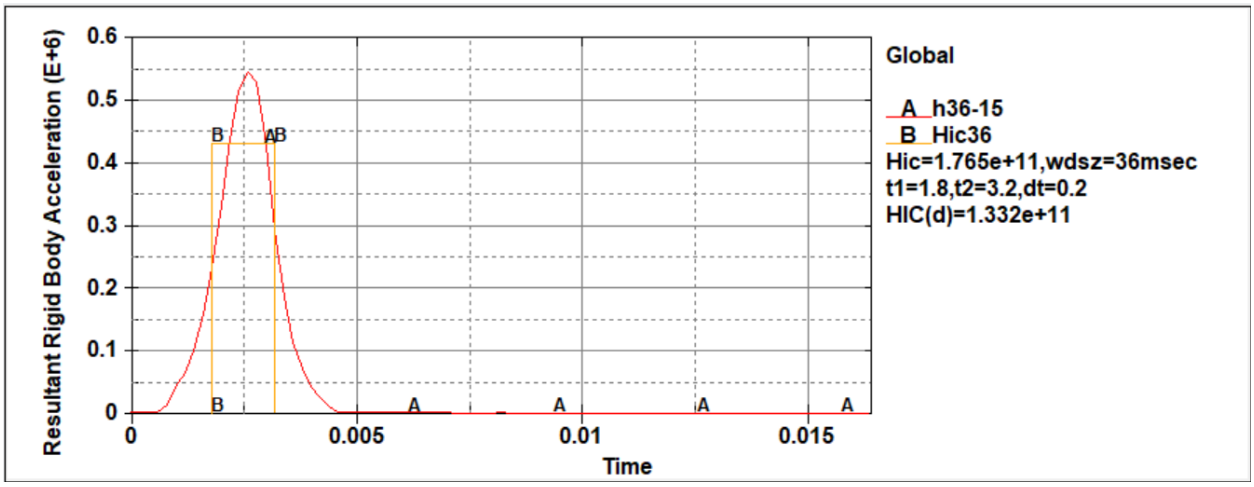

Figure 0.11. RLA distribution and HIC values at 15.5 m/s.

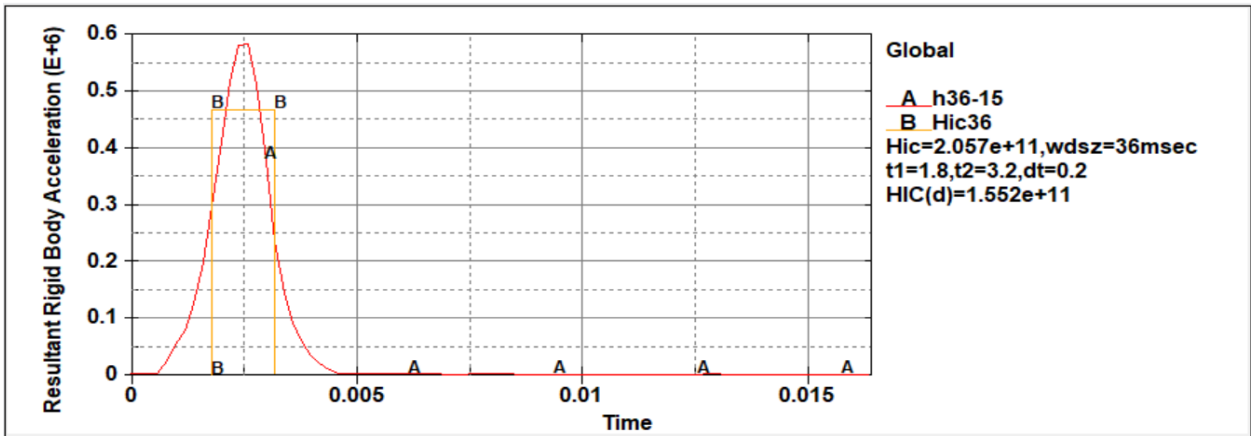

Figure 0.12. RLA distribution and HIC values at 16.5 m/s.

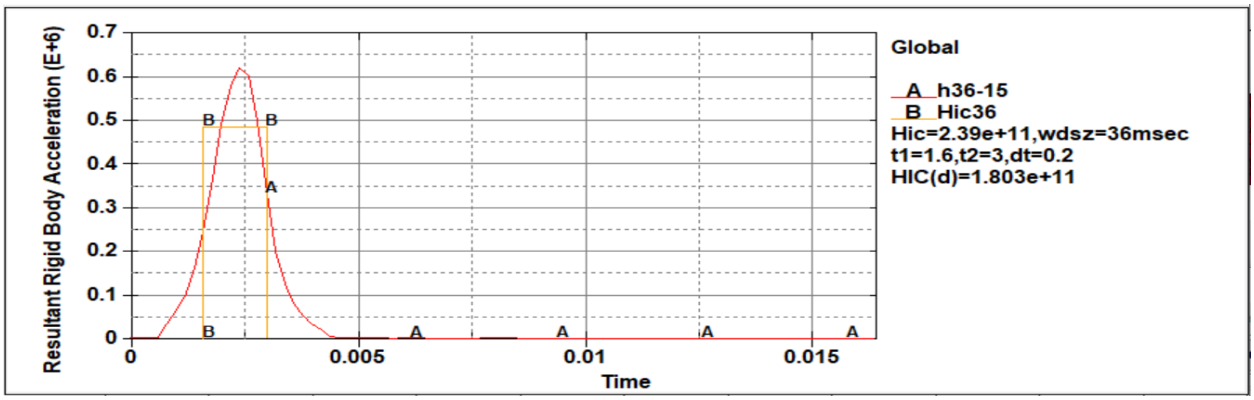

Figure 0.13 RLA distribution and HIC values at 17.5 m/s.

- The following figures are the representation of the results for the rear (R) impact position.

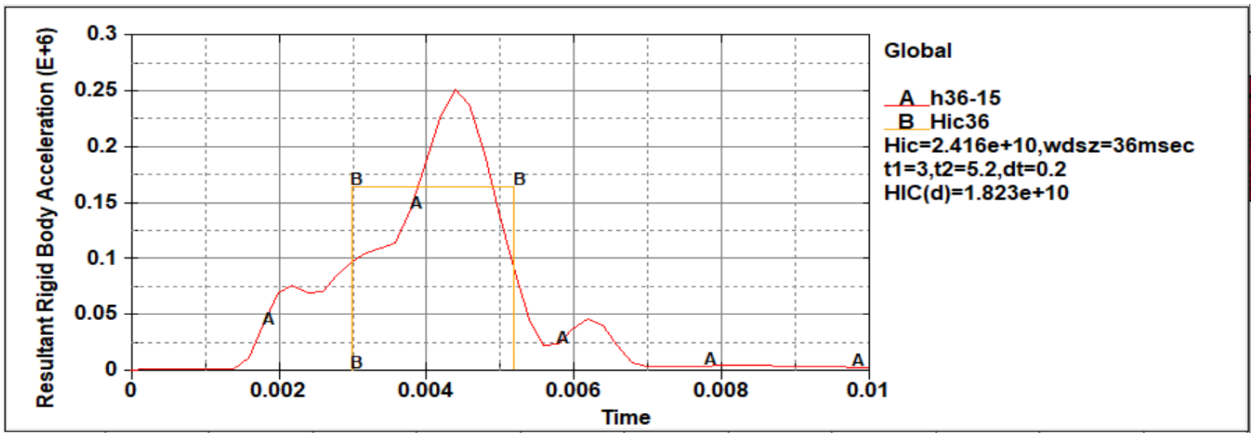

Figure 0.14. RLA distribution and HIC values at 7.5 m/s.

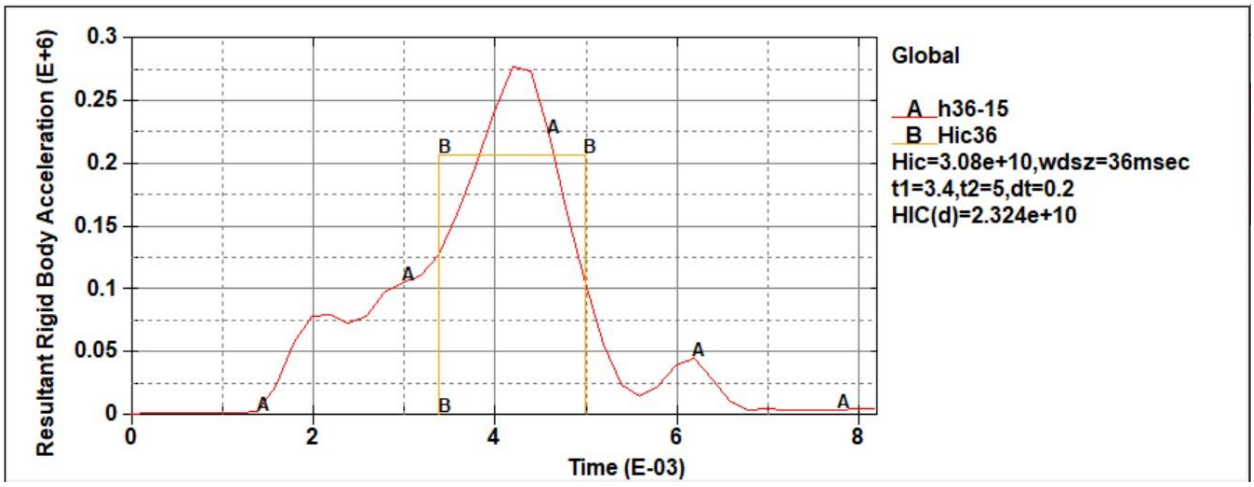

Figure 0.15. RLA distribution and HIC values at 8.5m/s.

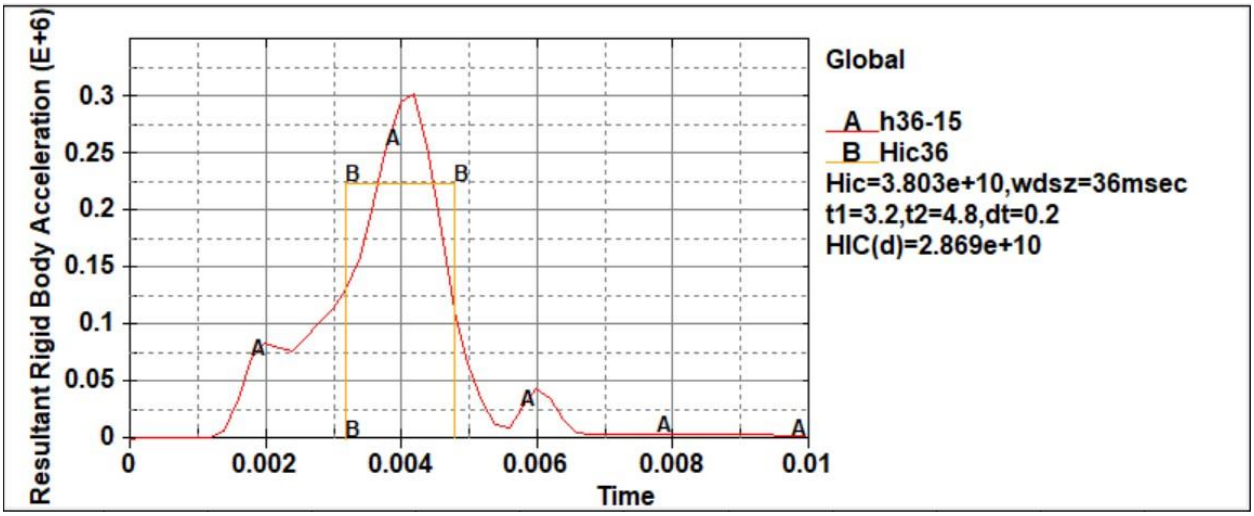

Figure 0.16. RLA distribution and HIC values at 9.5m/s.

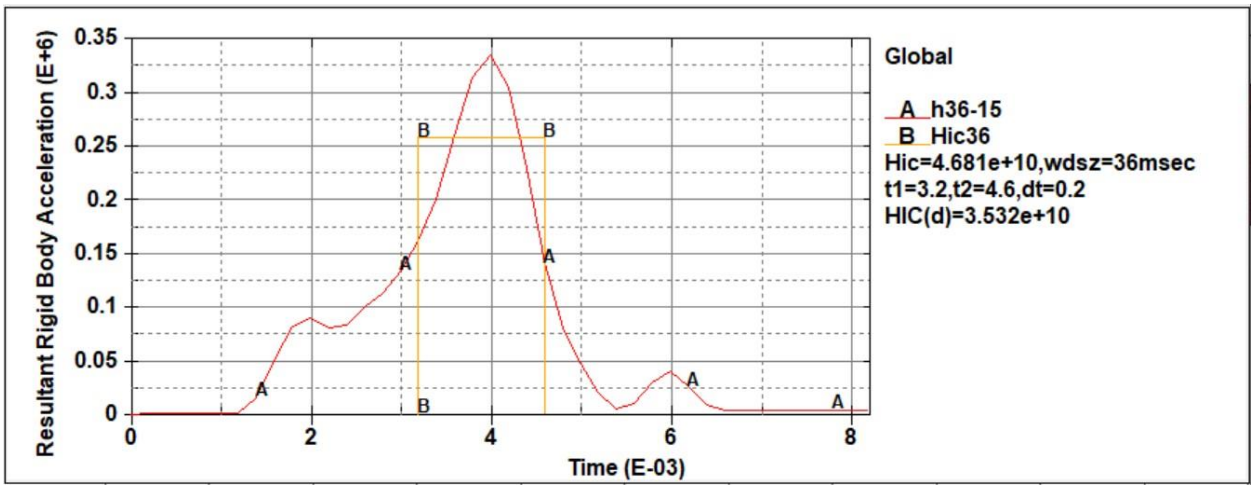

Figure 0.17. RLA distribution and HIC values at 10.5m/s.

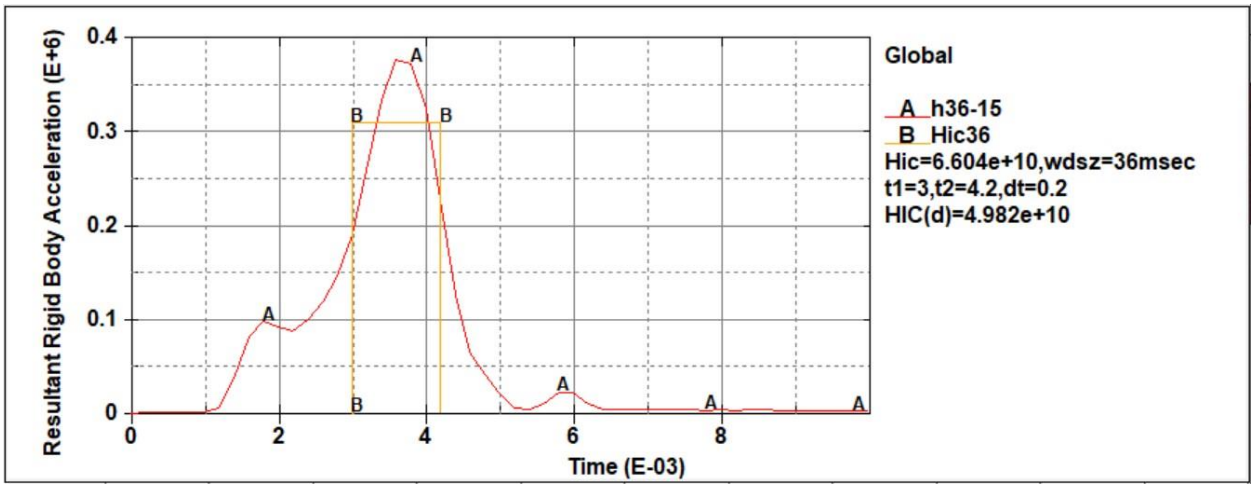

Figure 0.18. RLA distribution and HIC values at 11.5m/s.

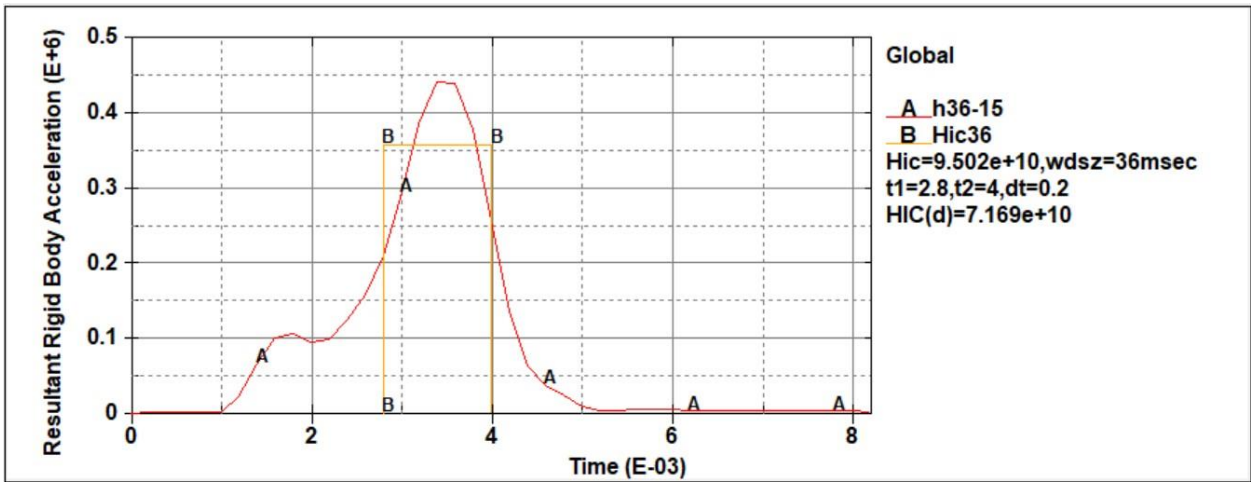

Figure 0.19. RLA distribution and HIC values at 12.5m/s.

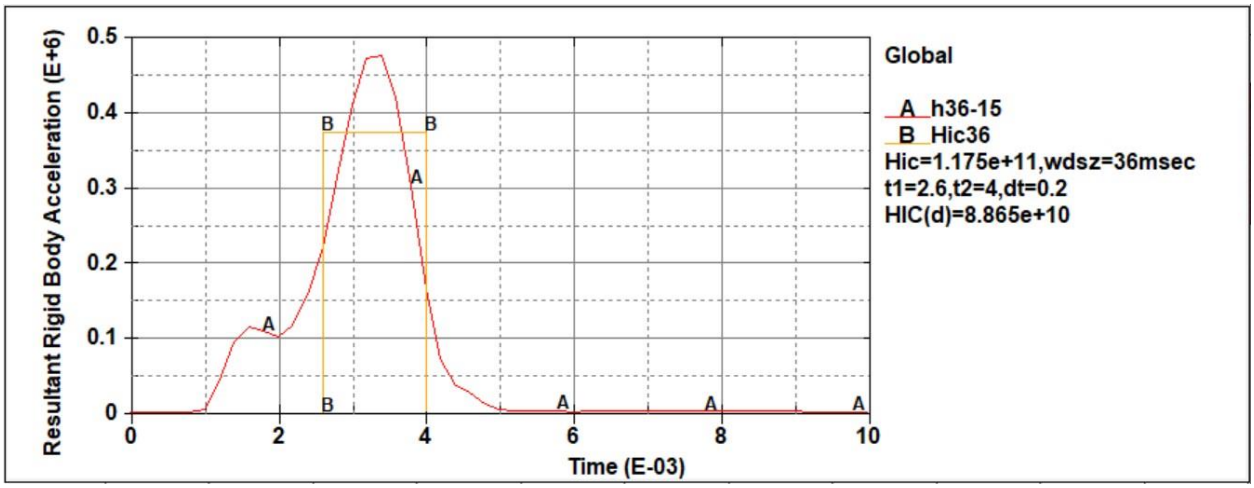

Figure 0.20. RLA distribution and HIC values at 13.5m/s.

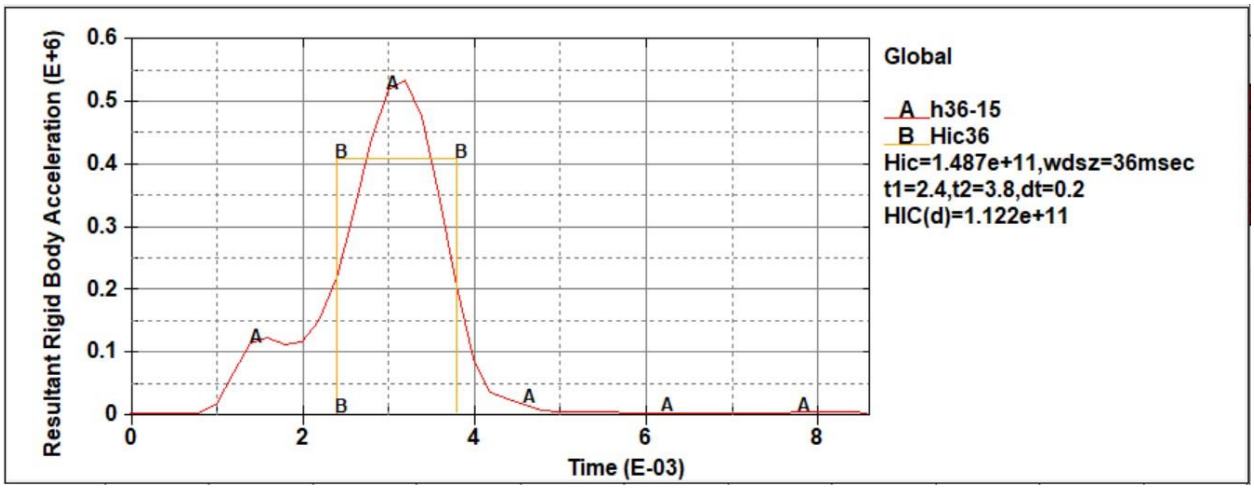

Figure 0.21. RLA distribution and HIC values at 14.5m/s.

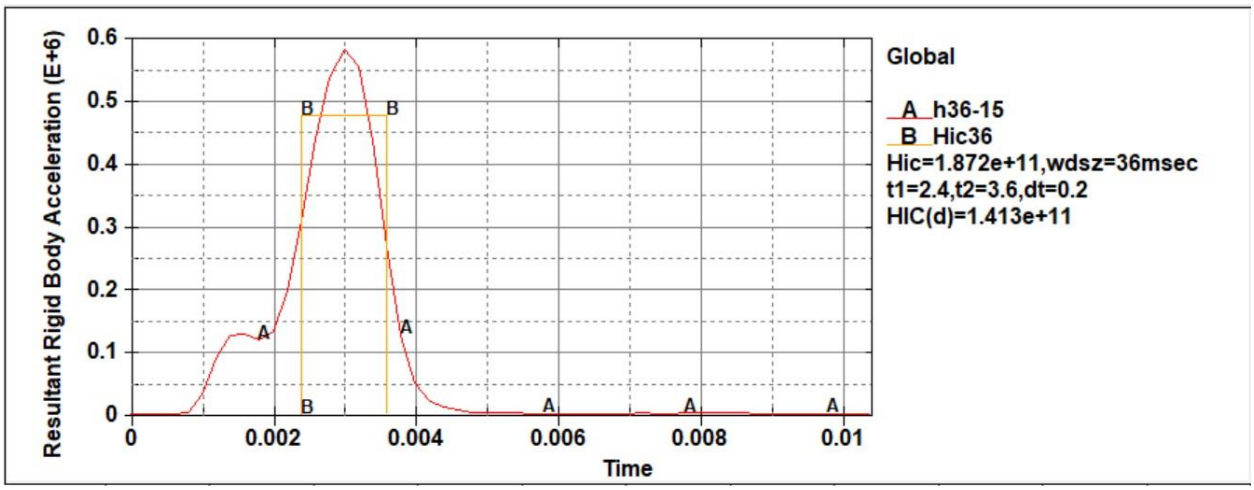

Figure 0.22. RLA distribution and HIC values at 15.5m/s.

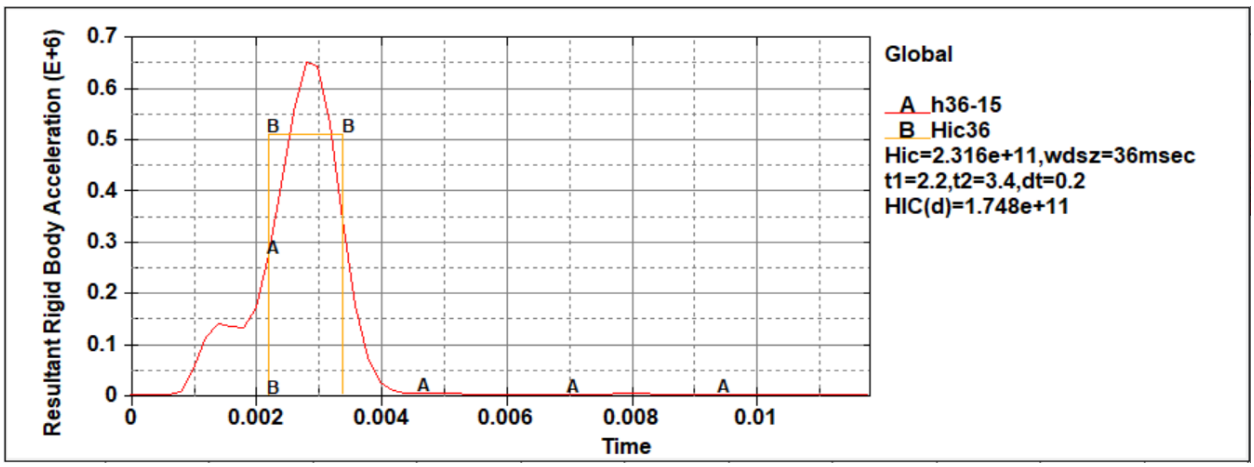

Figure 0.23. RLA distribution and HIC values at 17.5 m/s.

- The following figures are the representation of the results for the crown impact position.

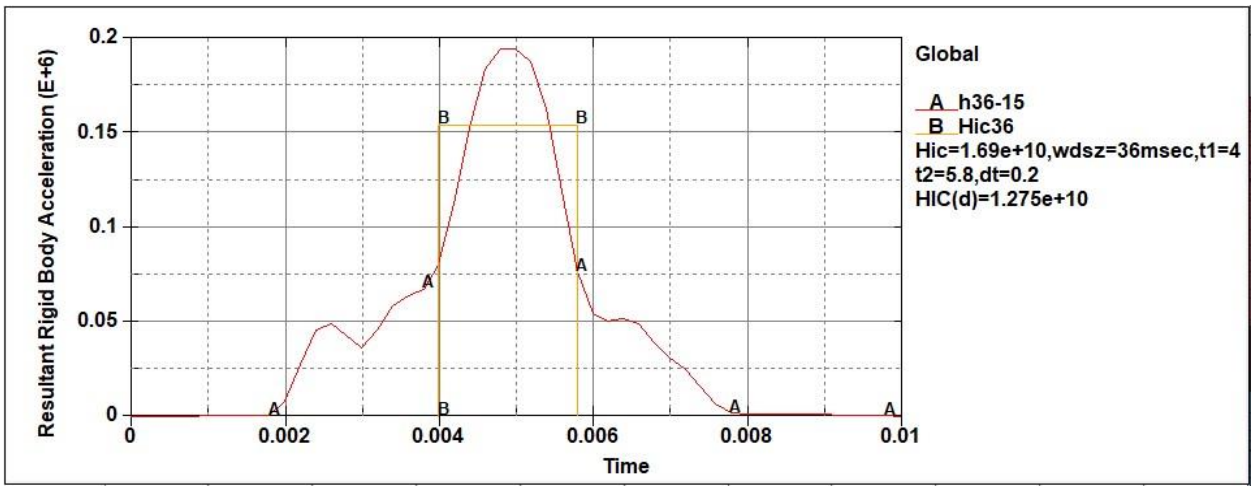

Figure 0.24. RLA distribution and HIC values at 7.5 m/s.

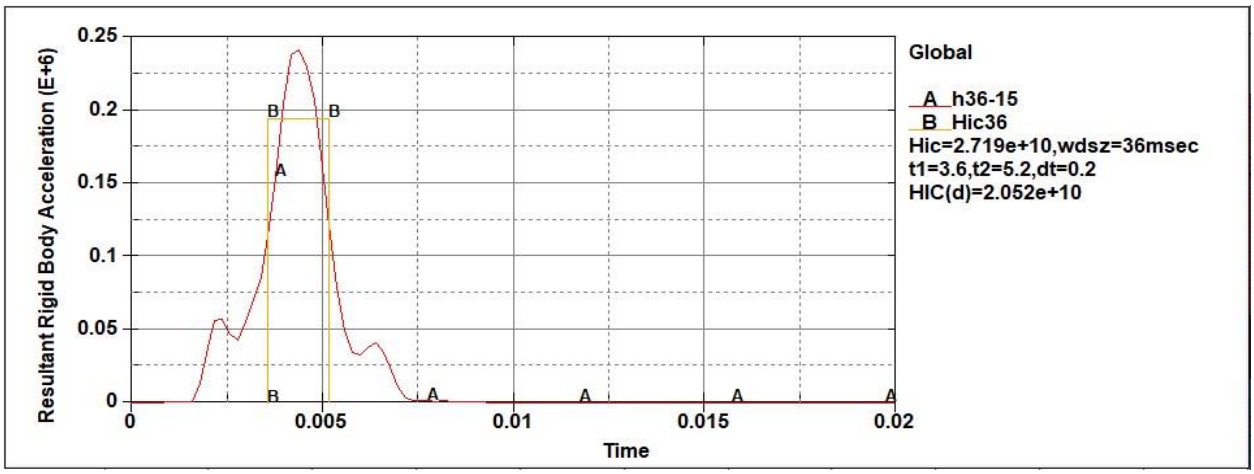

Figure 0.25. RLA distribution and HIC values at 8.5m/s.

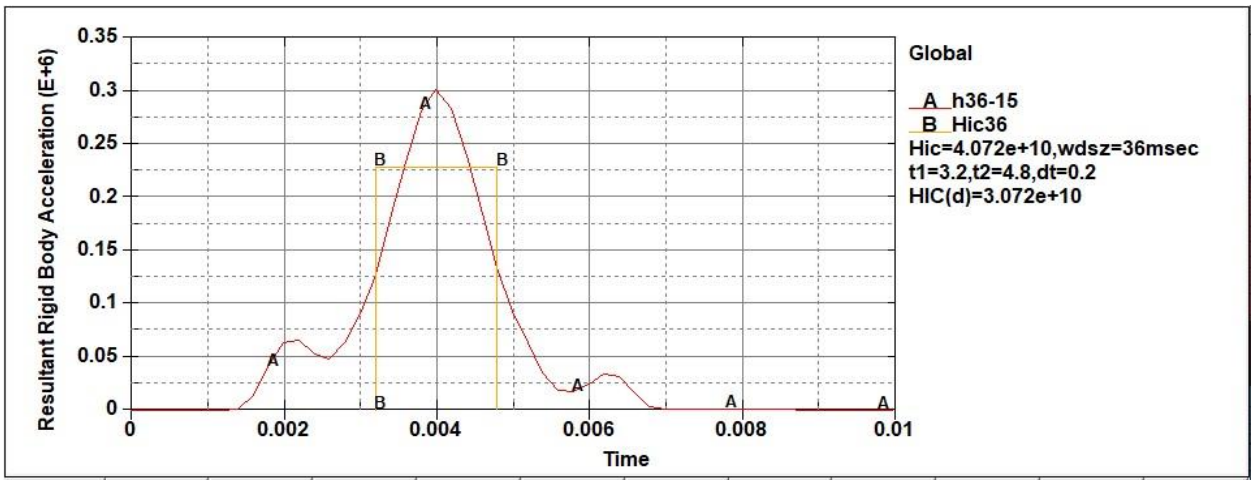

Figure 0.26. RLA distribution and HIC values at 9.5m/s.

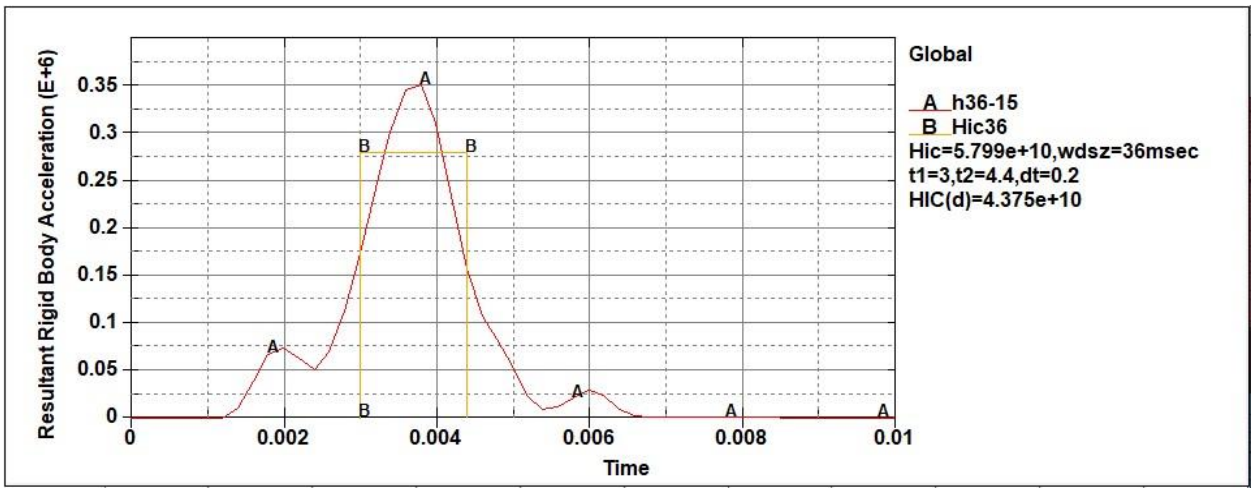

Figure 0.27. RLA distribution and HIC values at 10.5m/s.

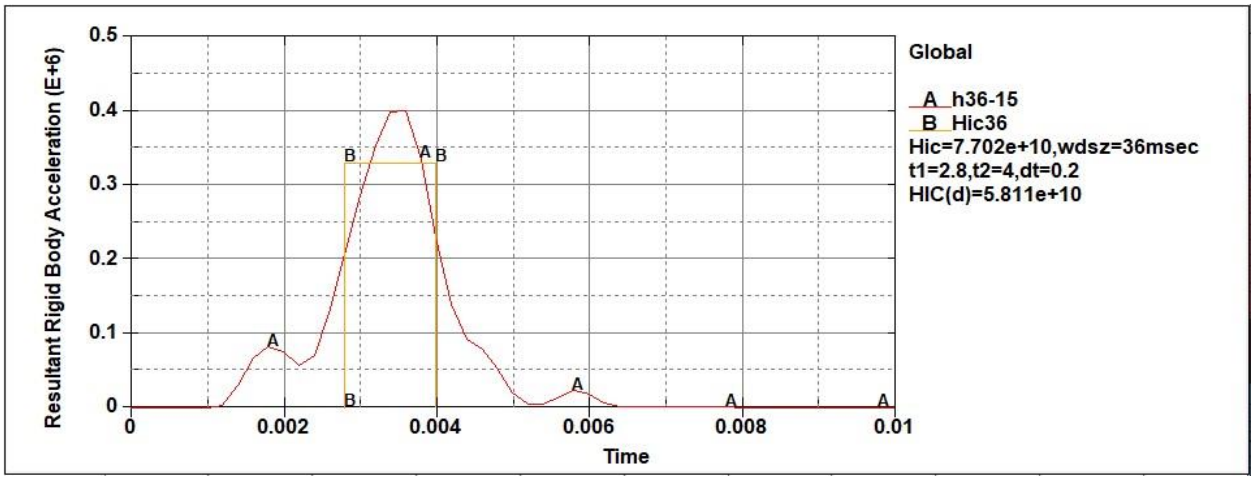

Figure 0.28. RLA distribution and HIC values at 11.5m/s.

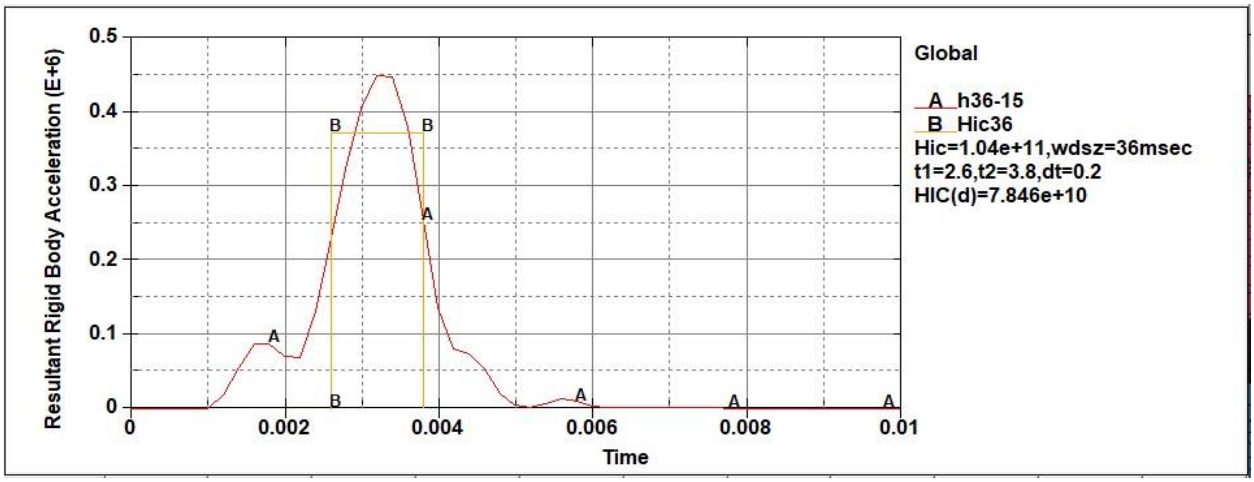

Figure 0.29. RLA distribution and HIC values at 12.5m/s.

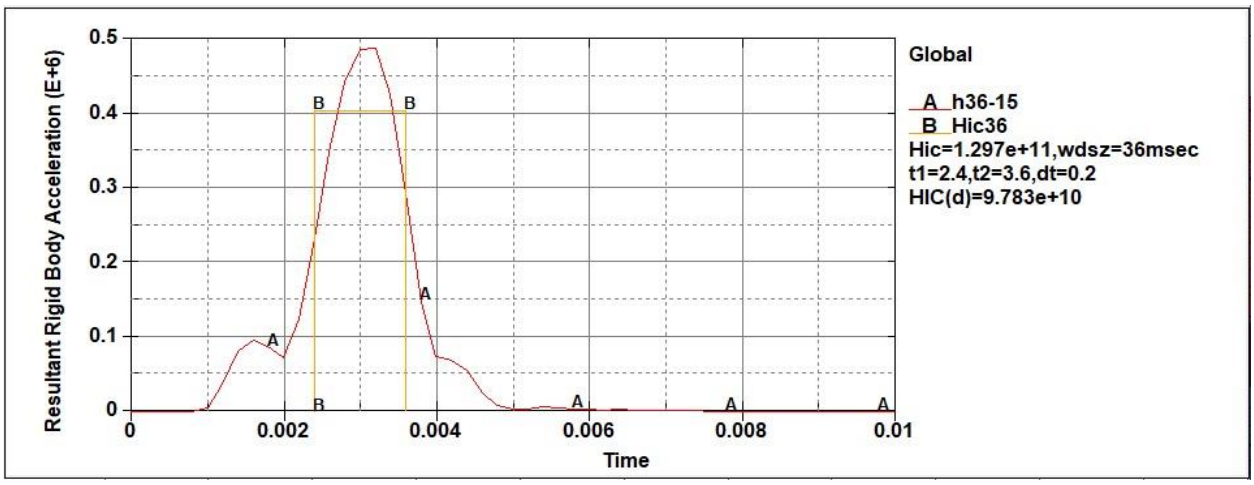

Figure 0.30. RLA distribution and HIC values at 13.5m/s.

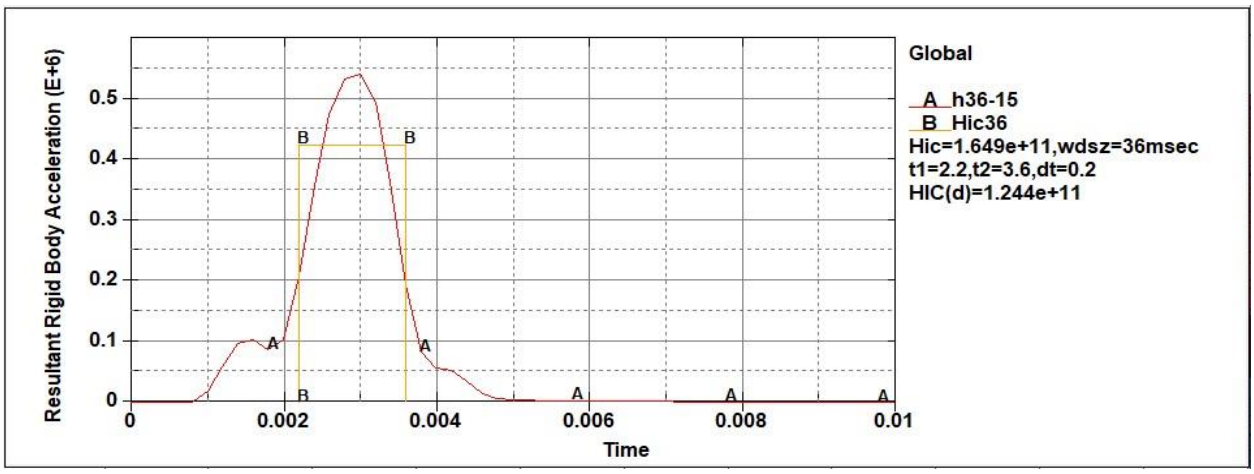

Figure 0.31. RLA distribution and HIC values at 14.5m/s.

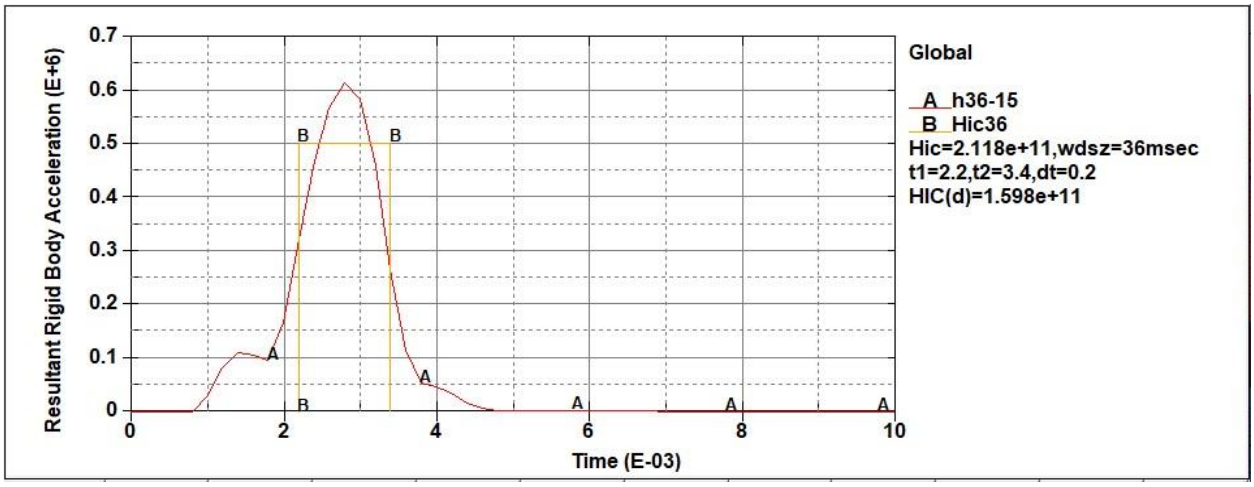

Figure 0.32. RLA distribution and HIC values at 15.5m/s.

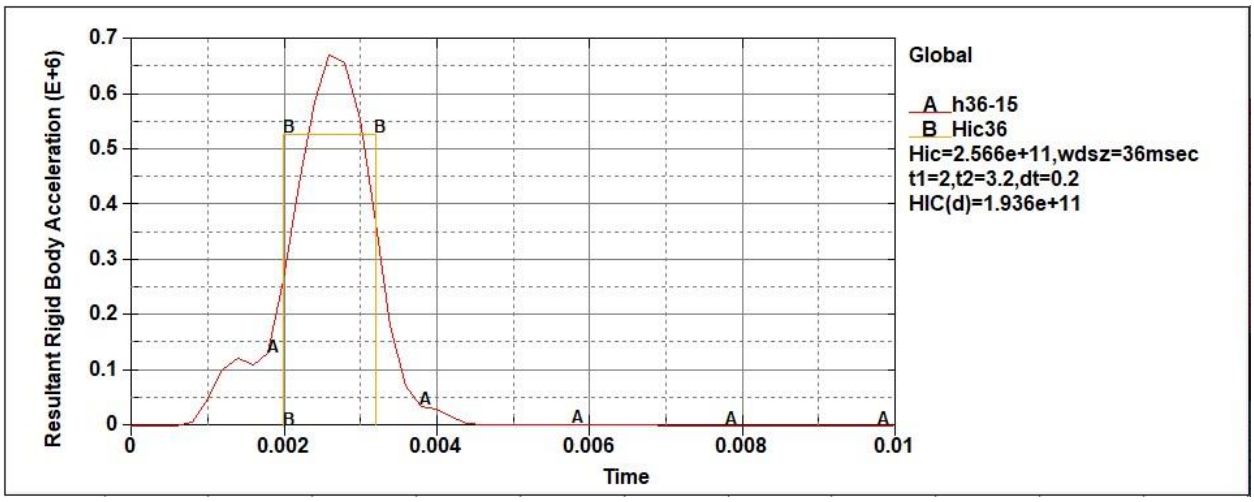

Figure 0.33. RLA distribution and HIC values at 16.5m/s.

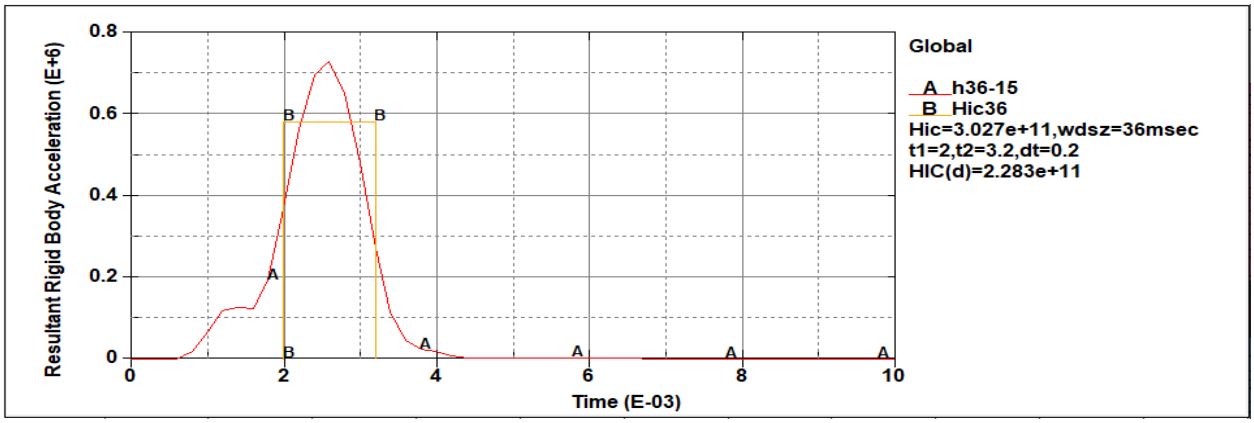

Figure 0.34.R LA distribution and HIC values at 17.5 m/s.

- The following figures the representation of the results for the lateral (S) impact position.

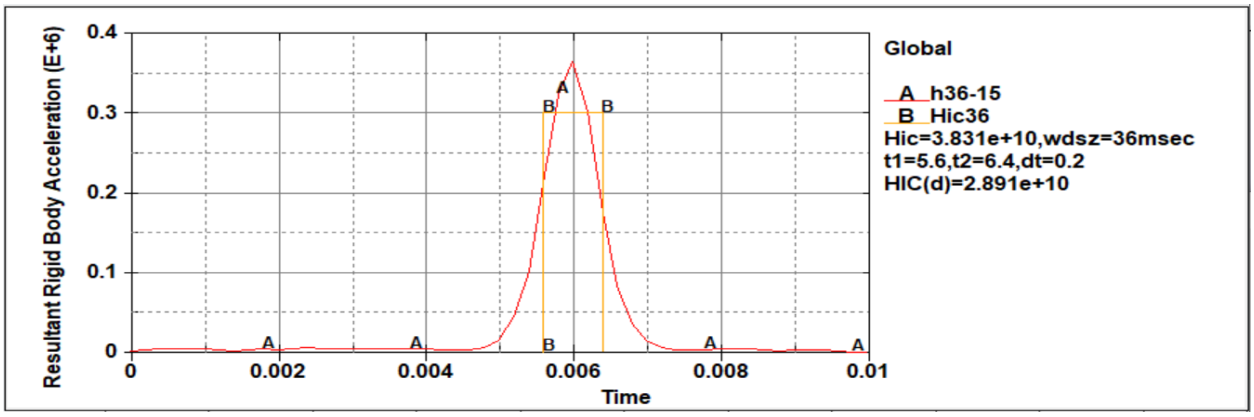

Figure 0.35. RLA distribution and HIC values at 7.5 m/s.

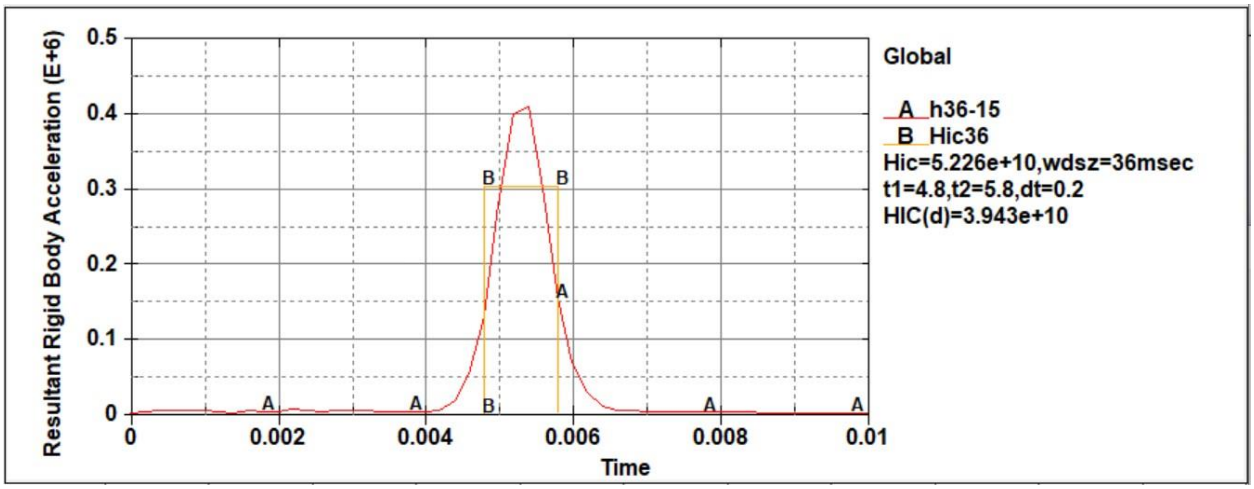

Figure 0.36. RLA distribution and HIC values at 8.5m/s.

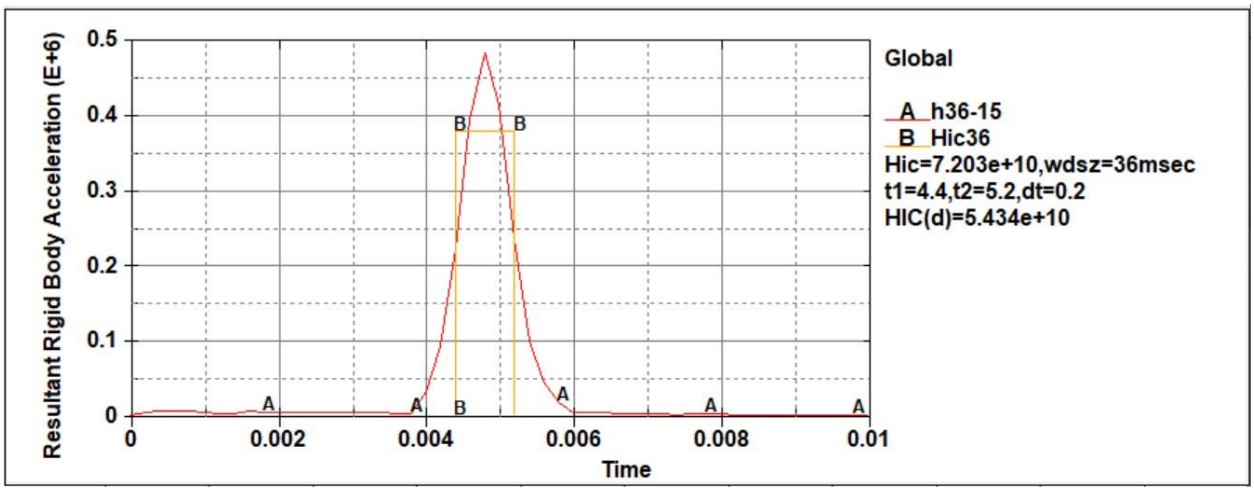

Figure 0.37. RLA distribution and HIC values at 9.5m/s.

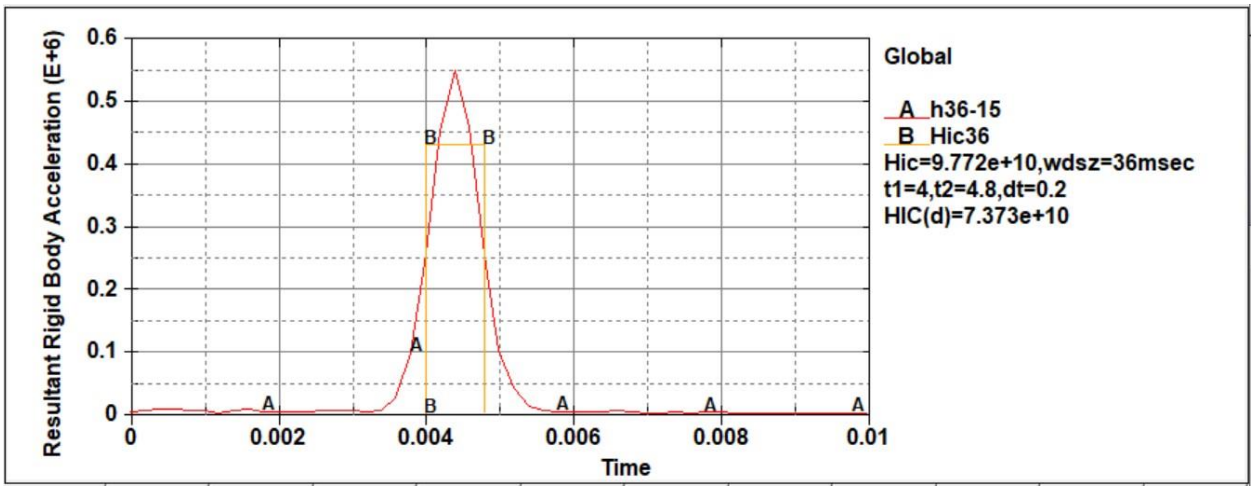

Figure 0.38. RLA distribution and HIC values at 10.5m/s.

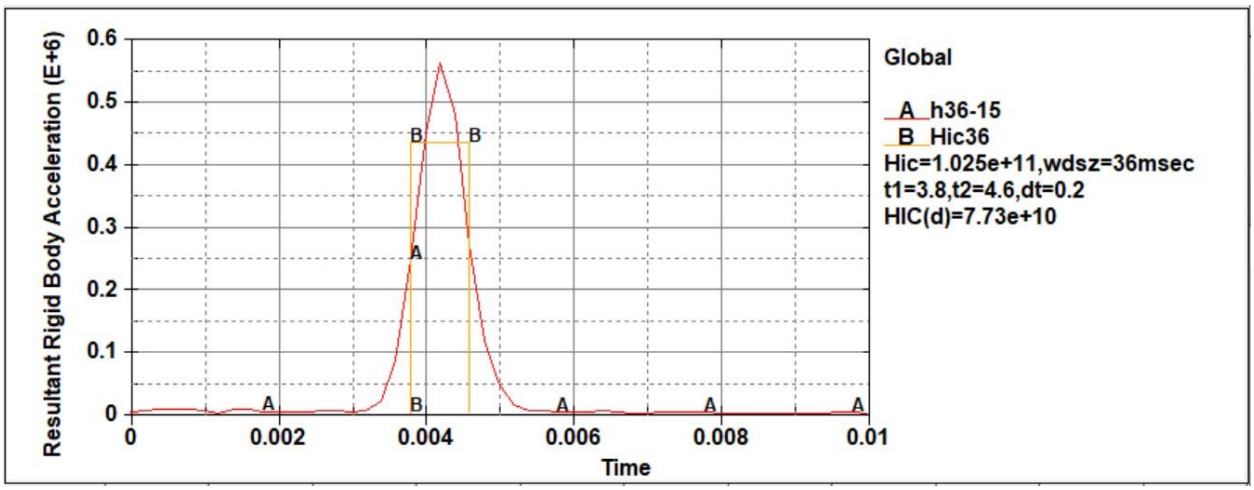

Figure 0.39. RLA distribution and HIC values at 11.5m/s.

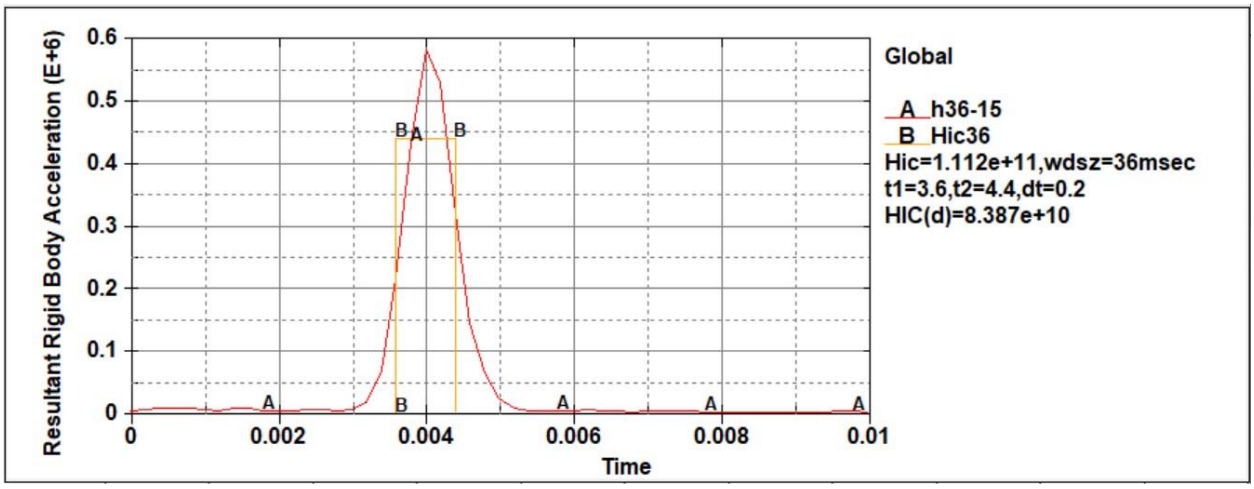

Figure 0.40. RLA distribution and HIC values at 12.5m/s.

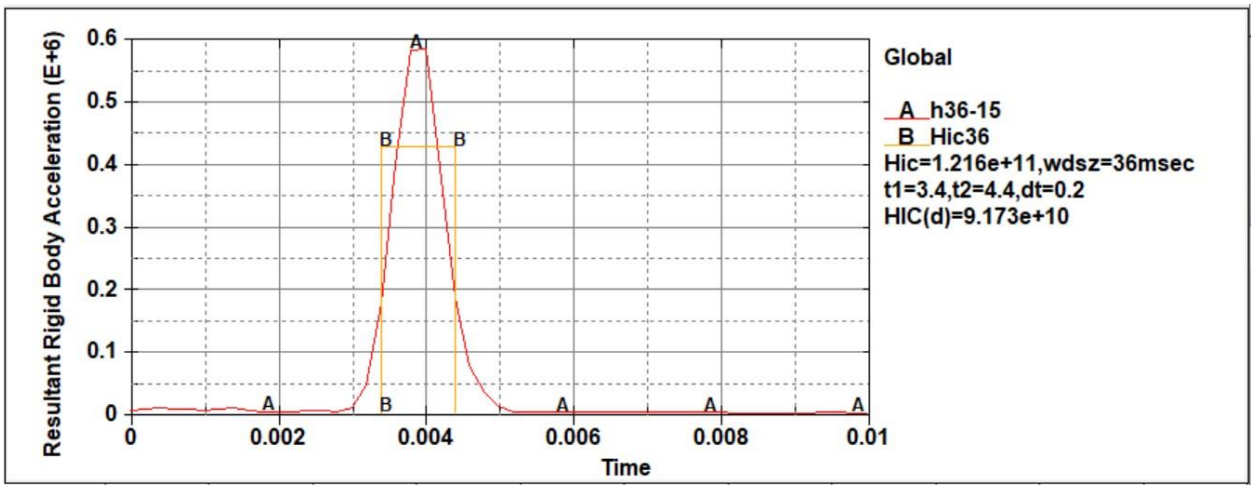

Figure 0.41. RLA distribution and HIC values at 13.5m/s.

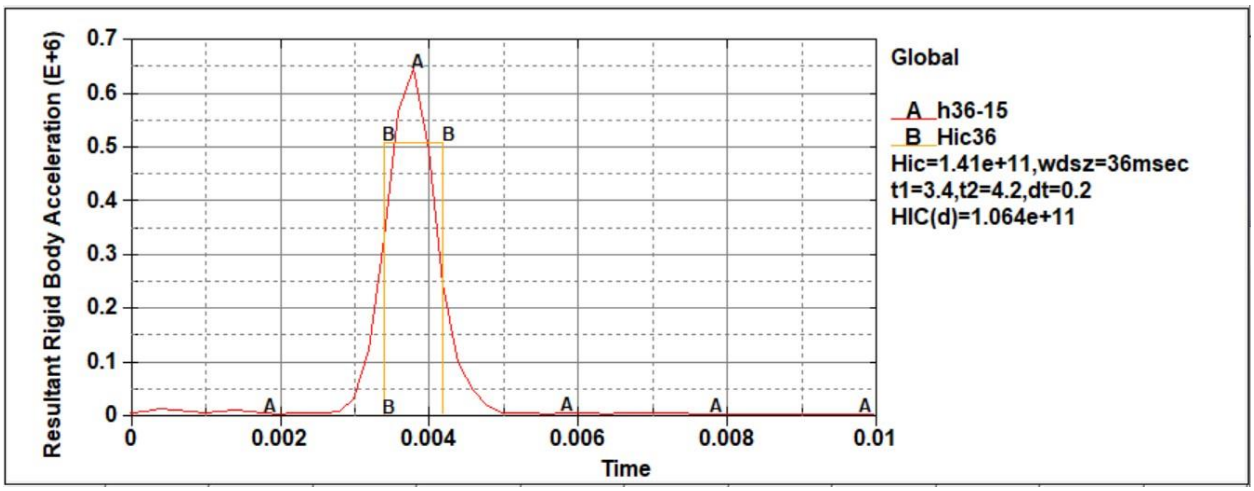

Figure 0.42. RLA distribution and HIC values at 14.5m/s.

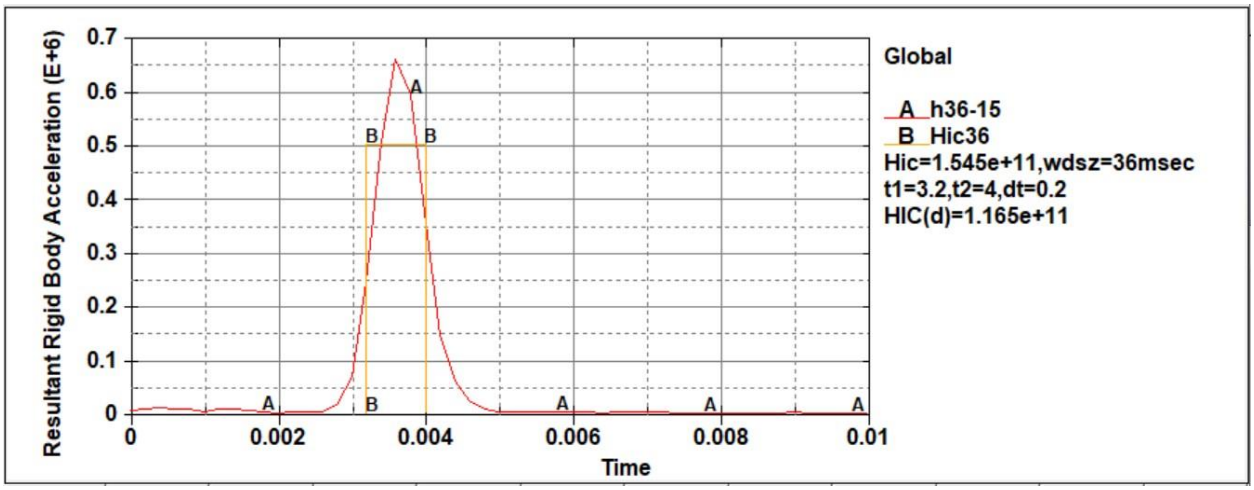

Figure 0.43. RLA distribution and HIC values at 15.5m/s.

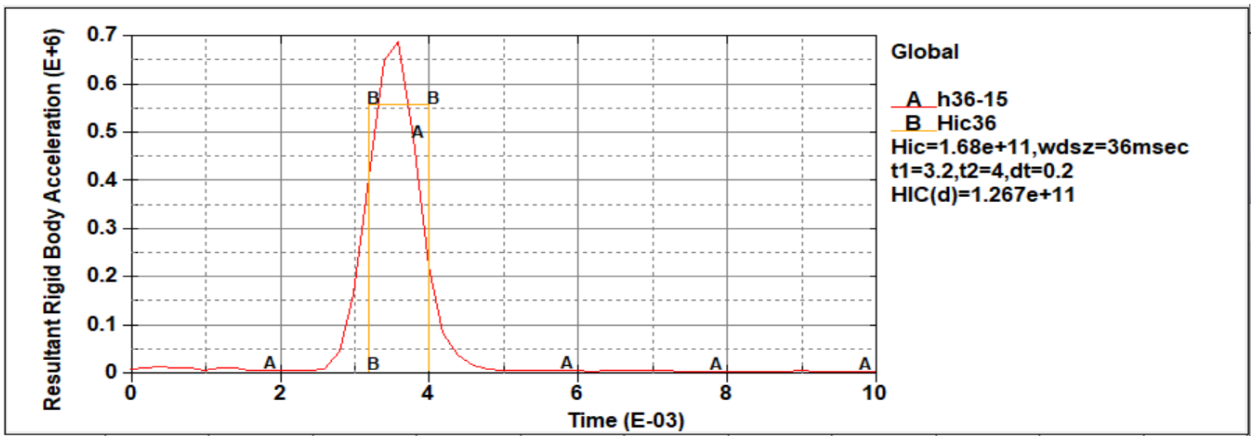

Figure 0.44. RLA distribution and HIC values at 16.5 m/s.